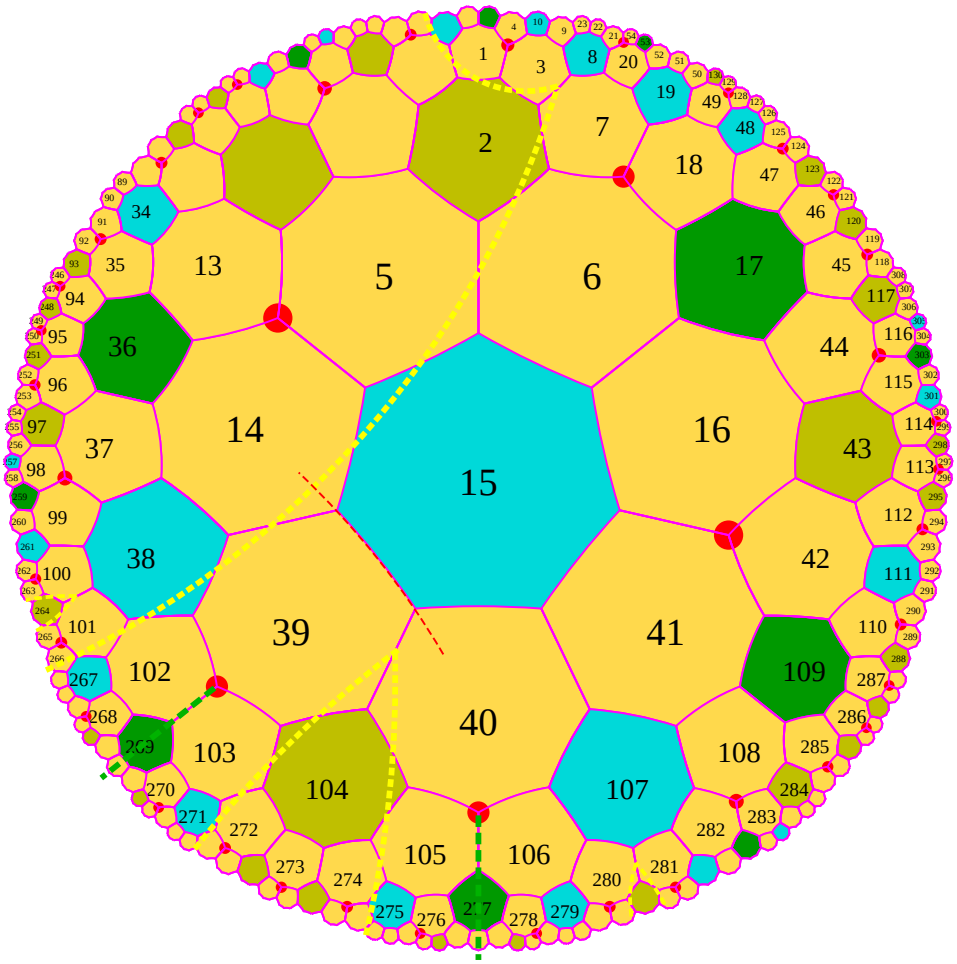

About the domino problem in the hyperbolic plane from an algorithmic point of view.

Maurice Margenstern

Publications du LITA, N° 2006-101

Service de reprographie de l'U.F.R. M.I.M., Université de Metz

Laboratoire d'Informatique Théorique et Appliquée, EA 3097 Université de Metz
Directeur de la publication : Maurice Margenstern

About the domino problem in the hyperbolic plane from an algorithmic point of view.

Maurice Margenstern

L.I.T.A., EA 3097, Université de Metz, I.U.T. de Metz,
Département d'Informatique,
Île du Saulcy,
57045 Metz Cedex, France,
e-mail : margens@univ-metz.fr

Abstract

In this paper, we prove that a generalized origin-constrained problem of tiling the hyperbolic plane with *à la* Wang tiles is undecidable.

Contents

1 Introduction

The question, whether it is possible to tile the plane with copies of a fixed set of tiles was raised by Wang, [30] in the late 50's of the previous century. Wang solved the *partial* problem which consists in fixing an initial finite set of tiles: indeed, fixing one tile is enough to entail the undecidability of the problem. The general case, when no initial tile is fixed, was proved by Berger in 1964, [1]. Both Wang's and Berger's proofs deal with the problem in the Euclidean plane. In 1971, Robinson found an alternative proof of the undecidability of the general problem in the Euclidean plane, see [28]. In this 1971 paper, he raises the question of the general problem for the hyperbolic plane. Seven years later, in 1978, he proved that in the hyperbolic plane, the partial problem is undecidable, see [29]. Up to now, the general problem is still open in the case of the hyperbolic plane.

In this report, we give the proof that a generalized origin-constrained problem is also undecidable in the case of the hyperbolic plane. It is interesting to note that our proof has several similarities with the proofs of Berger and Robinson, although it differs in its main character and in the result. The main difference is the presentation. In this report we consider that the tiling process is an algorithmic process which evolves in time.

We start from the initial idea of Berger's proof. It consists in simulating infinitely many computations of a Turing machine, indeed of the same Turing machine starting from an empty tape from which the set of prototiles is derived. The computations go as far as they can. If the Turing machine halts, the computations of the tiling which arrive until the halting state are stuck by this state and it is no more possible to tile. If the Turing machine does not halt, in general, the simulations are stopped by the limitations imposed on the tiling. But Berger, and after him Robinson, proved that among this infinity of computations in the case of a non-halting situation, either at least one of them can be performed without being interrupted, or there are arbitrary long computations. And, accordingly the plane can be tiled. And so, tiling the plane is possible if and only if the Turing machine does not stop. And this proves the undecidability of the problem.

Analysing the proof, we can see that the restricted amount of space in the Euclidean plane forces to find a way to generate infinitely many bounded domains whose size is exponentially increasing. The exponential size is needed to overcome the meeting problem. It is also needed from Wang's remarks of the 50's: if tilings of the plane are necessarily periodic, the general tiling problem is decidable. And, historically, Berger's proof had, as a side-product, the construction of a non-periodic tiling. This was not the goal of Berger's paper, but this was entailed by Wang's remark. As exponential signals are rather easily generated in the Euclidean plane, this was skillfully exploited by Berger. Also, the exponential growth guarantees the existence of at least an infinite sequence of increasingly longer and longer computations. This is performed in different very tricky ways connected with the structure of groups of symmetries of the square. On the other hand, the group structure makes it immediate to produce a situation where there is no privileged origin. At this point, it is important to focus on the fact that the constructions performed both by Berger and by Robinson in their respective proofs make a huge use of similarity. In his 1978 paper, speaking of the problem in the hyperbolic plane, Robinson remarks that *We cannot imitate Penrose construction, since similarity is impossible in the hyperbolic plane.* Indeed, this remark extends to Berger's proof and also to 1971 Robinson's proof.

The situation in the hyperbolic plane is very different than in the Euclidean plane, quite the opposite. Already Robinson's proof of the partial case witnesses at the key point: in the hyperbolic plane orientation and localisation are very difficult. This is what is expressed by Robinson in his 1978 paper: *The group of motions in the hyperbolic plane does not have a uniquely*

defined subgroup which plays the same role as the group of translations in the Euclidean plane. Indeed, the group of direct motions of the hyperbolic plane is simple which explains the impossibility of finding a *nice* subgroup as indicated by Robinson. Still in this 1978 paper, Robinson makes an interesting remark, asking whether *the undecidability and nonperiodicity results about tilings of the Euclidean plane have analogs for the hyperbolic plane*: *It is no longer clear that the two problems are related*. And it can be noted that the nonperiodicity problem for tilings of the hyperbolic plane has drawn more attention than the undecidability problem, see for instance [22, 7] for works in this direction. Here, our construction confirms Robinson's question as among continuously many realizations of the tiling which are possible when the simulated Turing machine does not halt, there are countably many of them which are periodic.

From the tools I devised to locate cells of a cellular automaton implemented in the hyperbolic plane, see [15, 16] for more complete references, it came to me that perhaps, this could provide us with a new angle to tackle the problem. Unfortunately, in my preliminary tools, the root of the tree which is used to locate cell plays a key rôle. It is even reinforced in other papers, [3]. Yet, these tools had the advantage to give much clear proofs for the partial case than Robinson's. I have several scenarios, although I published none of them on the subject. As a compensation, one of them is presented in this report as it is used in the proof of the main theorem. A bit later, in [18], I succeeded to give a representation of two tilings, $\{5, 4\}$ and $\{7, 3\}$ where there is no more a central root. However, in this representation, there are still many roots which are gathered in what could be called a highway. It is not still the requirement of the general problem.

It is worth noticing an interesting point. As it can easily be noted in Berger's and Robinson's proofs, if the first tile can be chosen at random, it can be a tile bearing the computation signs of a Turing machine. But as it may turn out that this tile can never be used, it cannot be placed. And this cannot be accepted. Consequently, the organisation of the tiling must force any computation to be started by a first tile corresponding to the starting of the Turing computation, which is the case in both Berger's and Robinson's proofs. And so, the first tile cannot be taken at random.

Is it not a contradiction with the statement of the general problem which requires that there is no condition on the set of prototiles? Indeed, there is no contradiction as we can see by the following argument.

Let us consider a finite set T of prototiles. The origin-constrained problem

means that we fix a tile a of T and we ask whether, a being placed, it is possible to complete the tiling to the whole plane with copies of elements of T. We shall express this by writing that there is a solution to the problem (T, a). In the general problem, a is not fixed, and so, a solution for T depends on T only. The connection between the two problems is the following. If there is a solution for T, taking at random a tile a in the tiling, this solution immediately gives a solution for (T, a). And so, there is a solution for T if and only if there is a in T for which there is a solution for (T, a). And so, when we look at the existence of a solution, it is possible to choose to start the construction from a fixed in advance tile. Now, when we try to see whether there is no solution, then we must try all problems (T, a) with a running over T. This means that we have to start from any tile. But as we wish to prove that there is no tiling, it is not needed to try to tile the whole plane. Starting from an arbitrary tile, if, continuing the tiling we can reach a tile from which we know that we can go on until we arrive at an impossibility, we are done. And if we have this property, we can always start from an origin, both for the positive and the negative tests. Berger's and Robinson's proof have this property. The skeleton fills up the plane and it guarantees that, starting from any point, an origin is eventually reached. And so, in the case when the Turing machine halts, starting from any arbitrary tile we can reach an origin and from this one we can find possibly another one from which we can process the whole computation of the Turing machine until we reach the halting state which blocks the construction of the tiling.

This point is not written in Berger's and Robinson's proofs. It was probably folklore at that time.

This forcing property is what is missing in the proof of this paper to solve the general problem. Our set of origins is not enough dense in the hyperbolic plane. However, in this proof, this set of origin has interesting properties, which are also shared by the analogous set in Berger's and Robinson's proof. The properties are the following ones:

> (*i*) *There is a positive number k such that in the ball of radius k around any origin ω, there are at least two origins ω_1 and ω_2 with ω, ω_1 and ω_2 not on the same line.*
> (*ii*) *There are infinitely many rays each one containing infinitely many origins.*

Accordingly, in the proof of this report, the set of origins satisfies a density property but with respect to itself. Of course, this is not enough. This is why

we call the problem obtained by requiring these properties a **generalized origin-constrained** problem of tiling the plane.

Note, that in Berger's and Robinson's proof, it is stressed that the copies of tiles of the initial set must be transported to their final place by using only **shifts** leaving the tiling invariant. In the hyperbolic case, this restriction cannot be observed: the shifts which leave the tiling invariant also generate the rotations which leave it invariant. However, in our construction, we forbid the possibility to take the reflection of a tile of the initial set.

The paper is divided in sections as follows. The second section recalls the prerequisites to follow the proof. In particular, we remind the reader what is needed from hyperbolic geometry. Then we shortly remind the basic tools used to deal with regular tilings of the hyperbolic plane, generated by tessellation. In the third section, we deal with the way to represent the tiling $\{7, 3\}$ which leads to the solution, starting from *flowers*, defined as balls in $\{7, 3\}$ of discrete radius 1 and continuing with the *mantilla*, a slight modification of the flowers creating a tiling in the spirit of the *carpets* which I introduced in [18]. Then, in section 4, we indicate a solution to the partial problem, and in section 5, we deal with the generalized origin-constrained problem. We use the partial solution of section 4 and also, at this occasion, we clarify a point about the simulation of Turing machines. In section 6, we give another application of the method, showing after [9, 24] that there is a finite set of tiles for which there is a non-recursive way to tile the hyperbolic plane but no recursive way to do so.

2 Tilings of the hyperbolic plane

2.1 Hyperbolic geometry

In order to simplify the approach for the reader, we shall present a model of the hyperbolic plane and simply refer to the literature for a more abstract, purely axiomatic exposition, see [23, 10] for instance.

As it is well known, hyperbolic geometry appeared in the first half of the 19^{th} century, in the last attempts to prove the famous parallel axiom of Euclid's *Elements* from the remaining axioms. Hyperbolic geometry was yielded as a consequence of the repeated failure of such attempts. Independently, Lobachevsky and Bolyai discovered a new geometry by assuming that in the plane, from a point out of a given line, there are at least two lines which

are parallel to the given line. Later, during the 19^{th} century, Beltrami found out the first models of the new geometry. After him, with Klein, Poincaré, Minkowski and others, a lot of models were discovered, some of them giving rise to the geometric material being used by the theory of the special relativity. The constructions of the models, all belonging to Euclidean geometry, proved by themselves that the new axioms bring in no contradiction with the other ones. Hyperbolic geometry is not less sound than Euclidean geometry is. It is also no more sound, in so far as much later, models of the Euclidean plane were discovered in the hyperbolic plane.

Among these models, Poincaré's models met with great success because in these models, hyperbolic angles between lines coincide with the Euclidean angles of their supports. In this paper, we take Poincaré's disc as a model of the hyperbolic plane.

2.1.1 Lines of the hyperbolic plane and angles

In Poincaré's disc model, the hyperbolic plane is the set of points which lie in the open unit disc of the Euclidean plane.

The lines of the hyperbolic plane in Poincaré's disc model are the trace of either diametral lines or circles which are orthogonal to the unit circle. We say that the considered lines or circles **support** the hyperbolic line, *h*-**line** for short, and sometimes simply **line** when there is no ambiguity.

Poincaré's unit disc model of the hyperbolic plane makes an intensive use of some properties of the Euclidean geometry of circles, see [12] for an elementary presentation of the properties which are needed for our paper.

Consider the points of the unit circle as **points at infinity** for the hyperbolic plane: it is easy to see that an h-line defines two points at infinity by the intersection of its Euclidean support with the unit circle. They are called points at infinity of the h-line. The following easily proved properties will often be used: any h-line has exactly two points at infinity; two points at infinity define a unique h-line passing through them; a point at infinity and a point in the hyperbolic plane uniquely define an h-line.

The angle between two h-lines are defined as the Euclidean angle between the tangents to their support. This is one reason for choosing this model: hyperbolic angles between h-lines are, in a natural way, the Euclidean angle between the corresponding supports. In particular, orthogonal circles support perpendicular h-lines.

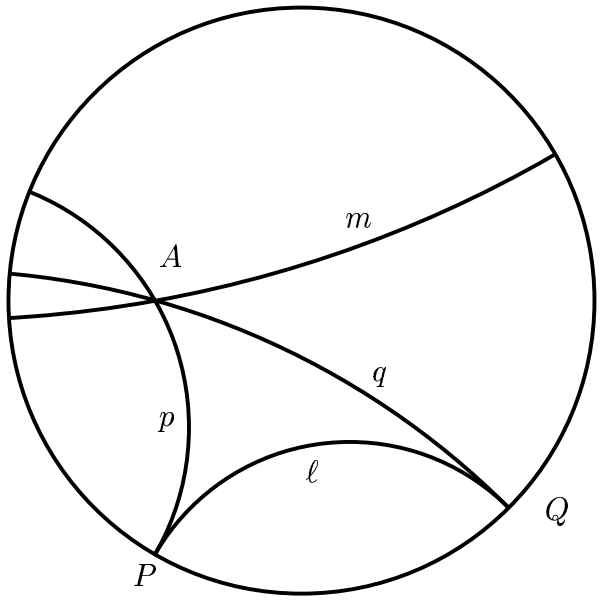

Figure 1 *The lines p and q are parallel to the line ℓ, with points at infinity P and Q. The h-line m is non-secant with ℓ.*

In the Euclidean plane, two lines are parallel if and only if they do not intersect. If the points at infinity are added to the Euclidean plane, parallel lines are characterized as the lines passing through the same point at infinity. Hence, as for lines, to have a common point at infinity and not to intersect is the same property in the Euclidean plane. This is not the case in the hyperbolic plane, where two h-lines may not intersect and have no common point at infinity: we say that such h-lines are **non-secant**. We shall call **parallel**, h-lines which have a common point at infinity. So, considering the situation illustrated by Figure 1 above, there are exactly two h-lines parallel to a given h-line which pass through a point not lying on the latter line. Also, there are infinitely many ones which pass through the point but are non-secant with the given h-line. This is easily checked in Poincaré's disc model, see Figure 1. Some authors call **hyperparallel** or **ultraparallel** lines which we call **non-secant**.

Another aspect of the parallel axiom lies in the sum of interior angles at the vertices of a polygon. In the Euclidean plane, the sum of angles of any triangle is exactly π. In the hyperbolic plane, this is no more true: the

sum of the angles of a triangle is **always less** than π. The difference from π is, by definition, the **area** of the triangle in the hyperbolic plane. Indeed, one can see that the difference of the sum of the angles of a triangle from π has the additive property of a measure on the set of all triangles. As a consequence, there is no rectangle in the hyperbolic plane. Consequently two non-secant lines, say ℓ and m, have, at most, one common perpendicular. It can be proved that this is the case: two non-secant lines of the hyperbolic plane have exactly one common perpendicular. But parallel h-lines have no common perpendicular.

In the Euclidean geometry, it is well known that if we fix three positive real number α, β and γ with $\alpha+\beta+\gamma = \pi$, there are infinitely many triangles which have these numbers as the measure of their interior angles. This property of the Euclidean plane defines the notion of **similarity**.

Another consequence of the non-validity of Euclid's axiom on parallels in the hyperbolic plane is that there is no notion of similarity in that plane: *if α, β, γ are positive real numbers such that $\alpha+\beta+\gamma < \pi$, ℓ and m are h-lines intersecting in A with angle α, there are exactly two triangles ABC such that $B \in \ell$, $C \in m$ and BC makes angle β in B with ℓ and angle γ in C with m.* Each of those triangles is determined by the side of ℓ with respect to A in which B is placed.

2.1.2 Reflections in a h-line

Any h-line, say ℓ, defines a **reflection** in this line being denoted by ρ_ℓ. Let Ω be the center of the Euclidean support of ℓ, and let be R its radius. Two points M and M' are **symmetric** with respect to ℓ if and only if Ω, M and M' belong to the same Euclidean line and if $\Omega M.\Omega M' = R^2$. Moreover, M and M' do not lie in the same connected component of the complement of ℓ in the unit disk. We also say that M' is obtained from M by the **reflection in** ℓ. It is clear that M is obtained from M' by the same reflection.

All the transformations of the hyperbolic plane which we shall later consider are reflections or constructed by reflections.

By definition, an **isometry** of the hyperbolic plane is a finite product of reflections. Two segments AB and CD are called **equal** if and only if there is an isometry transforming AB into CD.

It is proved that finite products of reflections can be characterized as either a single reflection or the product of two reflections or the product

of three reflections. In our sequel, we will mainly be interested by single reflections or products of two reflections. The set which contains the identity and the product of two reflections constitutes a group which is called the **group of displacements**.

At this point, we can compare *reflections* in a h-line with symmetries with respect to a line in the Euclidean plane. These respective transformations share many properties on the objects on which they operate. However, there is a very deep difference between the isometries of the Euclidean plane and those of the hyperbolic plane: while in the first case, the group of displacements possesses non trivial normal subgroups, in the second case, this is no more the case: the group is simple.

The product of two reflections with respect to lines ℓ and m is a way to focus on this difference. In the Euclidean case, according to whether ℓ and m do intersect or are parallel, the product of the two corresponding symmetries is a rotation around the point of intersection of ℓ and m, or a shift in the direction perpendicular to both ℓ and m. In the hyperbolic case, if h-lines ℓ and m intersect in a point A, the product of the corresponding reflections is again called a rotation around A. If ℓ and m do not intersect, there are two cases: either ℓ and m intersect at infinity, or they do not intersect at all. This gives rise to different cases of shifts. The first one is called an **ideal rotation**, it is a kind of degenerated rotation, and the second one is called a **hyperbolic shift** or **shift along** n, the common perpendicular to ℓ and m. A shift is characterised by the image P' of any point P on n. We shall say simply **shift** when the explicit indication of the common perpendicular is not needed.

For any couple of two h-lines ℓ and m, there is an h-line n such that ℓ and m are exchanged in the reflection in n. In the case when ℓ and m are non-secant, n is the perpendicular bisector of the segment which joins the intersections of ℓ and m with their common perpendicular.

For more information on hyperbolic geometry, we refer the reader to [23, 27].

2.2 Tilings of the hyperbolic plane

In the paper, we only consider tilings which are obtained by the following process: we consider a regular polygon P and we replicate P by reflection in its sides and, recursively, of the images in their sides. We say that P tiles the plane if two distinct images completely coincide or have disjoint interiors

and if the union of the images contains the whole plane. In this case, we say that P **tiles the plane by tessellation**. In the rest of this paper, as we only consider tilings of this kind, we shall simply say that P tiles the plane.

In the Euclidean plane, there are only three tilings by tessellation from a regular polygon: the square grid, the hexagonal grid and the triangular grid. They are based on the square, the regular hexagon and the equilateral triangle, respectively.

In the hyperbolic plane, there are infinitely many such tilings. This property is a result of the famous Poincaré's theorem, stated and proved by Poincaré at the end of the 19^{th} century. The theorem is based on the method of triangulation: if a tiling by tessellation exists, by subdividing the initial polygon on equal triangles sharing a common vertex at the centre of the polygon, we obtain a tiling by tessellation from this triangle. The converse is also true and Poincaré's theorem states a nice property for a triangle to tile the plane by tessellation:

We can now state the theorem:

Poincaré's Theorem, ([26]) – *Any triangle with interior angles* $\pi/\ell, \pi/m, \pi/n$ *such that*

$$\frac{1}{\ell} + \frac{1}{m} + \frac{1}{n} < 1$$

generates a unique tiling by tessellation.

As an immediate corollary of the theorem, tilings based on any regular polygon with p sides and interior angle $\dfrac{2\pi}{q}$ do exist, provided that $\dfrac{1}{p} + \dfrac{1}{q} < \dfrac{1}{2}$. Such a polygon and the corresponding tiling are denoted by $\{p, q\}$. Below we show the simplest tilings of this kind with $p = 5$ and $q = 4$ displayed by Figure 2. We call this tiling the **pentagrid**.

Another example, which we shall study in full details is the tiling $\{7, 3\}$ where $p = 7$ and $q = 3$. The basic tile is a regular heptagon whose interior angle is $\dfrac{2\pi}{3}$. We call this tiling the **ternary heptagrid**.

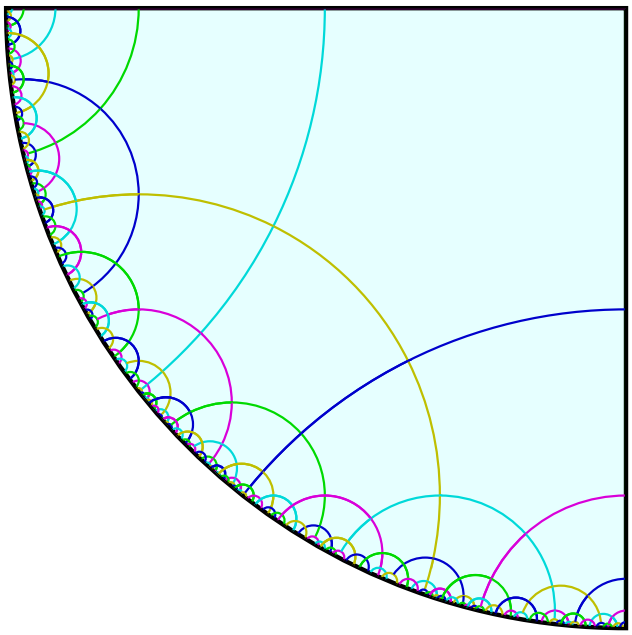

Figure 2 *A simple tessellation with right-angled regular pentagons.*

2.3 The splitting method

The splitting method was first defined in [13, 14]. The definition runs as follows:

Definition 1 *Let $S_0, \ldots, S_k$ be finitely many parts of some geometric metric space X which are supposed to be closed with non-empty interior, unbounded and simply connected. Let $P_1, \ldots, P_h$ with $h \leq k$ be finitely many closed simply connected bounded sets. Say that the S_i's and P_ℓ's constitute a* **basis of splitting** *if and only if:*

(i) X splits into finitely many copies of S_0,

(ii) any S_i splits into one copy of some P_ℓ, the **leading tile** *of S_i, and finitely many copies of S_j's,*

where **copy** *means an* **isometric image**, *and where, in condition (ii), the copies may be of different S_j's, S_i possibly included.*

As usual, it is assumed that the interiors of the copies of P_ℓ and the copies of the S_j's are pairwise disjoint.

The set S_0 is called the **head** *of the basis and the P_ℓ's are called the* **generating tiles** *and the S_i's are called the* **regions** *of the splitting.*

Say that a tiling of X is **combinatoric** if X has a basis of splitting and if the spanning tree of the splitting yields exactly the restriction of the tiling to S_0, the head of the basis.

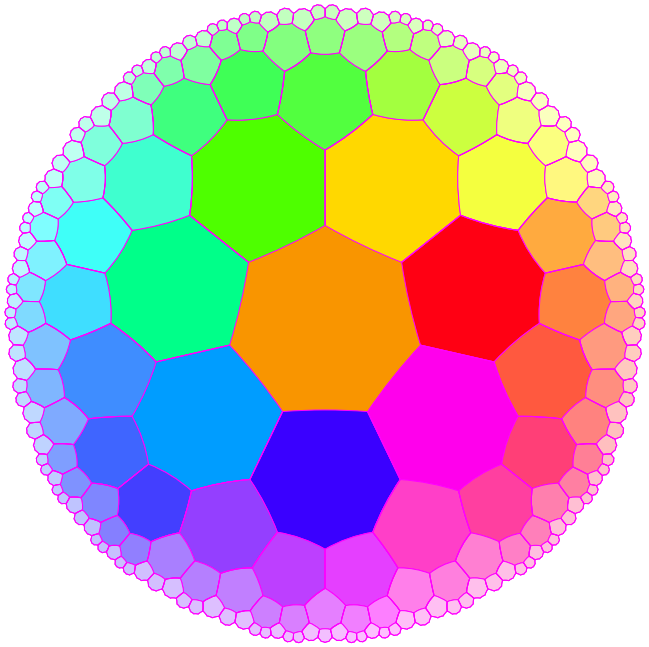

Figure 3 *Another tessellation: with regular heptagons where the interior angle is* $\frac{2\pi}{3}$.

Consider a basis of splitting of X, if any. We recursively define a tree A which is associated with the basis as follows. The **root** of A is the leading tile of S_0. Consider the region S_i associated to the considered node, say ν. Splitting S_i according to condition (ii) of the above definition, we take the leading tiles of the regions which are obtained as the sons of ν. This defines an infinite tree A with finite branching which we call the **spanning tree of the splitting**, where *splitting* refers to the basis of splitting with its regions $S_0, \ldots, S_k$ and its generating tiles $P_0, \ldots, P_h$.

The fact that the hyperbolic plane is able to embed infinite trees is not new. This is already known from Gromov's works, see [5] for instance, which

points at the tree structure as the key structure of a hyperbolic space. However, before [19], which exhibits the tree in a *natural* way, no *application* of that idea was done.

In [12], for instance, we proved that the pentagrid is combinatoric. We shall see in the next sub-section another example of a combinatoric tiling: the ternary heptagrid to which we shall apply the method.

Now, let us turn to the algebraic consequences of the definition.

When a tiling is combinatoric, we represent the splitting of the regions of the basis by an **incidence** matrix which we call the **matrix of the splitting**. Each row i is associated to a region S_{i-1} and on each column j, we have how many copies of S_{j-1} enter the splitting of S_{i-1} according to the condition (ii) of the definition. Now, when we have a square matrix M, we can attach to it its characteristic polynomial P. When M is the matrix of a splitting of a combinatorial tiling, we call **polynomial of the splitting** the just defined polynomial P possibly divided by the greatest power of X which it contains.

Let us see the connection of this polynomial with the tiling. Consider the spanning tree $\mathcal{A}$ of the head of the basis and number its nodes, level by level and, on each level, from the left to the right. Now, call u_n the number of nodes of $\mathcal{A}$ which are at level n. Then, the sequence of u_n's satisfies the linear recurrence relation associated with the polynomial of the splitting. Moreover, it turns out that in all cases which we studied, the polynomial of the splitting has a positive greatest real root β with $\beta > 1$. Then, it is possible to represent the positive numbers in the basis of the sequence u_n which we just defined. It is known, see [6, 11], that any positive number n can be written as $n = \sum_{i=1}^{k} \alpha_k u_k$, where $\alpha \in \{0..b\}$ with $b = \lfloor \beta \rfloor$. In general, this representation is not unique, but it can be made unique by choosing the maximal representation with respect to the lexicographic order on $\{0..b\}^*$. We call **coordinate** of node ν the maximal representation of the number attached to it in basis $\{u_n\}_{n>0}$. We call **language of the splitting** the language of the coordinates of the nodes of the spanning tree of the splitting.

Now, many tilings of the hyperbolic plane turn out to be combinatoric with a regular language of the splitting. There are detailed proofs for tilings $\{p, 4\}$ and $\{p, 3\}$. See [20] and [4] for, respectively $\{p, 4\}$ and $\{p, 3\}$. In [4], an interesting connection is established between both families of tilings: the spanning trees of the splitting of $\{p, 4\}$ and $\{p+2, 3\}$ are the same. There are also combinatoric tilings for which the language of the splitting is not

regular: the case of equilateral triangles, see [14], a tiling of the hyperbolic $3D$ space, see [21], and a tiling of the hyperbolic $4D$ space, see[17].

2.4 The tiling $\{7, 3\}$

In this section, we study the ternary heptagrid, a representation of which we gave by Figure 3, above. In this figure, we represent the tiling starting from any tile whose geometrical centre is put on the origin of Poincaré's disc, O.

2.4.1 The splitting

As we can see on Figure 5, we can split the hyperbolic plane into eight pieces: a heptagon and seven copies of the region which is displayed in the left-hand part of Figure 6 which we call S_0.

Call S_1 the regions which is displayed on the right-hand side of Figure 6. Due to the angle $\frac{2\pi}{3}$, regions S_0 and S_1 cannot be delimited by the lines which support the edges of a heptagon.

Here, in order to define these regions precisely, we introduce the following device, see also [3, 18]: we consider the lines of the **mid-points** of the sides of the heptagons which are defined by the tiling. More precisely, we take the lines which join the mid-points of two adjacent sides of the heptagon. Elementary considerations of hyperbolic geometry show that the mid-points of the heptagon on the ternary heptagrid lie on appropriate lines, see Figure 4. As we shall intensively use such lines in our sequel, we pay some attention to their construction.

Let σ denote the common sides of tiles $\mathcal{T}_0$ and $\mathcal{T}_1$. It is clear that $\mathcal{T}_1$ is the image of $\mathcal{T}_0$ by the reflection in σ. The bisector β of σ is an axis of reflection which leaves tiles $\mathcal{T}_0$ and $\mathcal{T}_1$ both invariant. It is not difficult to see that C is the image of A under the reflection in β followed by the reflection in σ. Consequently, the angle of AB with σ is equal to the angle of BC with σ and so, points A, B and C lie on the same line. Such a line is called **line of the mid-points**. Line AD is also another line of the mid-points.

Now, denote by S_0 the set of tiles which are centered inside the angle delimited by the two rays AC and AD in Figure 4.The angle is defined by two rays, each one being supported by a line of the mid-points in such a way that the bisector of the angle is a side σ of the ternary heptagrid, and the vertex of the angle is the middle of σ. Above, Figure 5 illustrates the

definition of S_0.

Figure 5 shows us that $\mathbb{H}^2$ splits into a tile $\mathcal{T}_0$ and seven copies of S_0. Each copy has a **leading tile** which has a common side with the central tile $\mathcal{T}_0$.

Next, in Figure 6, we also see the illustration of another region, S_1, which is also defined by lines of the mid-points. As indicated by Figure 6, S_1 is defined by three lines: two lines of the mid-points ℓ_1 and ℓ_2 and a side σ of the heptagrid which is supported by the common perpendicular of lines ℓ_1 and ℓ_2. Moreover, ℓ_1 and ℓ_2 pass through the mid-points of the sides of a tile which are adjacent to σ. Call **strip** $S(\ell_1, \ell_2, \sigma)$ one of the two regions which are defined as the intersection of three closed half-planes defined by these lines which contain both ℓ_1 and ℓ_2. Now, we define S_1 as the union of those tiles of the heptagrid which are centered in a strip $S(\ell_1, \ell_2, \sigma)$, where ℓ_1, ℓ_2 and σ are as just described.

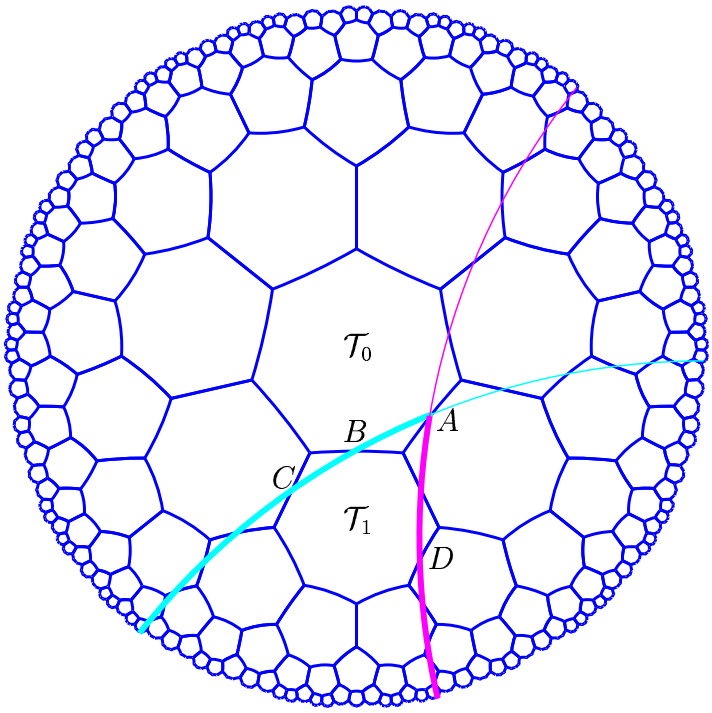

Figure 4 *Lines of mid-points defining a copy of* S_0.

Then, Figure 7 gives a closer look on copies of, respectively, S_0 and S_1, and Figure 7 shows how we can assemble copies of these regions in order to

define their splitting. At last, Figure 8 illustrates the proof that the splitting is indeed what is suggested by Figure 7.

The proof of the correctness of the splitting is given by the following arguments which are summarized by Figure 8.

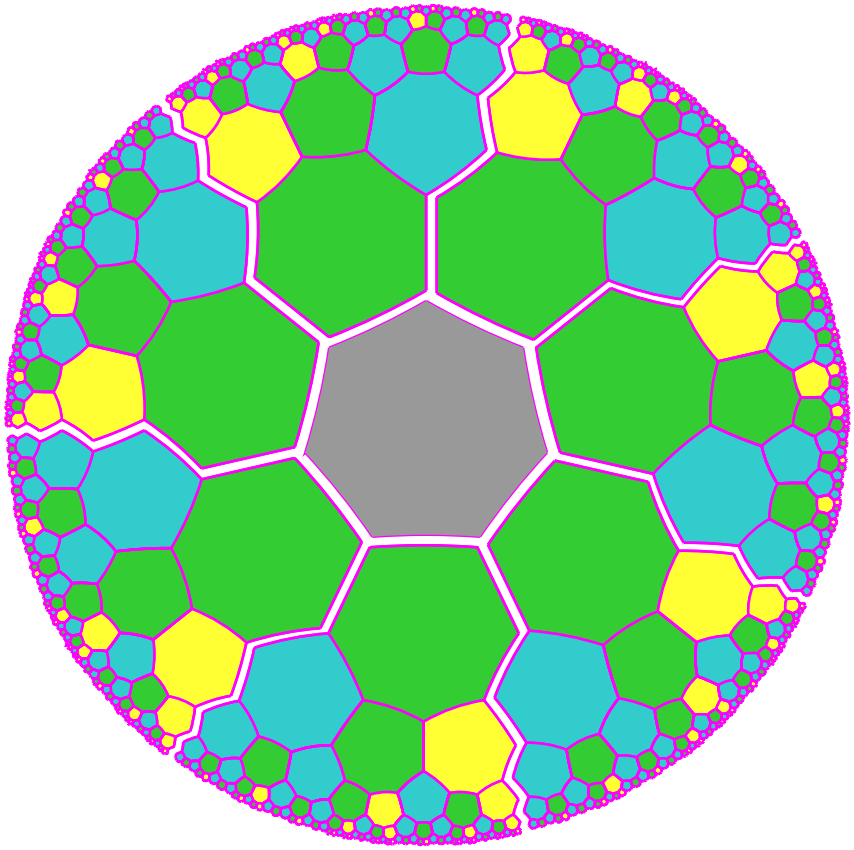

Figure 5 *$I\!H^2$ splits into a tile and seven copies of S_0.*

We can see that S_0 can be split into a tile and two copies of S_0 itself and one copy of S_1. This is proved as follows. Let τ be the leading tile of region S_0. There is a single vertex A of τ such that the bisector of the angle in A which is interior to τ is perpendicular to ℓ_2. Let τ_1 be the tile which is the reflection of τ in the side of τ which is also perpendicular to ℓ_2: there is a unique side $s1$ of τ with this property. Let δ_1 be the image of δ under the reflection in s_1. We note that ℓ_2 is the common perpendicular of δ and δ_1. Let σ be the shift along ℓ_2 which transforms δ into δ_1, see Figure 8. Note

that $\tau_1 = \sigma(\tau)$ and that also, $\delta_1 = \sigma(\delta)$. Shift σ transforms S_0 into a copy of it with τ_1 as its leading tile. Let us denote by S_0^1 this copy of S_0. It is defined by ℓ_2 which is invariant under σ and by $m_1 = \sigma(\ell_1)$, see Figure 8.

Let C be the centre of τ. It is clear that a rotation ρ around C with angle $\frac{2\pi}{7}$ transforms S_0^1 into another copy of S_0 with leading tile $\tau_2 = \rho(\tau_1)$. Call S_0^2 this new copy of S_0. It is defined by m_1 as we have also that $m_1 = \rho(\ell_2)$, and by $m_2 = \rho(m_1)$. The same rotation makes it clear that τ_2 is obtained from τ by a shift along a line of the mid-points of τ which makes an angle of $\frac{2\pi}{7}$ with ℓ_2. Indeed, this new shift is $\rho_\circ\sigma_\circ\rho^{-1}$ and it also transforms ℓ_1 into m_2. Note that τ_2 is also the image of τ under the reflection in $s_2 = \rho(s_1)$ which is the side of τ which is shared by τ_2.

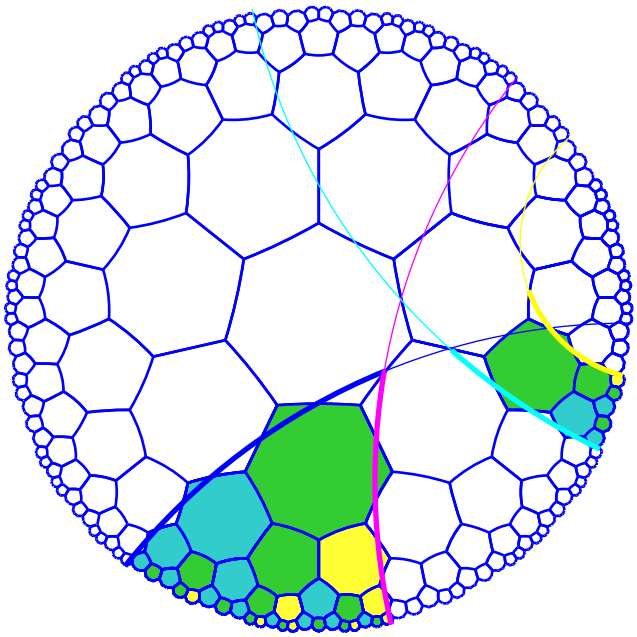

Figure 6 *Lines of the mid-points defining a copy of S_0 and a copy of S_1.*

Again, apply ρ to S_0^1. We get this time another copy of S_0, say S_0^3 with leading tile τ_3 and delimited by $m_2 = \rho(m_1)$ and $m_3 = \rho(m_2)$. We can also see that τ_3 is the image of τ under the reflection in $s_3 = \rho(s_2)$. Side s_3 belongs to both τ and τ_3.

Now, repeat with ℓ_1 the argument we provided with ℓ_2. This defines a shift which transforms τ into τ_3 and which transforms ℓ_2 into n_1. Now, we can see that s_3 is the common perpendicular of ℓ_1 and m_2: we obtain $s_3 \perp m_2$ from $\ell_2 \perp s_1$ by ρ^2, and we get that $s_3 \perp \ell_1$ by construction of ℓ_1. It is not difficult to see that what remains from S_0^3 when removing S_0^2 is a strip, namely $S(\ell_1, m_2, s_3)$, which is a copy of S_1. All these properties are illustrated by Figure 8.

At last, as m_3, m_2 and m_1 are defined from ℓ_2 by successive applications of ρ and as they successively define three copies of S_0, these copies do not overlap, *i.e.* the intersection of their interiors is empty.

Figure 7 also illustrates the splitting of S_0. Now, from what we have established and from the fact that a strip is obtained by removing a copy of S_0 from S_0, we obtain that a strip itself splits into a tile, a copy of S_0 and a copy of S_1.

This also can be seen on Figure 8: note that lines n_1 and ℓ_2 define a strip which splits into τ, the tile, S_0^1, a copy of S_0, and $S_0^2 \backslash S_0^3$ which is a copy of S_1 as it is $S(n_1, m_1, s_2)$.

From these remarks, we easily obtain:

Theorem 1 (see [4, 18]) – *The ternary heptagrid is a combinatoric tiling and the language of its splitting is regular.*

We refer the reader to [4, 18] for the details of the proof which are here omitted.

We note that for tiling $\{7, 3\}$, we can make use of the same Fibonacci tree as for the pentagrid, an important property found out in [12]. Accordingly, the same system of coordinates as for the pentagrid, see [12], can be used to locate the tiles of the heptagrid.

Above, Figure 9 indicates what we have to do in order to obtain the dual graph: on the figure, the edges which are added in order to get the dual graph of the pentagrid are indicated by red dotted arcs. The additional edges required for the heptagrid are indicated by blue dotted arcs in the same figure. These new edges of the graph correspond to the connections of a node with its immediate neighbour which are on the same level of the tree.

If we give number 7 to the side of the tile which is shared by its father and then if we go on the numbering modulo 7 turning counter clockwise, we

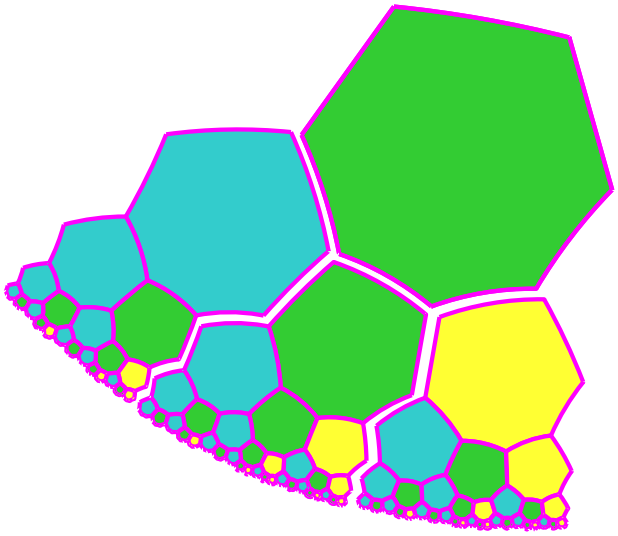

Figure 7 *The splitting of S_0 for tiling $\{7,3\}$.*

get that sides 2 and 6 in the case of a black node and sides 1 and 6 in the case of a white node are shared by another node on the same level of the tree.

This rule also holds for the nodes which are on the border of the tree: the corresponding neighbours belong to the next tree. On the left-hand border where we have black nodes, side 2 is shared by the white node which is on the right-hand border of the next tree, on the same level. Side 1 is shared by the father of this white node which is also a white node on the right-hand border of the next tree, but on the previous level. From this, we deduce that for a white node on the right-hand border of the tree, side 6 is shared by the node which is on the left-hand border on the next tree on the same level. Note that side 6 is shared by the left-hand son of this black node which is also on the left-hand border of the next tree, but on the next level.

3 The flowers and the mantilla

From now on, we are definitely in the tiling $\{7,3\}$. Flowers, as we shall define them soon, can be viewed as a grouping of tiles in *super-tiles* from which we define a new tiling of the hyperbolic plane.

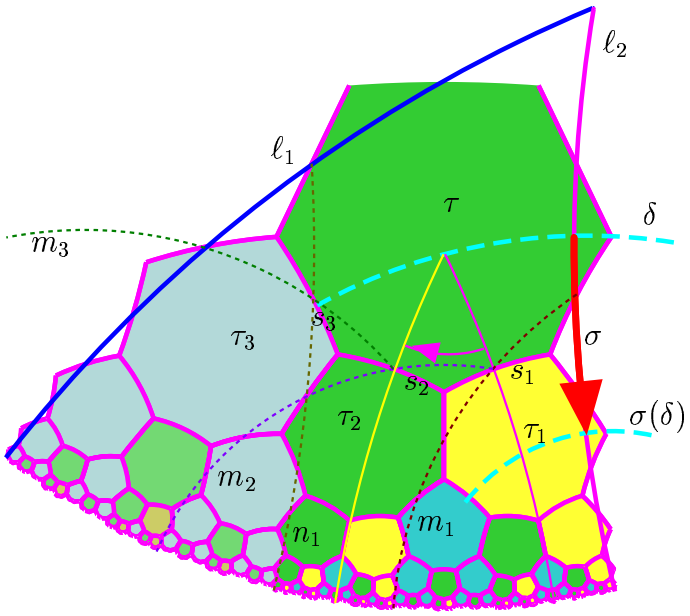

Figure 8 *The isometries defining the copies of S_0 for its splitting.*

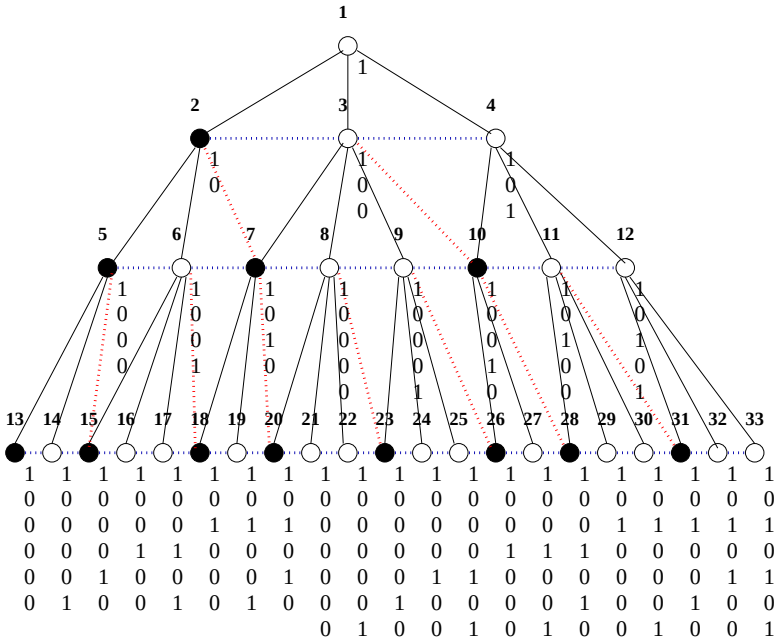

Figure 9 *Restoring the dual graph of the ternary heptagrid from its Fibonacci tree.*

3.1 The flowers

Remind that a **ball** is the set of tiles which are within a fixed distance from a fixed tile which we call its **centre**, where the **distance** of a tile to this centre is the number of tiles constituting the shortest path between the tile and the centre, the centre not being taken into account. The distance which defines the ball is called its **radius**. In what follows, we denote a ball of radius n by B_n. But as we shall be very often concerned by balls of radius 1 only, we give them a special name, we call them **flowers**.

We proved in our papers, and this will be published in a book to appear, that flowers tile the hyperbolic plane.

But here, we shall use another object in which we partially **merge** flowers. This will give rise to another way of tiling the ternary heptagrid which will be at the basis of our construction.

The idea of merging the flowers comes from the following consideration. Robinson's proof of the undecidability of tiling the Euclidean plane is based upon a simple tiling consisting of two tiles represented by Figure 10, below.

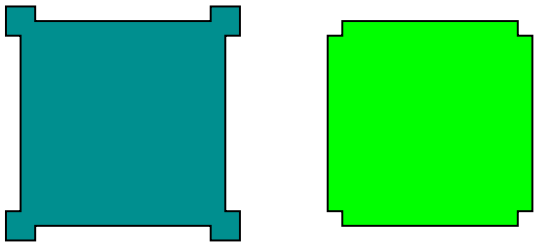

Figure 10 *Robinson's basic tiles for the undecidability of the tiling problem in the Euclidean case.*

In the Euclidean case, this fixes the tiling immediately and we refer the reader to Robinson's paper [28] to see the very nice consequences deduced from these simple tiles.

If we try to apply the same idea to the ternary heptagrid, we get the tiles of Figure 11.

It is not very difficult to see that this cannot work. Indeed, tile a requires seven copies of b around it and once we put three tiles a around a tile b, we arrive to an impossibility to go on.

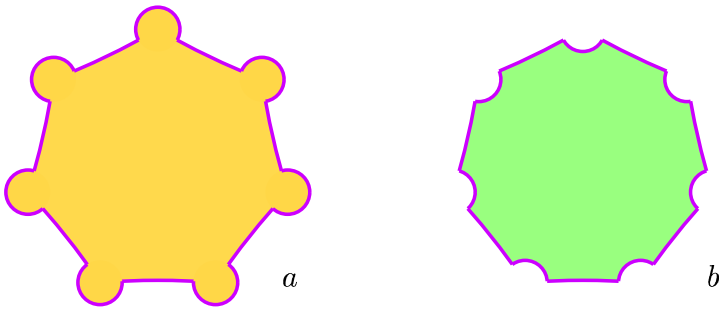

Figure 11 *A 'literal' translation of Robinson's basic tiles to the situation of the ternary heptagrid.*

However, it is not very difficult to change a bit the tile b to make things to work much better, perfectly well as will be seen later. Consider the new couple of tiles given by Figure 12.

This time we can see that we always must put seven copies of tile c around a tile a and that we need three copies of a around a tile c. Also, we can see that three tiles c abut around their untouched vertex.

What we shall call later the mantilla and the set of tiles which we shall later derive to represent it can be seen as a rigourous proof that there are tilings of the hyperbolic plane based only on tiles a and c of Figure 12. However, by contrast with the Euclidean case, we have here infinitely many such tilings, even continuously many of them.

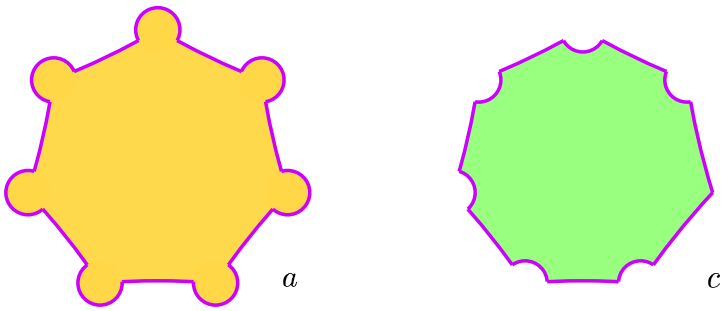

Figure 12 *An adaptation of Robinson's basic tiles to the ternary heptagrid.*

The seven copies of c around a tile a give immediately the idea of a flower. Also, we shall modify the representation in order to obtain strict *à la Wang*

tiles. Moreover, the tiles will abut simply, only requiring that abutting edges have the same colour.

Using the notion of flower, we introduce two kind of tiles: blank ones which, later on will be called **centres**, and the others will be called the **petals**. The tiles are represented by Figure 13. As can be more or less guessed, centres correspond to tile a of Figure 12 and petals correspond to tile c of the same figure. Petals can be seen as a *pedagogic* version of tile c: green and red marks indicate the edges where a petal abut with another petal, the other sides being shared with a centre.

The basic figure of the mantilla is the flower. Later, we will re-define the tiling in such a way that a condition will be put on the tiles: a centre may be surrounded by petals only; it cannot abut with another centre. A consequence of this constraint is that any petal belongs to three flowers and so, we can view petals and centres as meshes and holes of a vast crochet, whence the name *mantilla*.

It will turn out that there can be infinitely many mantillas if any. Indeed, we shall find an **algorithmic way** to combine petals and centres in order to get a tiling. We shall do this a bit later.

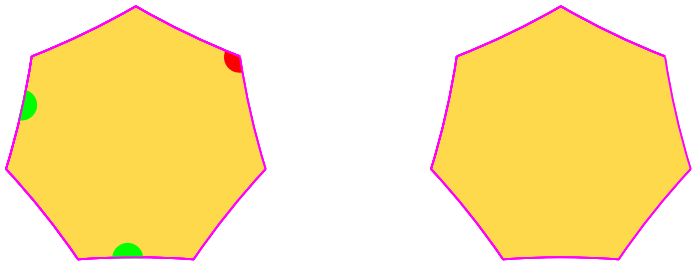

Figure 13 *The basic two kinds of tiles, translation of tiles a and c into dominoes.*

Assuming that solutions exist, let us investigate to what they look like. Considering a centre, it is not difficult to see that it is surrounded by centres, not immediately but at a small distance. Indeed, the first row of surrounding tiles are petals but on the second row, centres necessarily appear. Note in Figure 16 that the red vertex of three petals must be glued together. This will define the **red vertices** of the configurations we shall study. Also, two green dots are connected by the sides of two neighbouring petals. Accordingly, we say that the corresponding side is **green**. Now, we note that red vertices

are always at the end of a side where the other belongs to the border of a centre. We shall say that the considered red vertex is **at distance 1** from this centre. Note that any red vertex is always at distance 1 of exactly three distinct centres.

Lemma 1 *A petal can abut at a blank edge only with a centre. Two petals can abut either by their red-vertex and an edge of this vertex or by an edge with a green mark.*

Proof of Lemma 1. If we consider a petal, it cannot abut with itself or with another one by the blank edges. To see this point, we fix one petal and an edge and we make the other rotate three times in order to present all its blank edges to the chosen blank edge of the fixed petal. As we can see in Figure 14, in two cases, this would require a tile where two adjacent edges bear a green mark, which is impossible. In the remaining case, it would require a tile with an edge marked by a green side and an adjacent edge with, at the non-common vertex, a red vertex. This is also impossible.

The possibilities between two petals are indicated by Figure 15.

From Figure 15 which indicates the way of how petals can be connected we can see that the number of centres of the second row ranges in the interval $\{7..10\}$. Call **centre ring** the set of centres in the second row of tiles around a given centre. The centre defining the centre ring is again called the **centre** of the centre ring or simply centre if no confusion may arise. Then, it can be noted that the number of elements in the centre ring is directly connected with the number of red vertices which are at distance 1 from the centre of the centre ring. The correspondence is given by the following formula:

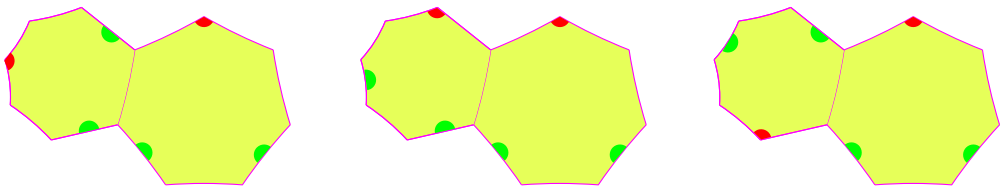

Figure 14 *The three ways of abutting petals along blank edges: in all cases, it is impossible.*

$$\#centres = \#red\_vertices + 7$$

This comes from the fact that a green side connects directly two centres, and that a red vertex is at distance 1 of three centres and for each of these three centres, both remaining centres belong to its centre ring. Accordingly, a red vertex generates 2 centres of the centre ring while a green side generates 1. Now,

$$\#red\_vertices + \#green\_sides = 7$$

and so,

$$\#centres = 2\#red\_vertices + \#green\_sides = \#red\_vertices + 7.$$

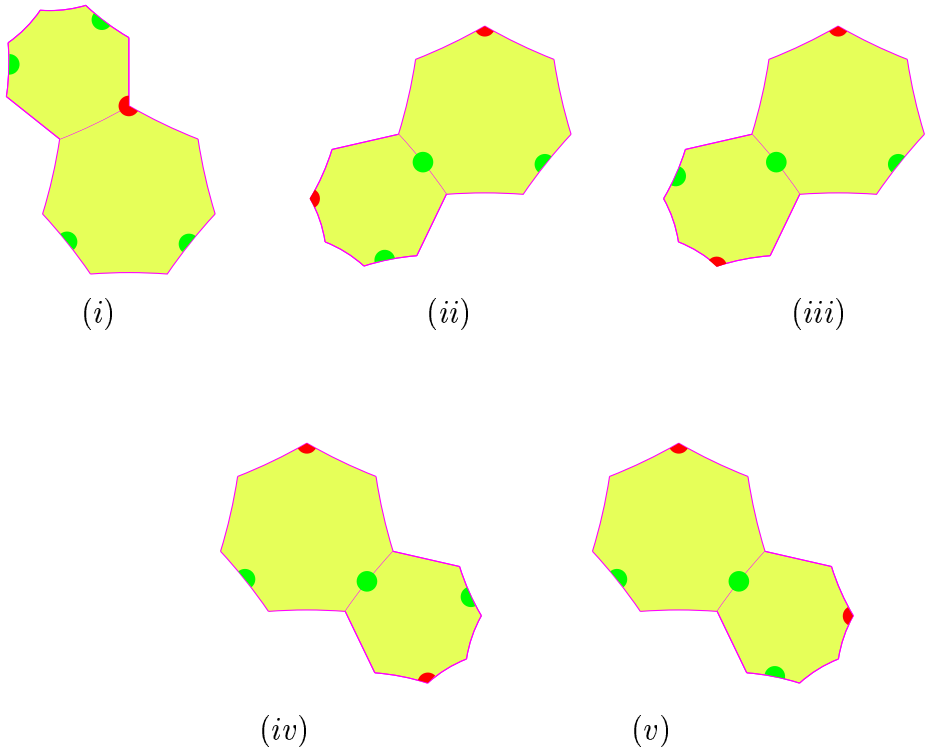

Figure 15 *There are six ways to correctly abut two petals. The three basic ones are indicated by* (i), (ii) *and* (iii). *The others are obtained by reflection in the vertical axis of the big heptagon. In this figue,* (iv) *and* (v) *are obtained in this way from* (iii) *and* (ii) *respectively.*

Next, it is not very difficult to see that there cannot be tilings where all centres have a centre ring of 7 elements or all centres have a centre ring of

10 elements. Indeed, if a centre is surrounded by seven green sides, then any element of its centre ring has at least two red vertices at distance 1 and so, the corresponding centre has a centre ring with at least 9 elements. The same remark applies also to a centre whose centre ring contains 8 elements. And so, there cannot be tilings of this kind where centres are all centres of a centre ring with 8 elements.

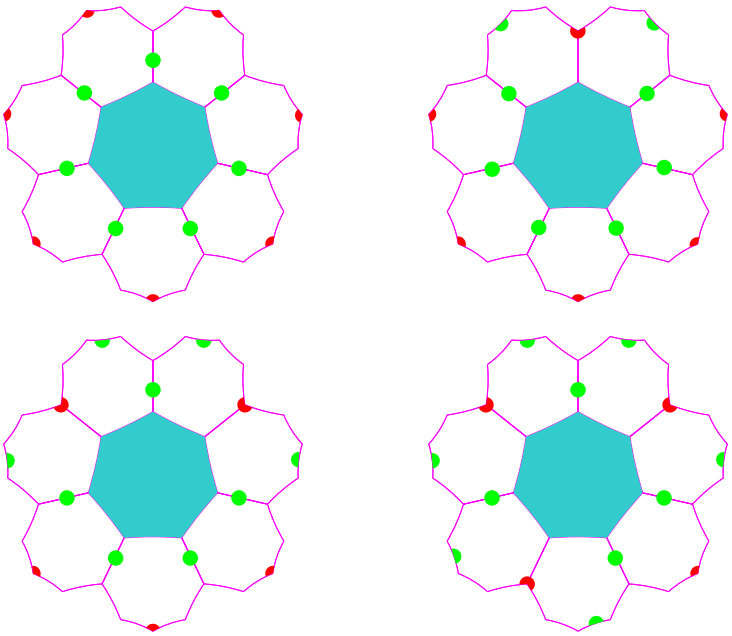

Figure 16 *Flowers with, respectively,* 7, 8, 9 *and* 10 *centres in their centre ring.*

It remains to see that all centres cannot have a centre ring with 10 elements. Indeed, consider a centre with a centre ring of 10 elements. As a red vertex at distance 1 of a centre defines two green sides in contact with the centre, the 3 red vertices of such a flower are separated either by a single green side touching the centre of the flower or by two such green sides. Now, consider two red vertices of a centre surrounded by 10 centres which are separated by a single green vertex. This green vertex connects the centre of the considered centre ring with another centre C. Now, from what we said, C has 3 consecutive green sides around itself and so, it cannot be the centre of a centre ring of 10 elements.

I don't know whether all centres can be surrounded by a centre ring of 9 elements. My conjecture is that this is the case, but I could not construct such a tiling algorithmically.

3.2 The mantilla

On the other side, we have the following:

Lemma 2 *There is a tiling of* $\{7, 3\}$ *with the petals and centres such that all flowers of the tiling have a centre ring of* 9 *elements or of* 8 *elements. Moreover, it is possible to algorithmically construct such a tiling.*

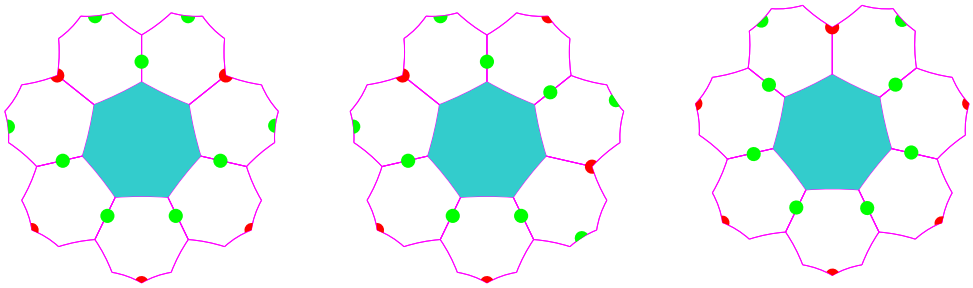

Figure 17 *The flowers of the mantilla : they consist of flowers with* 8 *or* 9 *elements in their centre ring. Note the representation of* **F-** *and* **G-flowers** *for the flowers with* 9 *centres.*

In this proof, we distinguish between flowers with 9 elements in a centre ring as there are two different possible patterns, see Figure 17. Indeed, the two red vertices of the flower may be separated by one green edge or by two, considering the shortest number between them in the centre ring. We call **F-flowers** the flowers for which the two red-vertices are separated by only one green edge. We call **G-flowers** the others: their red vertices are separated by two green edges. We shall call **8-flowers** the flowers with 8 elements in their centre ring.

Proof of Lemma 2. The proof consists in showing that the new tiling can also be generated by the splitting method. This is performed by induction.

Below, Figures 18, 19 and 20 indicate how we split F-, G- and 8-flowers. In the case of an F-flower, we call **parental petals** the petals of the flower which are between the two red vertices, considering the minimal possible number.

In the case of a G-flower, the parental petals are also taken among the three petals which realize the shorter path between the main two red-vertices of the flower. The central petal of this triple is a parental petal, call it p. The red vertex of p defines two centres which are in contact with the triple.

By induction on the splitting, we shall show that one of these two centres defines an 8-flower. The other non-parental petal of the G-flower is the petal which belongs to this 8-flower.

In the case of an 8-flower, the parental petals are the two petals which are in contact with the single red vertex.

Important convention: from now on, if not otherwise indicated, we shall not mention green sides, only red vertices in order to make the figures more easily readable.

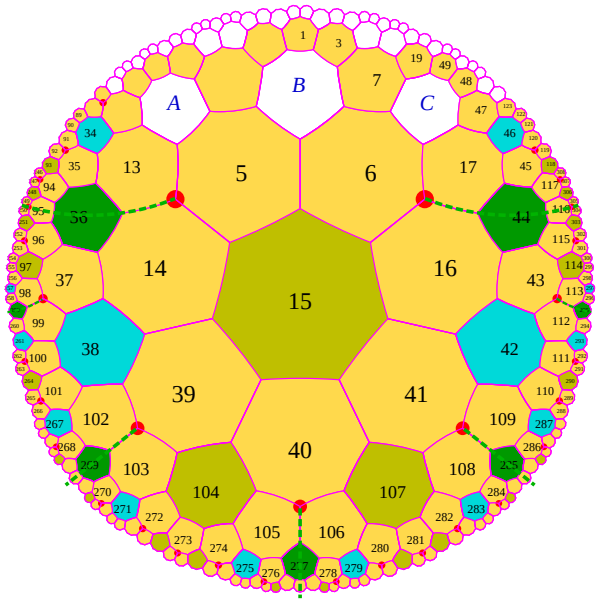

Figure 18 *Splitting the sector associated to an F-flower of the mantilla.*

In the case of F- and G-flowers, the splitting is defined as follows: let β_ℓ be the line which supports an edge of the non-parental petal sharing the left-hand red vertex and which is not in contact with the centre. We define β_r to be the reflection of β_ℓ in the bisector of the segment which joins the two red-vertices of the flower. We call F- or G-**sector** the region delimited by β_ℓ, β_r and the lower border of the non-parental petals of the considered flower.

Note that we have two kinds of G-flowers: left-hand side and right-hand side flowers, depending on the side of the 8-flower which is in contact with a parental flower. However, a G-sector is symmetric.

In the case of an 8-flower, let u and v be the parental petals and let p and q be the non-parental neighbouring petal of, respectively, u and v. Denote

by A the red vertex of p and by B the one of q. Note that B and q are the respective reflections of A and p in the line σ which passes through the red-vertex of the 8-flower and through the mid-point O of its centre.

Define the line which starts from O and which passes through A. Then denote by β_ℓ the ray on this line which is issued from A and which does not cut the centre of the flower. Symmetrically, define β_r to be the reflection of β_ℓ in σ. The **8-sector** is defined by β_ℓ and β_r and by the part of the lower border of the non-parental petals of the flower which falls inside inside the angular sector defined by β_ℓ and β_r.

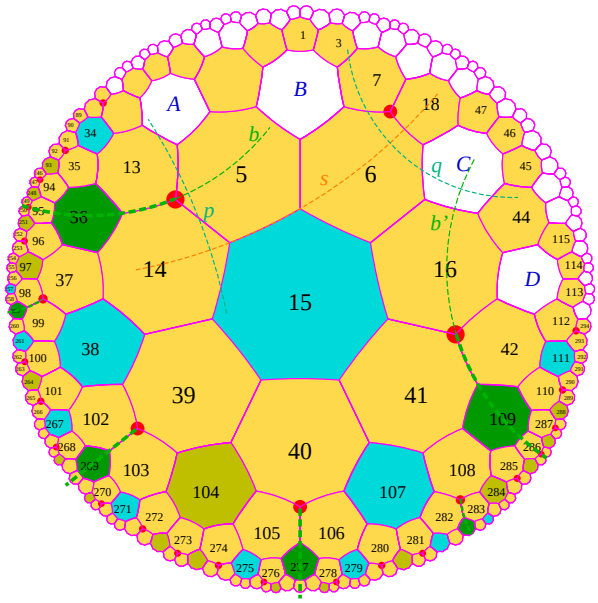

Figure 19 *Splitting the sector associated to a G-flower of the mantilla.*

We note that the parental petals also belong to another flower. They both belong to the same other flower in the case of an F-flower. They belong to different flowers in the cases of a G- or an 8-flower.

Note that the distinction between parental and nonparental petals introduces the notions of **top** and **bottom** in a flower of the tiling. In section 4.2.2. we shall come back to this point by the introduction of the notion of **levels** of the mantilla. In the above Figures 18, 19 and 20, we say that the central tile is the **head** of the sector.

It is not difficult to see how the splitting indicated in each case of Figures 18, 19 and 20 can go on *downwards*, from the non-parental petals of

the flower. The non-parental petals of the central flower of the pictures in Figures 18, 19 and 20 induce the flowers which are the head of the sectors into which the above sectors can be split.

In the case of an 8-flower, the splitting defines four sectors exactly. We consider that the G-flowers which appear outside the sector and around its head are defined by another flower: this property also belongs to the induction hypothesis. Also by induction, we will check the following property. Consider the three centres which are around a red vertex. Then, exactly one of them is the centre of an **8**-flower. The others are either both centres of F-flowers or one centre is from a G-flower, the other from an F-flower.

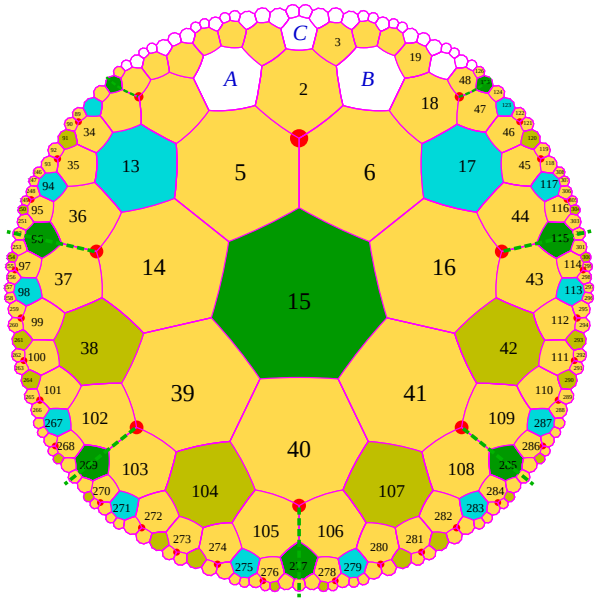

Figure 20 *Splitting the sector associated to an* 8*-flower of the mantilla.*

In the case of F- and G-flowers, beyond the side of the G-sector which is not shared by an F-sector, we have the half of an 8-sector: a right-hand half on the left-hand side and a left-hand half on the right-hand side.

Accordingly, as half- and right-hand sides are isometric, the splitting can be given by the following rules:

$$\begin{aligned} F &\longrightarrow 2F,\ 2G,\ 2\times\frac{1}{2}\mathbf{8} \\ G &\longrightarrow F,\ 2G,\ 2\times\frac{1}{2}\mathbf{8} \\ \mathbf{8} &\longrightarrow 4F \end{aligned}$$

For counting the elements of the spanning tree on the same level, we may replace 2 halves of an **8**-sector by a whole sector and so we get the following matrix:

$$\begin{matrix} 2 & 2 & 1 \\ 1 & 2 & 1 \\ 4 & 0 & 0 \end{matrix}$$

and so, the characteristic polynomial P of the splitting is:

$$P(X) = X^2 - 4X - 2.$$

We note that it is a Pisot polynomial whose greatest real root is $2 + \sqrt{6}$.

At this point, we note that we have a tiling of any sector, neglecting the fact the borders of a sector may involve half-tiles: we know that such halves will be completed by another sector which must necessarily be present.

Now, to tile the plane, we use the argument of [18]: consider a sector whose head is a flower **F**. The parental petals of **F** are non-parental petals of another flower **H**, **higher** than **F** in the tiling. It is clear that the sector Σ defined by **H** contains the sector defined by **F** as a sub-sector in the above tiling of Σ. Call **H** a **completing** sector of **F**.

It remains to prove that, whatever the choices are for the completing sector of the head of a given sector, we obtain a sequence of sectors whose union is the hyperbolic plane.

To prove this point, define the **augmented** sector of a given sector S to be the union of the sector and its heading flower, its parental petals being ruled out. Let B_n be the greatest ball around a once for all fixed origin O, contained in an augmented sector. Then, by completing the sector, we define a new sector of the splitting which, when augmented, contains S and B_{n+1} around O.

First, consider the case of an F-flower **F**. Figure 18 indicates three centres which share a petal with **F**. Call them A, B and C, from the left to the right in Figure 18.

Taking into account the already realised splittings, as the red-vertex shared by tiles 13, 5 and 14 is at distance 1 of the centre A and the 8-centre situated at tile 36, A cannot be the centre of an **8**-flower. It may be the centre of a 9-flower, either F or G. The same conclusion holds for C. Now, the following chains of consequences hold as the reader can easily check it:

$$\begin{aligned} A = F &\Rightarrow B = 8 \Rightarrow C = G \\ &\qquad\quad\ \Rightarrow C = F \\ &\Rightarrow B = F \Rightarrow C = G \\ A = G &\Rightarrow B = 8 \Rightarrow C = F \\ &\Rightarrow B = F \Rightarrow C = F \\ &\Rightarrow B = G \Rightarrow C = G \end{aligned}$$

We could also start with B and the above chains also indicate the possible choices: we note that B may be any kind of centre. But once it is fixed, it also fixes the choices for A and B when B is the centre of a G-flower, and we have two solutions in both cases when B is the centre of either an **8**-flower or an F-flower.

In all these situation, as tiles 5 and 6 in Figure 18 belong to the sector headed by B, the ball obtained from B_n by appending a new level of tiles is also in the sector. And this new ball is exactly B_{n+1}. And so, our claim is proved in this case.

Next, consider the case of a G-flower which is illustrated by Figure 19.

In this case, we have to discuss the situation of four centres denoted by respectively A, B, C and D in the figure.

It is not difficult to note that A and D are occupied by the centre of an F-flower. Indeed, A cannot be the centre of an **8**-flower, because there is already such a centre at distance 1 from the red vertex shared by tiles 13, 5 and 14 in Figure 19. Also, A cannot be the centre of a G-flower as there cannot be two adjacent G-sectors in the splitting of any sector. And so, A must be the centre of an F-flower. By symmetry of the figure, this is also the case for D.

Now, the possible cases for B and C are indicated by the following diagram:

$$\begin{aligned} B = 8 &\Rightarrow C = F \\ &\qquad\ C = G \\ B = F &\Rightarrow C = 8 \\ B = G &\Rightarrow C = 8 \end{aligned}$$

It is not difficult to check that, in all these cases, tiles 36, 13, 5, 6, 16, 42 and 109 do belong to the new appended augmented sector, either in B or in C and so, accordingly, the new augmented sector contains B_{n+1}.

At last, we remain with the case of an **8**-sector which is illustrated by Figure 20.

Here, we have the union of the four F-sectors defined by its splitting. The augmented sectors contains tiles 14, 15 and 16, as it can easily be checked.

As the red vertex shared by 5 and 6 is at distance 1 from the centre of the considered **8**-flower, A and B cannot be the centre of an **8**-flower as they are at distance 1 from this red vertex.

This leaves four cases a priori. But A and B cannot be both centres of a G-flowers, as two G-sectors cannot be adjacent. And so we remain with three cases: A and B are both centres of an F-flower, or A is the centre of a G-flower and B that of an F-flower or, conversely, B is the centre of a G-flower and A that of an F-flower.

In all cases, tiles 5 and 6 also belong to the union of the new augmented sectors and so, whatever which tile is next appended in C, it is the centre of a flower and the considered tiles together with 36, 13, 17 and 44 are in the sector defined by C.

And so, the following property is proved:

Lemma 3 *Completing a sector S by any of the possible centres which will give rise to a new sector Σ in which S enters its splitting, in at most two steps of such a completion, if S contains the ball B_n around a fixed in advance tile T, Σ contains the ball B_{n+1} around T.*

With this property, the proof of Lemma 2 is completed.

■

The tiling constructed in the proof of Lemma 2 is called the **mantilla**.

4 The partial problem

In this section, we provide the reader with an alternative solution of the partial problem. We remind the reader that the partial problem consists in fixing the first tile. It is well known that in the 1978 paper of Robinson mentioned in the introduction, see [29], there is a solution of the partial problem. As this solution deals with hexagons or quadrangles, it is not immediately suitable for our purpose. Accordingly, I here indicate a solution of my own which will be used for the generalized origin-constrained problem we consider. It is different in its spirit from Robinson's and it is adapted

to tiling $\{7, 3\}$ while Robinson's proof works only for to other grids of the hyperbolic plane, namely $\{4, 5\}$ and $\{6, 4\}$.

4.1 The harp

In this section, we first describe the setting in which we define a solution of the partial problem. We still consider the ternary heptagrid but now, taking advantage that the first tile is fixed, we inscribe it in a context which we force, thanks to the first tile.

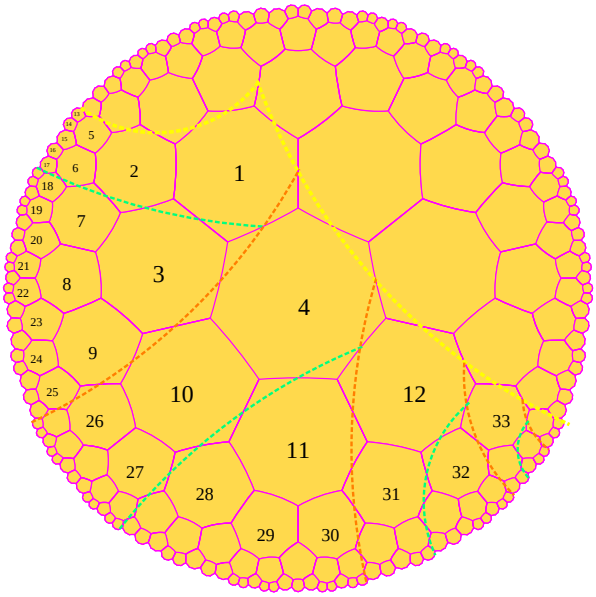

Figure 21 *The guidelines for the harp.*

In Figure 21, we illustrate the basic construction of our solution to the partial problem.

Indeed, the idea is to build a **harp** or a 'comb' in which we unfold the space-time diagram of the computation of a Turing machine. Without loss of generality, we may assume that during the computation of the Turing machine, the head never goes to the left of a cell which we call the leftmost position. Such a restriction is familiar and it is also used in Robinson's proofs for the Euclidean problem. The cells of the Turing tape will be represented by the **chords** of the harp. The time is represented by the levels of a Fibonacci tree and the head will go along levels during its travel from one cell to the

next one. After visiting a cell, the head will go down by one level as required in a space-time diagram.

The construction is based on a splitting which is different from the one used traditionally for the pentagrid or for the ternary heptagrid.

To this goal, we remember a notion which we used in [3, 18]. Call **mid-point line** any line d which joins mid-points of the edges of the tiling in such a way that if A and B are consecutive mid-points of edges of the tiling on d, A and B belong to consecutive edges of a tile, see Figures 21, 43 for an illustration. It was proved in [3, 18] that when two such mid-point lines meet at a vertex A, it is possible to define a Fibonacci tree in the angular sector determined by the smallest angle α defined by the lines. We call this **angular sector of the ternary heptagrid**. Most often, we shall say **angular sector** for short.

We split the initial angular sector S_0 into three regions: a **strip** C_0 which is the union of a strip as defined in section 2 and the leading tile of the sector; and two copies of the sector itself, U_0 and S_1. These copies are dispatched as indicated in Figure 21: C_0 is headed by the tile 1 and it is delimited by a yellow line β and a green line γ. Inside the strip we have, for the first two levels: the tiles 2, 5 and 6. The first copy of the sector, U_0 delimited by the line γ and an orange line δ. In the figure, U_0 is headed by tile 3 and the first level of its spanning tree consists of the tiles 7, 8 and 9. At last, S_1 is the remaining part of S_0. It is delimited by δ and by β_2, the other line delimiting S_0.

As shown in Figure 21, we repeat the splitting of S_0 in S_1 and, recursively, we define S_{n+1} by splitting S_n as we did for S_0 and by defining S_{n+1} as the second copy of S_0 in this splitting. Let C_n be the strip of S_n. Using the already introduced terminology of Fibonacci trees, consider that all the tiles which are intersected by the line which delimits the strip on its left-hand side are black nodes: this is what we call a **chord**. This choice of the status of the head of C_n automatically defines the status of the tiles inside C_n and inside U_n, the fist copy of S_0 inside S_{n-1}. Accordingly, the head of U_n is a white node. Repeating the construction inside S_{n+1}, we obtain that each leading tile of the S_n's are black nodes. An illustration of the chords is given by Figure 22.

4.2 The tiles for the harp

Our next task is to define tiles which can represent a sector and the chords of its harp. This is given by Figure 23 where six tiles are given.

The tiles have coloured edges which are represented by coloured strokes perpendicular to the edges. The leftmost tile of the first row of Figure 23 is marked with 1: it is the tile which must be first used. It is the root of the tree. It bears three strokes only: two for its sons and one for a nephew, the right-hand neighbour of its right-hand son on the same level of the tree. On the same row, we find the tiles for the borders. On the middle of the row, the tile for the leftmost border which consists of black nodes. It has no connection with a left-hand neighbour on the same level, nor with its left-hand uncle. Then, still on the first row, we have the tile for the right-hand border. It has no mark for the father and no mark for the right-hand neighbour on the same level. Later on, we shall speak of strokes only and we shall say **blank edge** for an edge which bears no stroke and **marked edge** for the one who bears a stroke.

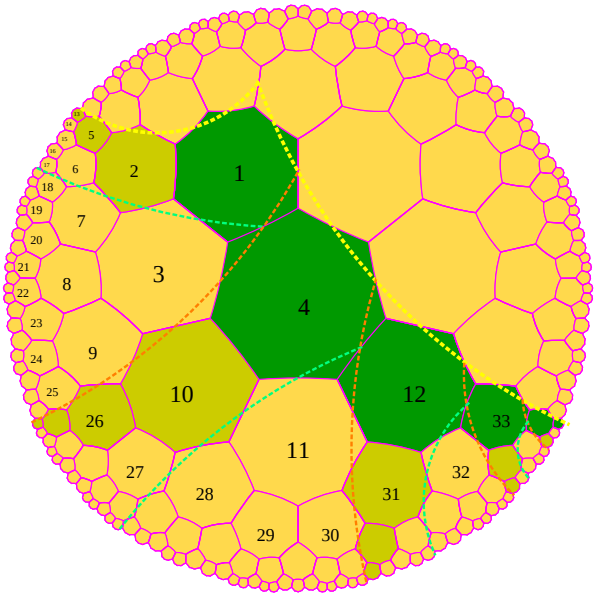

Figure 22 *The chords for the harp.*

On the second line, we have the tile for the chords: it is a black node with thick marks for the father and the son. Then we have the tile for black nodes and the tile for white ones.

Indeed, we have to prove that this set of tiles necessarily generates our tree, once the tile marked with 1 is put.

To this aim, first number the tiles from 1 up to 6, from the leftmost tile of the first row to the rightmost tile of the second row. Later, we denote tile i by $\textcircled{i}$.

First, we prove that tile $\textcircled{1}$ cannot abut with itself on its marked edges. The dark purple stroke cannot match with itself: looking at the blank edges, we can see that no tile can match in this way because of the position of the red stroke in the second copy of $\textcircled{1}$. The red stroke cannot abut with itself as by the fact that translations and rotation only are allowed, there is no tile with contiguous large blue and dark purple strokes. At last, the large blue stroke cannot abut with itself: this would require a tile with a red stroke contiguous to a blank edge.

Now, let us look at the dark purple stroke. As it cannot match with that of $\textcircled{1}$, it may match with one of $\textcircled{3}$. As a red stroke has no contiguous blank edge, it cannot match with the dark purple stroke of $\textcircled{3}$ which is adjacent to the red stroke. And so, it can only match with the dark purple stroke of $\textcircled{3}$ which is adjacent to the green stroke. And so, we could assemble $\textcircled{1}$ together with $\textcircled{3}$ in a unique way.

At this stage, we assume $\textcircled{1}$ and $\textcircled{3}$ assembled together as just indicated. Now things are easier. The red stroke of $\textcircled{1}$ and the green stroke of $\textcircled{3}$ force the matching with $\textcircled{6}$ as the single possibility. Assume that $\textcircled{6}$ is appended to the assembled tiles in the indicated way. Now, to complete the common vertex of $\textcircled{1}$ and $\textcircled{6}$ which is not yet so, we could put $\textcircled{2}$ or $\textcircled{4}$. But $\textcircled{4}$ requires a tile where a red or a light purple stroke is adjacent with a blank edge. And so, we can assemble only $\textcircled{2}$. Accordingly, we assembled the root and the first level of the tree.

Note that if we started with the large blue stroke of $\textcircled{1}$, a similar argument works. This large blue stroke cannot match with that of $\textcircled{3}$ as there is no red stroke contiguous to a blank edge. But it also cannot match with the large blue strokes of $\textcircled{4}$ for the same reason for the blue stroke of $\textcircled{4}$ which is contiguous to a red stoke. It cannot match with the other large blue stroke of $\textcircled{4}$ for a similar reason: there is no light purple stroke which would be contiguous to a blank edge. And so, the large blue stroke of $\textcircled{1}$ matches with the large blue stroke of $\textcircled{2}$ which is contiguous to a green stroke. Then the assembly of the first level goes on easily, as above.

By induction, assume that we assembled the tree up to level k, all nodes on this level being included. In this assembly, the root being excepted, the

left-hand border consists of copies of (2) only and the right-hand border of copies of (3) only. Also, we assume that for the other nodes of the assembled tiles, black nodes are represented by copies of (5) and them only, the chords being excepted, which are represented by copies of (4). We also assume that all white nodes are represented by copies of (6) and them only.

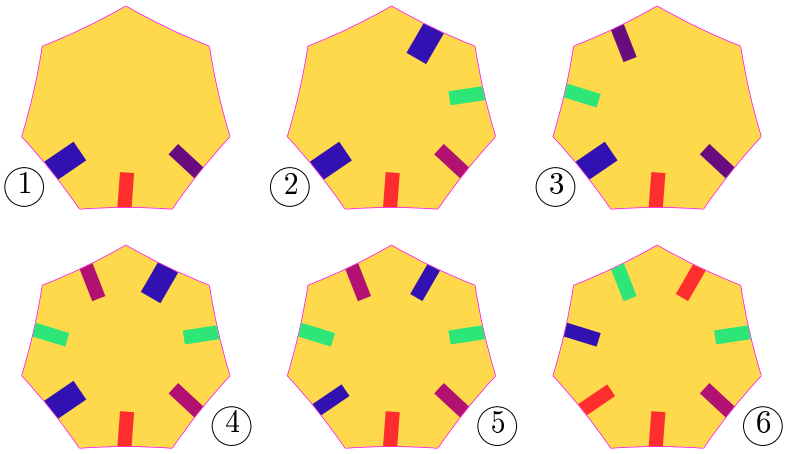

Figure 23 *The tiles for the harp. On the first row, to the left, the root of the tree. Then, on the same row, the tiles for the leftmost branch and then for the rightmost one. On the second row, to the left: the tile for the chords. Then the tile for the block nodes and then, for the white ones.*

Consider level $k+1$. First look at the first and second nodes on level k starting from the left-hand side of the level. By induction, we have a copy of (2) and of (6), respectively. We note that the tile which completes the non completed common vertex of (2) and of (6) is necessarily a copy of (5) because of the adjacent light purple and thin blue strokes. This copy of (5) being assembled, it requires a copy of (6) to match with the red stroke of (2). Once we assembled this copy of (6), the large blue stroke of (2) requires either a new copy of (2) or a copy of (4). But the same argument with the root works here also: (4) would require a tile with light purple stroke adjacent to a blank edge and such a tile does not exist. Now, we proved that the sons of the first node of level k can be assembled in a unique way and that it is also the case for the first son of the second node of level k. With white nodes, the green strokes force the correct tile to be assembled and now, it is easy to see, by induction on the rank of the node on level k, that its sons can also be assembled in a unique way. The situation is a bit different with the last

node. In this case, as we are at the last node of level $k+1$, we need a tile which must match with a copy of (6), the previous node on level $k+1$, and a copy of (3), the last node of level k. For the same reason as with the root and the copy of (3) on the first level, the dark purple stroke of the copy of (3) on level k cannot accept a copy of (1) nor the stroke of (3) which is adjacent to a red stroke. Accordingly, only a copy of (3) in the expected position can match and this completes our first part of the proof.

It is also easy to check that the chord is generated by copies of (2) for the leftmost chord and of (4) for all the others and only by these tiles.

At this moment, we can see that the tree and it only can be constructed in this way, but we did not look at what we can put to the left of the left-hand border or to the right of the right-hand border.

To this aim, we go back to the root and look at how we can complete its blank edges. Only the copies of tiles (1), (2) and (3) can be used. In fact they all can contribute and, as we shall soon see, there are infinitely many solutions.

The first think we can note is that the tiles have a top and a bottom. For tiles of the first row of Figure 23, the bottom consists of the edge with the red stroke and the top consists of the two opposite edges. This definition also holds for tiles (4) and (5). For tile (6), the bottom is the edge with a red stroke with another red-stroked edge to the left and a light-purple-stroked edge to the right. Now, we note that tiles (2) and (3) have blank edges which can match together. Also tiles (2) can be assembled by their blank sides. The same remarks also holds for tiles (3).

Accordingly, a first solution consists in placing four roots around the first one we considered. As it can be noted in Figure 24, five trees dispatched in this way do not cover the plane: they are numbered from I up to V in the left-hand picture of Figure 24. There is still room for a sixth one, whose root is at distance 1 from the initial root which we placed there, between sectors I and V in the left-most picture of the figure.

On the right-hand picture of Figure 24, we moved sector VI by a counter-clockwise rotation of $\frac{2\pi}{7}$. This entails a small change in sectors IV and V. The same transformation can be repeated, to create sector VI between sectors III and IV, or II and III or I and II. This gives us five different solutions. Now, on both pictures of Figure 24, we can see that at least one mid-point line is complete. Now, it is not difficult to note that the tiles which are cut by this line are always cut at blank edges. This means that we can make each

half-plane defined by this line move independently of each other along this line. Or, which is the same, we can decide to fix one, for instance the half-plane containing sector I, and to make the other move along the line. For each mid-point line, this provides us with infinitely many solutions indexed by $\mathbb{Z}$. Let us call them IV_n, V_n and VI_n for instance, taking the case of the yellow line of the right-hand picture of Figure 24 as an example.

There are also two other solutions attached to a mid-point line: in the just considered example, one such solution is obtained by taking the limit of IV_n, V_n and VI_n as n tends to $+\infty$, the other by taking the limit as n tends to $-\infty$. In both cases, the limit corresponds to a half-carpet in the sense of Fibonacci carpets as defined in [18]

Before turning to the Turing computation, let us note how the tiles belonging to the chords can algorithmically be characterised. Indeed, it is not difficult to locate them thanks to their coordinates.

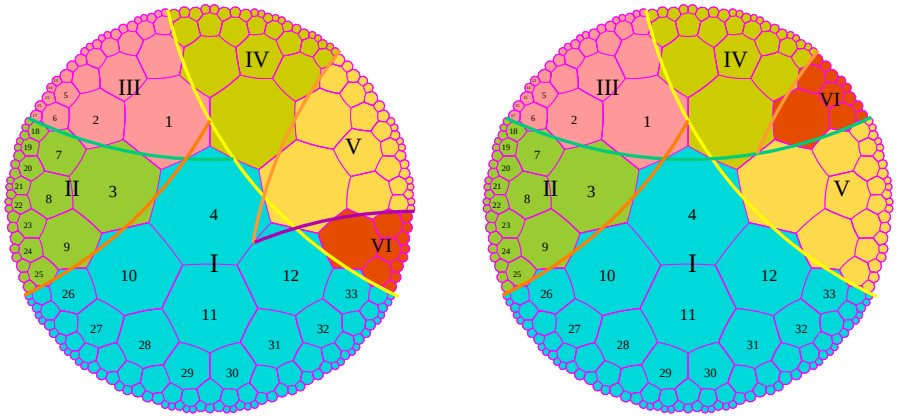

Figure 24 *The possible solutions around the initial root, tile* 4 *in the figure.*

To this purpose, note that in the splitting represented by Figure 21, sector S_1 is obtained from the initial sector S_0 by a shift along the right-hand mid-point line defining the sector, namely the shift which transforms tile 1 into tile 4. Accordingly, under this shift, the level k of the tree T_0 spanning S_0 is transformed into the level $k{+}1$ of the tree T_1 which spans S_1. Now, we know that the level k of the Fibonacci tree contains f_{2k+1} nodes. Hence, the level $k{+}1$ contains f_{2k+3} nodes. Now, by definition of the Fibonacci sequence, $f_{2k+3} = f_{2k+2}{+}f_{2k+1}$. And so, the image of the level k of T_0 under the shift in T_0 itself consists of the last f_{2k+1} nodes of the level $k{+}1$ of T_0. Now, the first node on the level k of T_0 has number f_{2k} and the first node on the level $k{+}1$

has number f_{2k+2}. The number of the root of T_1 is 4 in T_0, whose coordinate is 101, and $4 = f_3 + f_1$. By induction on k, assume that the first node ν_k on the level k of T_1 is $f_{2k} + f_{2k+3}$ whose coordinate is 10010^{2k-1}. Then, from the preferred son property of the Fibonacci tree, see [12], as T_1 is also a Fibonacci tree, ν_{k+1} is the preferred son of ν_k. Accordingly, from [12], the coordinate of ν_{k+1} is 10010^{2k+1} which represents $f_{2k+2} + f_{2k+5}$. And so, the induction hypothesis is proved.

We have now the coordinates of the nodes on the chord.

Lemma 4 *If x runs over the coordinates of the nodes of the level k in T_0 which belong to a chord, the coordinates of the nodes of the level k+1 in T_0 which belong to a chord are $10x$, where the writing of x is taken with $2k$+1 digits, possibly padding 0's to the left, to which we have to append the node of coordinate 10^{2k+1}, the first node of the level k+1 in T_0.*

4.3 The Turing computation

Now, we turn to the tiles which represent the computation of a Turing machine. We represent them by the set of tiles of Figure 25 which we call the **set of prototiles** for the partial problem, after the terminology introduced by Berger in its proof.

Let us explain in detail how the prototiles work.

Figure 25 contains 17 tiles which are based on the six tiles used for the construction of the harp. The first five tiles, (a), (b), (c), (d) and (e), simply assume the transportation of the signals of the space-time diagram of the Turing machine: the content of the cells and the state of the head. The other tiles implement the execution of the instructions of the Turing machine.

Starting from the root represented by tile (r), the computation goes on by tile (k) as the head of the Turing machine cannot go the left of the first cell. As we may assume that the head of the Turing machine always move, then it must move to the right. In the general case, an instruction is triggered by the meeting of a state signal with a cell signal. This means that the signal of the Turing head meets a chord which bears the cell signal. The tile where the meeting takes place is represented by one of the other tiles, tiles (h) and (k) being excepted. The general case, when the head is inside the tree is represented by tiles (f), (g), (i) and (j). Indeed, we have four cases as we take into account the direction from which the state signal arrives to the

meeting tile and to which direction the new state goes. Accordingly, tiles (f) and (i) deal with signals arriving from the left while tiles (g) and (j) are concerned by a signal which arrives from the right. Symmetrically, tiles (f) and (g) deal with the signal of a new state going to the left while tiles (i) and (j) deal with the signal of a new state going to the right.

At this point, we have to remember that for the next meeting with a chord, the head must go down by one level deeper. This is performed by the above tiles: the motion to the right is sent to the red son of the chord tile which is a black node. The motion to the left is sent to the blue son which corresponds to a black node and, in this case, which is also a tile of the chord. However, there is no danger with confusing this tile with an instruction tile as in an instruction tile the state signal always arrive through an edge with a green stroke. Once the new state signal arrives to the next level, tile (k), when the move is to the right, or tile (h), when it is to the left, sends the new signal to the neighbouring tile on the same level and in the expected direction. Another way to see this point is to note that the new state enters its new level through the father edge of the next tile, while in an instruction case, the state arrives by a neighbour edge.

The tiles of Figure 25 are called **prototiles** because they are not the actual tiles for a given Turing machine. They are simply the patterns followed by the actual tiles. In the actual tiles, the symbols a, b, p, q and s which occur in Figure 25 are replaced by actual states and tape symbols taken from the table of the Turing machine. In this regard, the set of prototiles of Figure 25 could be called a **protoset** of prototiles. The only actual symbol which is present in Figure 25 is B which represents the blank of the Turing tape. This symbols occurs in tile (k) as it is the root and also in tiles (m) and (n) as they deal with the right-hand border of the tree.

The right border represents the body of the harp and, from the point of view of the simulation of the Turing computation, it represents the successive initialisation of the cells of the tape. Recall that we have to simulate a Turing machine which starts its computation form an empty tape. And so, the tiles of the right-hand border propagate the blank which is the initial content of any chord. In the construction, the blank signal is always present on the right-hand border when a state signal arrives to it, necessarily from the left. We remark that for the left-hand border, we have a single tile, (ℓ), which corresponds to the required property that the head of the Turing machine never goes to the left of the initial leftmost cell which is represented by the first chord in the simulation.

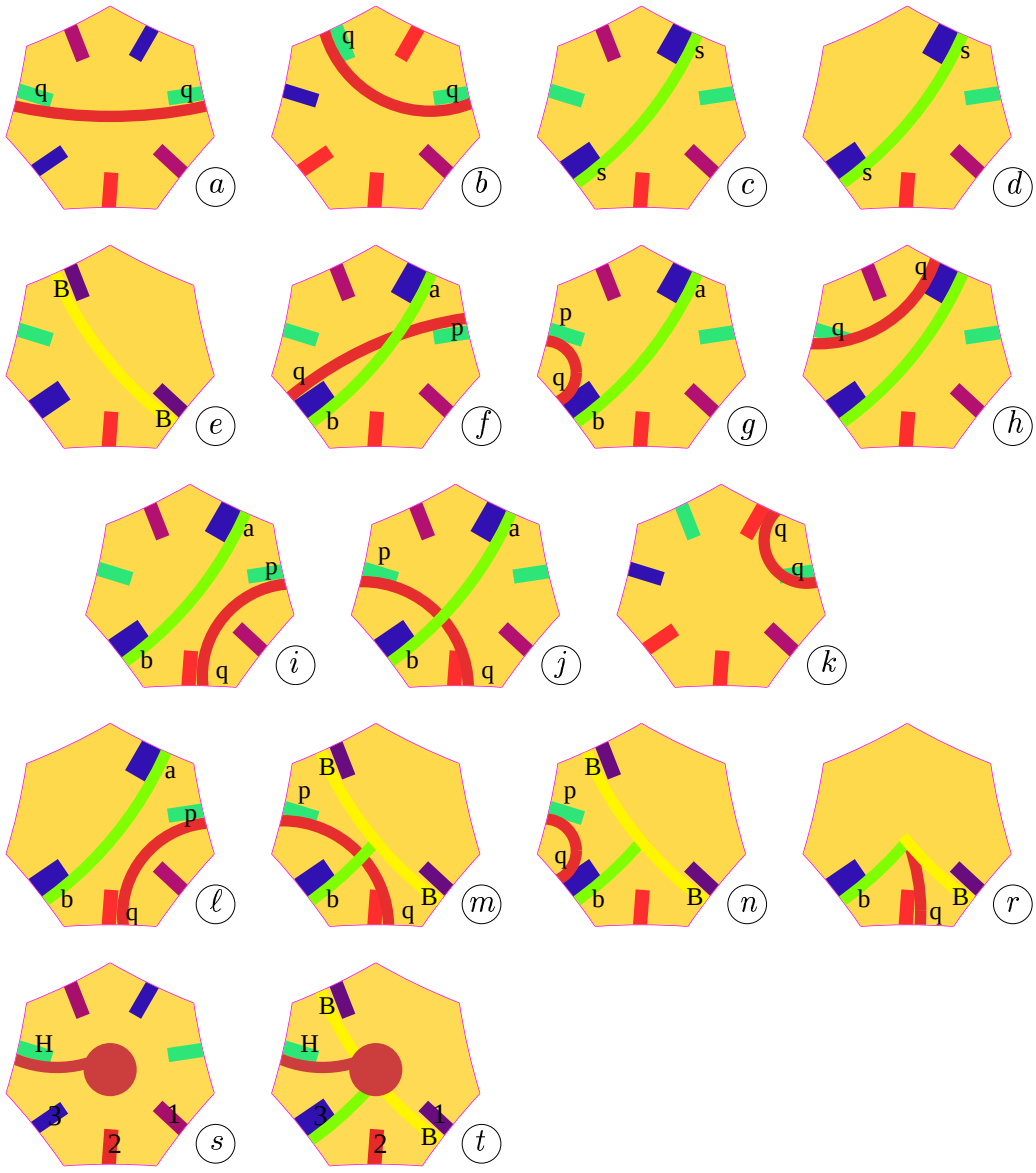

Figure 25 *The tiles for the Turing computation.*
The transportation of the signals: tiles a up to e. The rest of the tiles is devoted to the implementation of the instructions of the Turing machine.

A last word for the halting. It is assumed by tiles (*i*), (*k*), (*s*) and (*t*). Tile (*i*) takes the information of the halting state H. It transfers it to the

terminating tiles (s) and (t) through (k). Tiles (s) and (t) stop the tiling: the black numbers can abut only with themselves and thanks to angle $\frac{2\pi}{3}$, this leads to an impossibility.

With these indications, we can see that the above set of prototiles allows to simulate the computation of any Turing machine starting from an empty tape. Accordingly, we proved the following result:

Theorem 2 *The sets of prototiles defined by Figure* 25 *together with the assortments associated to given Turing machines constitute a family of tiling sets for which the partial tiling problem is undecidable. Note that when the Turing machine associated to the set of prototiles does not halt, there are infinitely many solutions for the tiling, each of them containing at least three roots and at most six ones.*

5 The generalized origin-constrained problem

5.1 The basic principles

We call **general solution** the solution which we shall construct for the generalize origin-constrained problem. It differs from the partial solution in this point that the first tile is not fixed and that it must be used infinitely often as any other tile of the skeleton. In the partial problem, the first tile is used to be the starting point of the computation of a Turing machine. In the setting of our generalzed problem, the starting point of the computations should be chosen at random among infinitely many ones distributed according to the conditions (i) and (ii) of the introduction. Here, we have a bit more: all the tiles of the skeleton will be infinitely often. The condition of density uniformity will be satisfied as follows: within a ball B of radius 6 around any point of the tiling constructed by the skeleton, there is at least one starting point of a computation.

In this proof, following the general pattern of Berger's and Robinson's proofs, we define an infinite family of frames in which we shall proceed to the computation of the Turing machine. As in Berger's and Robinson's proof, there will be infinitely many such computations and infinitely many of them will go on endlessly in the case when the Turing machine does not halt, providing this way a solution for tiling the hyperbolic plane.

Due to the relative lack of space in the Euclidean plane, where truly planar infinite regions interfere between one another, the definition of computing regions is rather intricate in the case of the Euclidean plane. Here, in the hyperbolic plane, taking advantage of the large amount of space everywhere present in this plane, we can define an infinite family of unbounded regions. They may interfere, but it will be simpler than in the Euclidean plane: two such regions are either disjoint or one is embedded in the other. It will be enough to provide a mechanism to rule out embedded regions. This is not a simple question, we shall later precisely see this in the proof.

Before turning to the precise description of the computation, we have to formulate an important remark.

In both papers by Berger and by Robinson, they first indicate the construction of a homogeneous tiling which Berger calls the **skeleton** where infinitely many regions of size 2^n, for all values of $n \geq 3$, are delimited with no overlapping, only embeddings. Then, in these regions, they *draw signals* corresponding to the computation of the Turing machine, *starting* from the initial time. And this starting point happens in infinitely many places, of course, finitely often at each time of the construction of the tiling. This amounts to put the following constraint as we already noted in our introduction: the first tile does not contain computing signal except, possibly, the initial one. Now, this restriction is easily justified: if we relax this restriction, we may introduce configurations which do not correspond to a starting configuration, and it is impossible to backtrack the computation as the accessibility problem is undecidable for Turing machines.

Accordingly, we shall use the same restriction, and for the choice of the first tile, we take any one which does not bear a computing signal except, possibly, the initial one. Also, our construction obeys the same principles as the construction of Berger's and Robinson's proofs: all tiles needed to construct the skeleton must be present for the choice of the first tile. We note that the number of tiles to be taken as the first one is twenty one. However, we depart from the *drawing* signals: once a tile is placed, and the algorithm may take some time to decide to place it or to take another one, it cannot be removed. The reason of our choice is that the tiling constructed by the skeleton only is connected and its complement in the hyperbolic plane is exactly the union of all computing areas.

The second remark is that as in Berger's proof, we define **times** which allow to locate the process in time. From an algorithmic point of view, the skeleton and the computations are both constructed in time and they must

occur simultaneously. Moreover, the region of the plane which consists of the tiles assembled at some time must be controlled up to a point. Otherwise, it might be possible to go on the process without covering the plane, simply because we would put tiles in one direction only. This problem seems to be specific to the hyperbolic plane. It is the price to pay for the large amount of space which is available at any place.

And so, there is an initial time. For the reason already mentioned, the first tile belongs to the skeleton with, possibly, the initial signal of a computation.

From Lemma 2, we know that each sector entails the construction of a tree, the spanning tree of the splitting. Considering a sector S, we define S_n as the set of all tiles which are contained in a flower whose centre belongs to level k of the tree attached to S with $k \leq n$.

In our construction, we have a sequence of times t_n where t_0 is the initial time and t_n, for $n \geq 1$ indicates that we completed a sector which contains a ball B_n around the first tile and with at least $2n$ levels of the sector: this guarantees that the process will tile the plane if the Turing machine does not halt.

5.2 The set of tiles

As in Berger's and Robinson's proofs, we have two kinds of tiles: the tiles for the **skeleton**, *i.e.* the basic pattern which delimit the regions in which the computations hold; and the tiles for the computation. First, we describe the tiles of the skeleton.

5.2.1 The skeleton

For the skeleton, we have to implement the construction of F-, G- and **8**-flowers and the rules of generations of the carpet structure of the mantilla. We have also to implement the delimitation of the trees which are candidate for a computation using the harp model of the solution to the partial problem.

To this aim, remember that in the flowers we have two categories of tiles: the petals and the centres. Also remember that we started with two kind of tiles: tiles with a red vertex and two green sides and tiles with no marks. We already mentioned a way to prevent basic tiles of the second kind, *i.e.* without red or green marks, to tile the plane alone. This way consists in labelling the edges of such a tile by numbers from 1 up to 7. It is very easy to check that with such a labelling, the tiles of the second kind cannot alone

tile the plane as the labels cannot match. This property is not specific to tiling $\{7, 3\}$, indeed it is shared by any regular tiling $\{p, 2q+1\}$[1]. Due to the matching condition on edges, the tiles of first kind should be dotted with similar labels. Indeed, the labels are needed only on the edges of tiles of the first kind which are shared by tiles of the second kind. A priori, this would give 7^3 different tiles for the initial set of tiles which, after Berger, we call the **prototiles**. As we shall soon see, we need only 29 prototiles for the skeleton, including petals and centres.

To see this, let us fix where we put number 1 in a tile which is a centre. For F-flowers, it may seem natural to put 1 and 7 at symmetric places with respect to the vertical axis of reflection of the flower. It is also easy to fix 1 and 7 for an **8**-flower: the red vertex is exactly on the vertical axis of reflection of the flower. We have a different situation with G-flowers. We already noted that there are left-hand and right-hand side flowers. Here, we shall stress on this difference by giving to G-flowers a different numbering: instead of clockwise increasing around the edges of the tile, the numbers will increase while **counter-clockwise** going around the edges of the tile. Also, in order to distinguish between petals, we introduce two sets of numbers: we shall consider **marked** and **unmarked** numbers. Unmarked numbers in $\{1..7\}$ are those which we ordinarily use. Marked numbers are in $\{\overline{1}..\overline{7}\}$. The difference appears below, on table 1 and Figure 26.

We remark that the new numbers do not change the fact that central tiles alone, even by mixing the labels, cannot tile the plane by themselves.

	2	3	4	5	6
F	2	$\overline{3}$	$\overline{4}$	$\overline{5}$	6
G_ℓ	$\overline{6}$	$\overline{5}$	4	3	2
G_r	6	5	4	$\overline{3}$	$\overline{2}$
8	$\overline{2}$	3	$\overline{4}$	5	$\overline{6}$

Table 1 *Table of the distribution of colours on the sides of the central tiles. The labels are given for sides numbered from* 1 *up to* 7 *clockwise running around the tile. For centres of G-flowers, we indicate the reverse ordering on the labels. The labels* 1 *and* 7 *are not indicated: they are the same for F- and* **8***-flowers, and they are exchanged for G-flowers.*

[1]The property does not hold for $\{p, q\}$ when q is even.

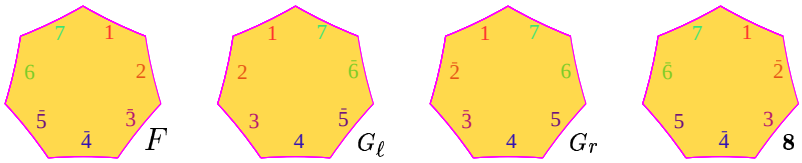

Figure 26 *The prototiles for the centres: F-, $\mathbf{8}$-, G_ℓ- and G_r-centres.*

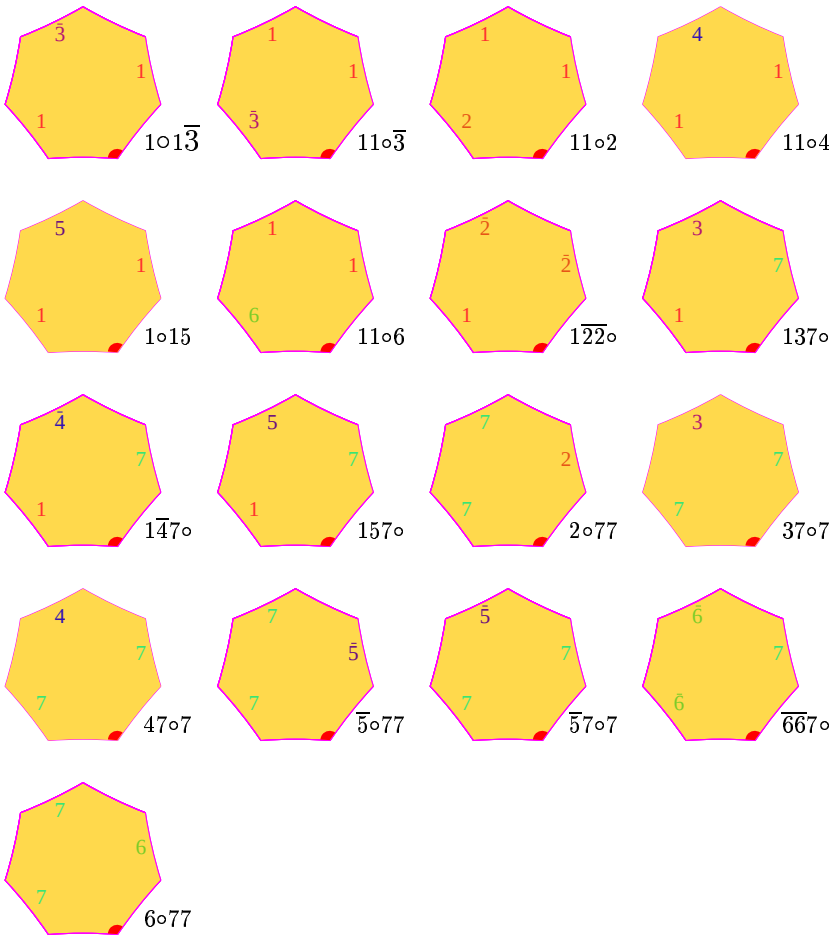

Figure 27 *The prototiles for the non-parental petals.*

From this, we deduce 15 prototiles from the petals, looking at the different configurations of petals attached to edges numbered from 2 up to 6 of all

possible centres. In this respect, we define such tiles as the **non-parental** tiles which will be the meaning of this expression until the end of the report.

Above, Figure 27 displays all possible figures. Further, Figure 42 displays the complete set of 21 tiles of the skeleton.

The non-parental petals can be grouped according to the flowers in which they occur. This is given in table 2, below. In this table, the position of the red-vertex in the petal is indicated by the occurrence of symbol $\circ$. The labels are indicated by putting in first position the lowest label according to the alphabetic order and then by by following the occurrence of the other labels and of the red vertex while running around the tile clockwise.

	2	$\overline{2}$	3	$\overline{3}$	4	$\overline{4}$	5	$\overline{5}$	6	$\overline{6}$
F	$2\circ 77$			$1\circ 1\overline{3}$		$1\overline{4}7\circ$		$\overline{5}7\circ 7$	$11\circ 6$	
G_ℓ	$11\circ 2$		$37\circ 7$		$1\circ 14$			$\overline{5}\circ 77$		$\overline{66}7\circ$
G_r		$1\overline{22}\circ$		$11\circ\overline{3}$	$47\circ 7$		$1\circ 15$		$6\circ 77$	
8		$1\overline{22}\circ$	$137\circ$			$1\overline{4}7\circ$	$157\circ$			$\overline{66}7\circ$

Table 2 *Table of the non-parental petals according to their parent flower.*

Table 2 results from a careful checking. It is not difficult to check, in each case, that the configuration of each petal is unique, even when the same tile may appear in different contexts.

In this line, we note that the following petals appear only in a fixed centre:

$2\circ 77$, $1\circ 1\overline{3}$, $\overline{5}7\circ 7$ and $11\circ 6$ for F-flowers;
$11\circ 2$, $37\circ 7$, $1\circ 14$ and $\overline{5}\circ 77$ for G_ℓ flowers;
$11\circ\overline{3}$, $47\circ 7$, $1\circ 15$ and $\circ 77$ for G_r-flowers;
$137\circ$ and $157\circ$ for **8**-flowers.

For the other petals:

$1\overline{4}7\circ$ is common to F- and **8**-flowers;
$\overline{66}7\circ$ is common to G_ℓ- and to **8**-flowers;
$1\overline{22}\circ$ is common to G_r and **8**-flowers.

Now, we have to establish a converse of the table. Starting from a tile, we necessarily obtain what can be deduced from the table and nothing else.

To this aim, we first prove :

Lemma 5 *The set of tiles defined by table* 2 *together with the four tiles for the centers entail the mantilla. Namely, starting from a tile, we precisely have the contacts which can be deduced from the table.*

In order to prove the lemma, we first note that a corollary of Lemma 1 is the following result:

Corollary 1 *A petal can abut at a numbered edge only with a centre, at the edge which bears the same number. If the number on the edge of the petal is marked, the same number on the edge of the centre must also be marked.*

Proof of Lemma 5. We prove the lemma by looking at the four cases successively. Now, we make a general remark. A bit further, when we say that we start with that and that case of centre, we do not use the properties of the flower attached to the center. We only consider tiling matching and we shall find out that the constraints due to matching entail the properties which we know about the corresponding flowers.

First, we start with an F-flower. In this case, we can see that edge $\overline{4}$ can abut with a single petal, namely $1\overline{4}7\circ$.

Then, look at what can be put to abut with edge $\overline{5}$ of the centre. Looking at Figure 42 we find that only two tiles can match with mark $\overline{5}$ at this edge: either $\overline{5}7\circ7$ or $\overline{5}\circ77$. Now, as $1\overline{4}7\circ$ has its two green sides radiating from its edge $\overline{4}$, tile $\overline{5}\circ77$ is ruled out: it requires to share its red vertex with $1\overline{4}7\circ$ which is not possible. Accordingly, we have $\overline{5}7\circ7$ as indicated in Figure 28.

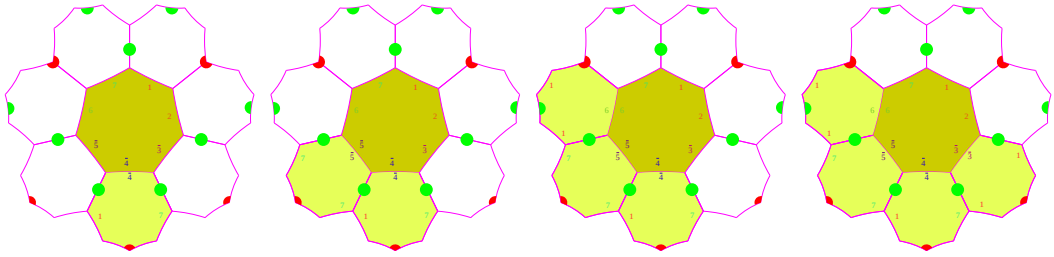

Figure 28 *The non-parental tiles induced by an F-centre but the last one.*

Next, we consider the edge 6 of the centre. There are two possibilities, *a priori*: $6\circ77$ or $11\circ6$. In order to choose the right one, we make use of an argument which we shall repeat very often in this proof. The argument consists in noticing that in a centre, edges are marked by consecutive numbers

and, in particular, there cannot be two adjacent edges with identical numbers. Let us call this property the **uniqueness constraint**. We use this property in the following situation. Consider two adjacent petals sharing a common green side. As a consequence, both petals are around two centres: the one which we consider and another one, say a. Now, by our construction, $\overline{5}7\circ 7$ has a common edge 7 with a. Accordingly, by the uniqueness constraint the petal at edge 6 cannot abut with a with again a 7. And so, the petal at edge 6 must be $11\circ 6$ as indicated in table 2 and in Figure 28.

Now, we go on the construction on the other side of $1\overline{4}7\circ$. For edge $\overline{3}$ we have either $1\circ 1\overline{3}$ or $11\circ\overline{3}$. Now, in case of the latter petal, the red-vertex of $11\circ\overline{3}$ would be in contact with $1\overline{4}7\circ$, but this does not match with the position of the red vertex of $1\overline{4}7\circ$. And so, here we have $1\circ 1\overline{3}$.

At last, for the edge 2, we have either $11\circ 2$ or $2\circ 77$. But the uniqueness constraint rules out $11\circ 2$ as $1\circ 1\overline{3}$ contributes with a 1 to the other centre. And so, the last non-parental petal for an F-flower is $2\circ 77$. We find again the tiles indicated by table 2 for an F-centre. The complete image of non-parental petals is also displayed in Figure 34.

Now, let us turn to an **8**-centre, which is illustrated by Figures 29 and 34.

As for an F-centre, we start by petal $1\overline{4}7\circ$ which is the single possible petal for an edge marked with $\overline{4}$. This time, we turn counter-clockwise. Accordingly, for edge 3, we have $37\circ 7$ or $137\circ$. Now, $37\circ 7$ is ruled out by the uniqueness constraint. Indeed, $1\overline{4}7\circ$ already contributed with an edge 7 for the other centre. And so, we have $137\circ$ at edge 3. At edge $\overline{2}$ we necessarily have $1\overline{22}\circ$. A refinement of the uniqueness constraint is that we should have **consecutive** numbers for two adjacent petals of the same centre, considering that 1 and 7 are consecutive. We shall call this the **successor constraint**. But 7 and 2 cannot be consecutive and this rules out the wrong position of $1\overline{22}\circ$ at edge $\overline{2}$ of the **8**-centre. The right position is characterised by the fact that the edge 1 of $1\overline{22}\circ$ is adjacent to the edge 7 of $137\circ$ around the **8**-centre.

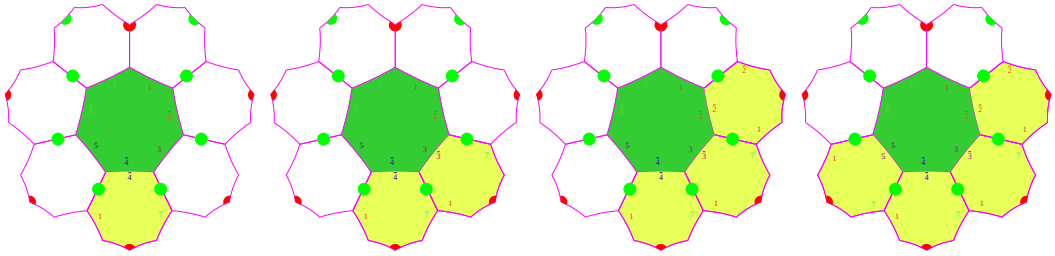

Figure 29 *The non-parental tiles induced by an* **8***-centre but the last one.*

Let us now turn to the other side of $1\overline{4}7\circ$. At edge 5 we have either $1\circ 15$ or $157\circ$. By the uniqueness constraint on 1, this rules out $1\circ 15$ and so, the expected tile is $157\circ$.

At last, for edge $\overline{6}$ we have again a unique tile but with two possible positions depending on whether edge $\overline{6}$ is in contact in the first or the second $\overline{6}$ in $\overline{66}7\circ$. If it is with the first, then the successor constraint is violated and so, it must be the second as displayed in Figure 34.

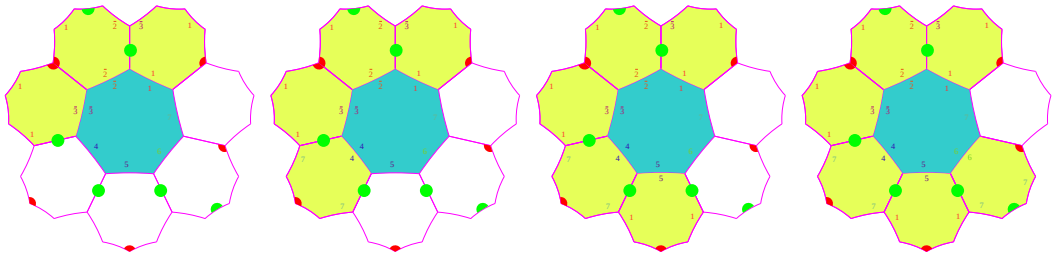

Figure 30 *The non-parental tiles in a wrong assumption for a G_r-centre.*

Now, let us turn to G-centres.

First, we shall consider G_r-centres. Let A be one of them.

We start with edge $\overline{2}$ for which there is a single tile: $1\overline{22}\circ$. Now, this tile can be put in two positions as at first glance any $\overline{2}$-edge of the tile may abut with the $\overline{2}$-edge of the centre.

In Figure 30, we assume that we put a tile $1\overline{22}\circ$ in such a way that its first $\overline{2}$ abut with that of A. For edge $\overline{3}$ of A, we may have either $1\circ 1\overline{3}$ or $11\circ\overline{3}$. The latter cannot be put with the considered position of $1\overline{22}\circ$. Otherwise, the red-vertex of $11\circ\overline{3}$ would be shared by $1\overline{22}\circ$, which is not possible in the considered position. As noted, two adjacent petals are in contact with two centres. In Figure 30, we consider that tiles $1\overline{22}\circ$ and $11\circ\overline{3}$ are fixed for A, and we consider the other centre, say B. We make use of Figure 30 to look at the tiles which can be put around B. Tile B itself has a $\overline{2}$-edge due to the second one of the petal $1\overline{22}\circ$ we considered. It has also a petal at 1 by tile $1\circ 1\overline{3}$. The order of the petal at A induces that B is a G-centre. As one of its edges is $\overline{2}$, it is also a G_r-centre. Now, note that the position of $1\overline{22}\circ$ at B is different from its position at A. The position of the red vertex of $1\overline{22}\circ$ at B forces tile $11\circ\overline{3}$ at the edge $\overline{3}$ of B as illustrated by Figure 30. Next, we consider the edge 4 of B. We may put either $1\circ 14$ or $47\circ 7$. But the uniqueness constraint rules out $1\circ 14$ and so, we put $47\circ 7$. At edge 5, we could put $1\circ 15$ or $157\circ$. If we put the latter, we need to put $11\circ 6$ at the

edge 6 of B but in this case, the red vertex of 11∘6 should be shared with 157∘ which is not possible. And so we need to place 1∘15 at edge 5 which entails 6∘77 at edge 6 by the uniqueness constraint. But now, as illustrated by Figure 30, the red vertex of 6∘77 and that of 1∘1$\overline{3}$, the petal at the edge 1 of B, must be shared by the petal at 7. This is impossible for a petal and so, this rules out the position which we first considered for tile 1$\overline{22}$∘ at the edge $\overline{2}$ of A.

Accordingly, 1$\overline{22}$∘ abuts with A at the second $\overline{2}$ of the petal. But this is the position which we had for B which is also a G_r-centre. From the argument we had for B, we conclude that the petals we put around B from edge $\overline{2}$ up to 5 are correct. As at edge 5 we put 1∘15, we put 6∘77 at edge 6 as 11∘6 is ruled out by the uniqueness constraint. And so, also here, we find the indication of table 2.

Now, we come to our last case for a centre: G_ℓ-centres. Again, call A one of them.

For the edge 2 of A, we may have 2∘77 or 11∘2. For edge 3, we may have 37∘7 or 137∘. Note that these last two tiles have their red-vertex at the same place with respect to edge 3. Now, the position of the red vertex of 2∘77 is unique when the tile abuts with its edge 2 and this position requires the red vertex to be shared by the tile which is put at the edge 3 of A. As shown in Figure 32, it is impossible as the red vertex of the tile at the edge 3 of A cannot be there whichever tile with 3 is placed.

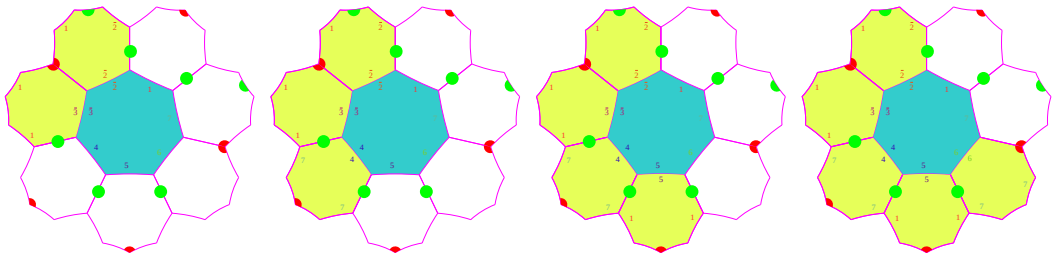

Figure 31 *The non-parental tiles for a G_r-centre.*

And so, we need to place tile 11∘2 at the edge 2 of A and this entails tile 37∘7 at edge 3 by the uniqueness constraint. The uniqueness constraint also forces to place 1∘14 at edge 4, the other possibility being ruled out. For edge $\overline{5}$, there are two possibilities: $\overline{5}$∘77 or $\overline{5}$7∘7.

Assume that we put $\overline{5}$7∘7. Then this tile and 1∘14 are also adjacent around another centre, call it B. With respect to B, 1∘14 and $\overline{5}$7∘7 abut

with the centre at edges 1 and 7, respectively. Note that the position of the red-vertices of these tiles with respect to B are those of an F-flower but, as indicated at the beginning of this argument, we cannot use this property. Note also that the order of the edges of $1\circ 14$ and $\overline{5}7\circ 7$ which are in contact with B induces that B is a G-centre. But at this stage, we cannot use this contradiction.

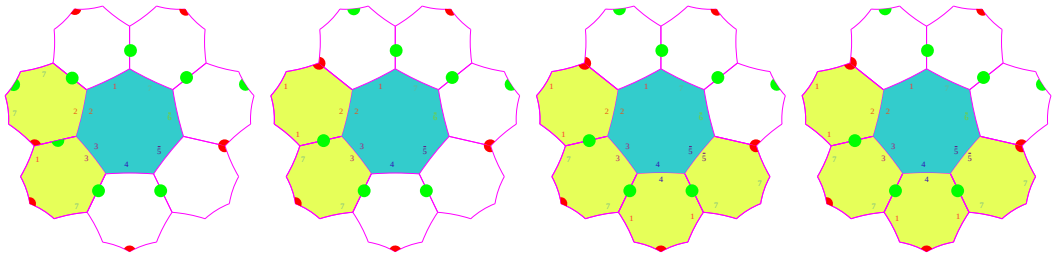

Figure 32 *The first non-parental tiles for a G_ℓ-centre. Leftmost picture: a wrong assumption on the first two tiles.*

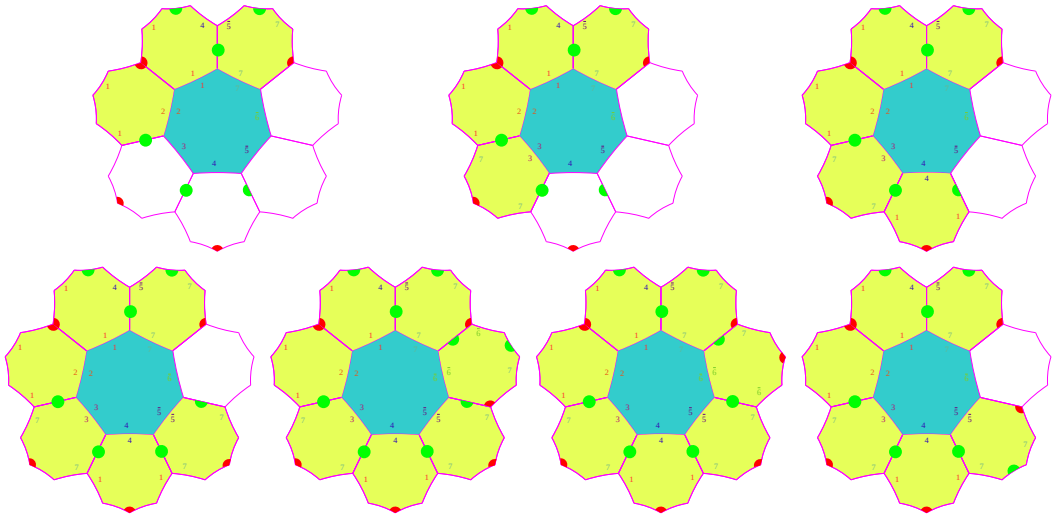

Figure 33 *Illustrating the proof of wrong assumptions on a G_ℓ-centre.*

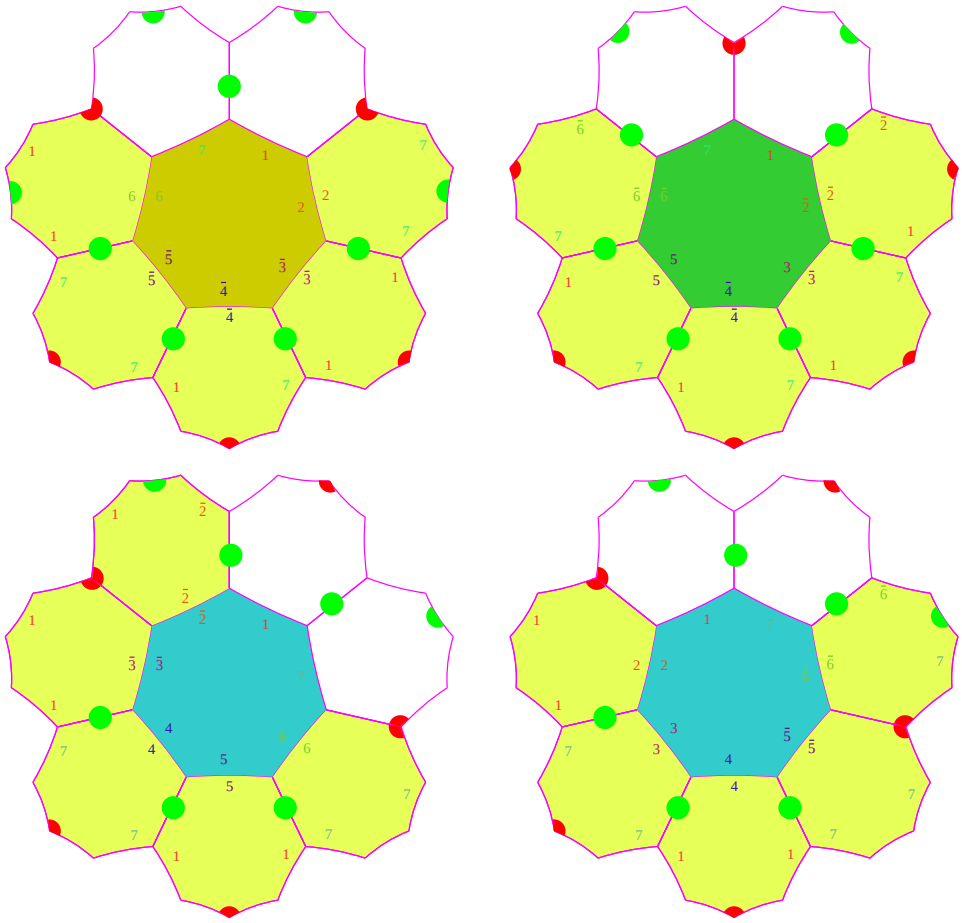

Figure 34 *All the non-parental tiles induced by the centres: above, left-hand side, an F-centre; right-hand side, an* **8***-flower. Below, left-hand side, a G_r-centre; right-hand side, a G_ℓ-centre.*

Starting with the edge 2 or $\overline{2}$ of B, we can use the position of the red-vertex of 1∘14. This position rules out both possibilities with tile $1\overline{22}\circ$ as the red vertex cannot occur just before a $\overline{2}$ while turning clockwise around the petal. For the same reason, 2∘77 is ruled out and so, we remain with 11∘2. This indicates that B is a G_ℓ-centre. From 11∘2 and the edge 3 of B, the uniqueness constraint indicates the choice of 37∘7 as the single possibility. In its turn, this selection entails that we have 1∘14 at the edge 4 of B, again by the uniqueness constraint. Next, we meet edge $\overline{5}$. Two petals could be put: $\overline{5}\circ77$ or $\overline{5}7\circ7$. If we put $\overline{5}7\circ7$, as illustrated by Figure 33, both positions of $\overline{66}7\circ$ lead to a contradiction: as from the tile which abuts at the edge 7 of

B there is already a red-vertex in contact with the petal at edge $\overline{6}$, the red vertex of $\overline{66}7\circ$ should match with it which cannot be the case. This forces the edge to be 6, which is impossible for B which is a G_ℓ-centre. And so, we have to put $\overline{5}\circ 77$ at the edge $\overline{5}$ of B. But in this case, the red vertex of $\overline{5}\circ 77$ is also in contact with the petal to be placed at the edge $\overline{6}$ of B. This is incompatible with the other red-vertex imposed by the petal at edge 7. And so, we are led to a contradiction, as expected.

From this contradiction, we conclude that we have to put $\overline{5}\circ 77$ at the edge $\overline{5}$ of A. And this matches with $\overline{66}7\circ$, provided that we take the position in which the red vertex of $\overline{66}7\circ$ abuts with that of $\overline{5}\circ 77$. This is possible as indicated in Figure 34.

Again we find the line of table 2.

Now, the rest of the proof is easier.

We first note that in most petals, we can write the numbering of its edges in the form α, β, γ with $\alpha \in \{2..6\} \cup \{\overline{2}..\overline{6}\}$ and $\beta, \gamma \in \{1, 7\}$. In such a case, we consider α and, in many cases, there is a single centre which abuts with α.

The following tiles belong to these cases:

$2\circ 77$, $1\circ 1\overline{3}$, $\overline{5}7\circ 5$ and $11\circ 6$ require an F-flower;
$137\circ$ and $157\circ$ require an **8**-centre;
$11\circ 2$, $37\circ 7$, $1\circ 14$ and $\overline{5}\circ 77$ require a G_ℓ-centre;
$11\circ\overline{3}$, $47\circ 7$, $1\circ 15$ and $6\circ 77$ require a G_r-centre.

There are three remaining tiles: $1\overline{22}\circ$, $1\overline{4}7\circ$ and $\overline{66}7\circ$.

First, let us consider $1\overline{4}7\circ$. The problem comes from the fact that this tile may belong either to an F-flower or to an **8**-one. The tile itself cannot determine the choice between these two kinds of centre. However, if we take a neighbouring tile, it is necessarily of the form α, β, γ as above indicated and α fixes the choice: F-centre when $\alpha = \overline{3}$, then it must be $1\circ 1\overline{3}$, **8**-centre when $\alpha = 3$ and it must then be $137\circ$. Similarly, the choice is F-centre when $\alpha = \overline{5}$ and it must be $\overline{5}7\circ 7$, and it is **8**-centre when $\alpha = 5$ and then the tile must be $157\circ$.

Consider the case when the tile is $1\overline{22}\circ$. In this case, the tile may belong either to a G_r-centre or to an **8**-one. Here, the tile for 3 determines the choice: if it has a side marked with $\overline{3}$, the required centre is a G_r-one; if it has a side marked with 3, it is an **8**-centre. Now, we can note that the abutting of the tile with the centre is not the same. We know that $1\overline{22}\circ$ may

abut a centre in two ways, depending on which one of its $\overline{2}$'s is in contact with the centre.

Looking at Figure 34, we can see that petal $1\overline{22}\circ$ abuts with an **8**-centre by its first $\overline{2}$ while it abuts with a G_r-centre by its second $\overline{2}$. From the already seen arguments, if we choose the position, it forces the choice of the centre. Indeed, imagine that we have a G_r-centre abutting at each $\overline{2}$ of petal $1\overline{22}\circ$. Then, looking at Figure 30, we have a situation where petal $1\overline{22}\circ$ is in such a configuration. And we have then seen that the parental couple constituted by petal $1\overline{22}\circ$ with petal $1\overline{3}1$ over a G_r centre induces a contradiction when we arrive at the petal for edge 7. If we assume that each $\overline{2}$ of petal $1\overline{22}\circ$ abuts to the edge $\overline{2}$ of an **8**-centre, the discussion is simpler.

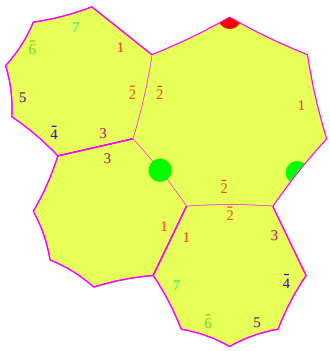

Figure 35 *An impossible situation: two* **8***-centres abutting petal* $1\overline{22}\circ$ *by both its two* $\overline{2}$*-edges.*

As indicated in Figure 35, there is another petal between both centres. It has an edge 1 and an edge 3 and there is no tile where 1 comes immediately after 3 when we run clockwise around the tile. And so this situation also is impossible.

At last, consider the case of a tile $\overline{66}7\circ$. From what we established, two centres can have such a tile: a G_ℓ-centre or an **8**-one. However, as in the case of tile $1\overline{22}\circ$, there is a difference in the position of the red-vertex of this tile with respect to the centre. When the red-vertex is the closest to the centre, this means that its second $\overline{6}$ is in contact with the $\overline{6}$-edge of the centre which necessarily is a G_ℓ-centre. In the other case, when the tile abuts the centre by its first $\overline{6}$-edge, the centre must be an **8**-one. Accordingly, the same tile

abuts at the same time to a G_ℓ-centre and to an **8**-one. Also, it cannot abut by both its $\overline{6}$-edges with two **8**-centres or with two G_ℓ-centres. We can see this point directly as in the case of tile $1\overline{22}\circ$.

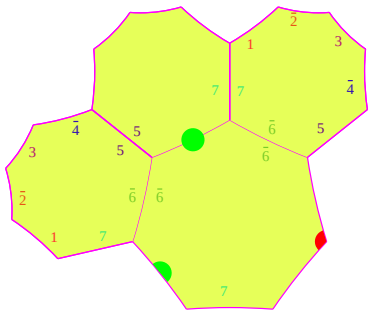

Figure 36 *An impossible situation: two* **8***-centres abutting petal* $\overline{66}7\circ$ *by both its two* $\overline{6}$*-edges.*

Indeed, if we have two **8**-centres, Figure 36 shows that between the two $\overline{6}$-edges of the tile this requires another tile with a 7-edge just before a 5-edge when turning clockwise around the tile. We can check in Figure 42 that there is no such tile.

If we have two G_ℓ-centres, in fact the argument is symmetric to the one we used for $1\overline{22}\circ$ tiles with two G_r-centres. This means that we have to look at how we find the tiles around a G_ℓ-tile starting from tile $\overline{66}7\circ$.

And so, for one $\overline{6}$-edge we have the expected position for a G_ℓ-centre, while for the other $\overline{6}$-edge, we have another position with the G_ℓ-centre. Let B be the second G_ℓ-centre with tile $\overline{66}7\circ$ abutting to the $\overline{6}$-edge of B by its second $\overline{6}$-edge. Denote by A the other G_ℓ-centre. It is not difficult to see that with $\overline{66}7\circ$ abutting as indicated at the $\overline{6}$-edge of B, necessarily, the $\overline{5}$-edge of B receives tile $\overline{5}7\circ7$. With the other possibility, namely $\overline{5}\circ77$, the red-vertex would have to be shared with $\overline{66}7\circ$, which is not possible. And so, this gives $\overline{66}7\circ$ and $\overline{5}7\circ7$ as parental tiles for A where tile $\overline{66}7\circ$ abuts the $\overline{6}$-edge by the first $\overline{6}$-edge. Then, turning around A, we successively find that the $\overline{5}$-edge of A must abut with tile $\overline{5}\circ77$ due to the necessity to share its red vertex with tile $\overline{66}7\circ$, which is now possible. Then, by the uniqueness constraint, edge 4 must receive tile $11\circ4$. By the same reason, edge 3 must

receive tile 37∘7 and, similarly, edge 2 receives tile 11∘2. Now, the petal at edge 1 has already a red vertex from the side of edge 7 where tile $\overline{5}$7∘7 abuts and it also has to share another red vertex on the side of edge 2 by the red vertex of 11∘2. As this is impossible, we conclude that the two $\overline{6}$-edges of a tile $\overline{66}$7∘ cannot receive two G_ℓ-centres.

The correct solution is a G_ℓ-centre at one $\overline{6}$-edge, the first one, and an **8**-centre at the other $\overline{6}$-edge, the second one.

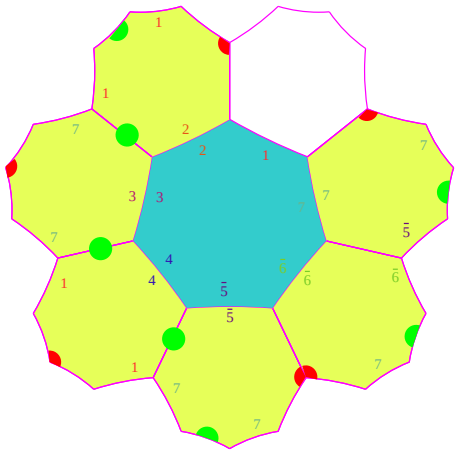

Figure 37 *An impossible situation: two G_ℓ-centres abutting petal* $\overline{66}$7∘ *by both its two* $\overline{6}$*-edges. The tiles around one of them with a contradiction.*

At this point, we proved that the mantilla can be constructed **downwards** in any sector. We have to see that the considered set of tiles allows us to go **upwards** also.

It is not difficult to see that the first thing we have to do is to determine what the parental tiles are.

Our first remark is that we should check that parental tiles do not bring in new types of tile. Indeed, a parental tile in a given flower is also a non-parental tile in another one. Accordingly, we should have already all possible types of tiles.

As previously, this checking will be performed from the tiles themselves. We look at the marks and do not take into consideration the results we obtained from the splitting process. Indeed, it will turn out that we find again the results of Lemma 2.

First, we consider an F-flower. And so, we look at the tiles which can be put at edges 7 and 1 of the F-centre. Taking into account that these tiles

are also non-parental tiles of another flower, we look among the tiles defined by table 2.

Consider the configuration defined by the two red vertices of the flower which are at another end of an edge in contact with the centre. Starting from the edge of the centre and clockwise running around the expected petal, we find that its pattern must be of the form $7\circ xy$ for the edge 7 and $1uv\circ$ for the edge 1 of the centre. Moreover, edges y and u are consecutive in the new centre and, accordingly, the successor constraint applies to them.

Looking at table 2, we find that the possible patterns for these petals are:

- edge 7: $7\circ 1\overline{4}$, $7\circ 7\overline{5}$, $7\circ 73$, $7\circ\overline{66}$, $7\circ 74$, $7\circ 13$ and $7\circ 15$.
- edge 1: $1\overline{3}1\circ$, $1\overline{4}7\circ$, $141\circ$, $1\overline{22}\circ$, $151\circ$, $137\circ$ and $157\circ$.

Let us start with the edge 7 of the centre.

Consider $7\circ 1\overline{4}$. Table 2 indicates either an F-flower or an **8**-one. We get $y = \overline{4}$ and so, $u =\in \{3, \overline{3}\}$ from the successor constraint, as the orientation of F- and **8**-centres are the same. If we take $u = 3$, due to $\overline{4}$, we deal with an **8**-centre and so the tile at edge 1 is $137\circ$. If we take $u = \overline{3}$, we deal with an F-flower and now, the petal at edge 1 is $1\overline{3}1\circ$.

Consider $7\circ 7\overline{5}$. From table 2, it requires an F-centre. As $y = \overline{5}$, we get $u = \overline{4}$ and so we have petal $1\overline{4}7\circ$ at edge 1. Note that $1\overline{4}7\circ$ is also $7\circ 1\overline{4}$, but the position of the tiles is not the same with respect to the initial F-centre. It is also not the same in the new centre.

Consider $7\circ 73$. From table 2, it belongs to a G_ℓ flower. Accordingly, the successor constraint and the orientation give $u = 4$ and so, we obtain $141\circ$ for edge 1.

Consider $7\circ\overline{66}$. This can be either an **8**-flower or a G_ℓ-flower. The successor constraint and the different orientation give us $u \in \{5, \overline{5}, 7\}$. Now $u = 7$ means a tile with pattern $17v\circ$. Table 2 has no tile with this pattern. This rules out the case of a G_ℓ-centre. For an **8**-centre, we necessarily have $u = 5$ and so we get tile $157\circ$.

Consider $7\circ 74$. From table 2, this requires a G_r-centre only. From $y = 4$, the orientation and the successor constraint give us $u = 5$. And so the petal at edge 1 is $151\circ$.

Consider $7\circ 13$. From table 2, this requires an **8**-centre only. By the successor constraint and the orientation we get $u = \overline{2}$ and so, the petal at edge 1 is $1\overline{22}\circ$.

At last, consider $7\circ 15$. From table 2, this again requires an **8**-centre only. The successor constraint and the orientation yield $u = \overline{4}$. Accordingly, the

petal at edge 1 is $1\overline{4}7\circ$.

This information is gathered in table 3, below.

	F_ℓ	F_r	G_ℓ	G_r	$\mathbf{8}_1$	$\mathbf{8}_2$	$\mathbf{8}_3$	$\mathbf{8}_4$
1	$1\overline{4}7\circ$	$1\circ1\overline{3}$	$1\circ14$	$1\circ15$	$1\overline{22}\circ$	$137\circ$	$1\overline{4}7\circ$	$157\circ$
7	$\overline{5}7\circ7$	$1\overline{4}7\circ$	$37\circ7$	$47\circ7$	$137\circ$	$1\overline{4}7\circ$	$157\circ$	$\overline{66}7\circ$

Table 3 *The possible values of the parental tiles of an F-flower.*

We note that the table gives additional information about the position of the flower induced by the indicated parental petals. In what we computed, we see that there are a single case for G_ℓ- and G_r-flowers which corresponds to the fact that in a G-flower, there is a single F-son. For an F-flower, we have two cases which corresponds to the fact that an F-son has two F-sons. One is on the left-hand side, it is determined by petals $\overline{5}7\circ7$ and $1\overline{4}7\circ$ as we can see in Figure 34. This is why table 3 indicates F_ℓ. The other F-son of an F-flower is determined by petals $1\overline{4}7\circ$ at edge 7 and $1\circ1\overline{5}$ at edge 1 as we can see in Figure 34. From this we understand the indication F_r of the table. Now, it is easy to understand the indications $\mathbf{8}_i$, $i \in \{1..4\}$ of the table. An **8**-flower has four F-sons and, numbering them from 1 up to 4, going clockwise around the centre as we can see from Figure 34 we obtain: the first F-son is determined by petals $1\overline{22}\circ$ at edge 1 and $137\circ$ at edge 7, the second by $137\circ$ at edge 1 and $1\overline{4}7\circ$ at edge 7, the third by $1\overline{4}7\circ$ at edge 1 and $157\circ$ at edge 7 and the last one by $157\circ$ at edge 1 and $\overline{66}7\circ$ at edge 7. These are exactly the indications of table 3.

Now, consider the case of a G_ℓ-flower.

The configuration of the parental petals which can be seen in Figure 34 indicate that the pattern of a tile put at edge 7 is of the form $7u\circ v$ while it is of the form $1\circ xy$ for a petal at edge 1. We have also that y and u must observe the successor constraint. Now, we note that the tile at edge 7 is also in contact with the petal at $\overline{6}$ which is $\overline{66}7\circ$. From the first part of this proof, we know that the other edge $\overline{6}$ of the petal is in contact with an **8**-flower, and it is not difficult to check that this edge $\overline{6}$ and v must also satisfy the successor constraint. As we now know that there is an **8**-centre at this place, the orientation indicates that $v = 7$ and so, the tile at edge 7 has the pattern $7u\circ7$. From table 2, the possibilities are exactly: $72\circ7$, $7\overline{5}\circ7$ and $76\circ7$.

On another side, the possibilities of the pattern $1\circ xy$ for the petal at edge 1 are exactly the following, taken from table 2: $1\circ1\overline{3}$, $1\circ14$ and $1\circ15$.

Consider 72∘7. From table 2, this matches with an F-centre only. Accordingly, due to the successor constraint and the orientation, $u = \overline{3}$. And so, among the above three possible petals at edge 1, only $1\circ 1\overline{3}$ is possible.

Consider $7\overline{5}\circ 7$. Table 2 indicates that this petal matches with a G_ℓ-centre only. From the successor constraint and the orientation, $u = 4$. And so, this selects 1∘14 from the three possibilities for the petal at edge 1.

Consider 76∘7. From table 2, we know that this matches only with G_r-centres. Accordingly, we get $u = 5$ from the successor constraint and the orientation. This selects 1∘15 as the single possibility for the petal at edge 1 among the possible three ones.

This gives us the information given in the left-hand side table of tables 4.

	F	G_ℓ	G_r
1	$1\circ 1\overline{3}$	1∘14	1∘15
7	2∘77	$\overline{5}\circ 77$	6∘77

	F	G_ℓ	G_r
1	11∘6	11∘2	$11\circ\overline{3}$
7	$\overline{5}7\circ 7$	37∘7	47∘7

Table 4 *The possible values of the parental tiles of a G-flower. On the left-hand side, the case of a G_ℓ-flower. On the right-hand side, the case of a G_r-flower.*

Now, consider the case of G_r-flowers. We argue in a very symmetric way with respect to the case of G_ℓ-flowers as can be expected from Figure 34.

Indeed, we first determine the patterns of the petals at edge 7 and edge 1. From Figure 34, we can see that the patterns are $1x\circ y$ for the petal at edge 1 and $7uv\circ$ for the petal at edge 7. We have also the successor constraint on edges y and u. Now, petal $1\overline{22}\circ$ which abuts the G_r-centre by its second edge $\overline{2}$ also abuts an **8**-flower by its first edge $\overline{2}$. Now, this $\overline{2}$ and x must obey the successor constraint. Due to the orientation, we obtain that $x = 1$. And so, the pattern for a petal at edge 1 is $11\circ y$. Table 2 indicates that the possible patterns are exactly: 11∘6, 11∘2 and $11\circ\overline{3}$.

On another side, table 2 indicates that the patterns $7uv\circ$ are exactly: 772∘, $7\overline{5}7\circ$, 737∘, $77\overline{5}\circ$, 747∘ and 776∘.

Consider 11∘6. From table 2, this petal belongs to F-flowers only. Accordingly, from the successor constraint and the orientation, $u = \overline{5}$. The single possibility for an F-centre is $7\overline{5}7\circ$.

Consider 11∘2. From table 2, we can see that this petal occurs for G_ℓ-centres only. The successor constraint and the orientation fix $u = 3$ which yields 737∘, again from table 2.

Consider $11\circ\overline{3}$. From table 2 we obtain that this petal belongs to G_r-centres only. From the successor constraint and the orientation we conclude that $u = 4$. Table 2 indicates $747\circ$ as the single possibility.

This gives us the information which is displayed by the right-hand side table of table 4.

We have an important remark from these arguments and the table: the parent of a G-flower is either an F-flower or a G-flower. It is never an **8**-flower.

Now, let us turn to the case of an **8**-flower.

From Figure 34, we note that the pattern of the parental tiles are of the form $7xy\circ$ for the petal at the edge 7 of the centre and $1\circ uv$ for the petal at edge 1. Contrarily to the previous cases, this time y and u are not in contact with the same centre. Accordingly, we shall obtain two flowers and, there will probably be some choice. However, as we shall see, the choice cannot be arbitrary as the considered flower are not completely independent: they share a petal which we shall call the **third petal**, which shares the red-vertex belonging to both parental petals. We denote $\alpha\beta\gamma\circ$ the pattern of this petal. We note that the successor constraint applies to y and α as they are in contact with the same centre and adjacent with respect to it and that, for a similar reason, it also applies to γ and u.

Now, we note that the petal at the edge $\overline{6}$ of the centre is $\overline{66}7\circ$. As we noted in the previous study, such a petal abuts to both an **8**-flower and to a G_ℓ-flower by its edges $\overline{6}$. Accordingly, the other edge $\overline{6}$ of the petal is in contact with a G_ℓ-centre and as x is adjacent to that $\overline{6}$, the successor constraint and the orientation entail that $x = 7$. Accordingly, the pattern of the parental petal at edge 7 is $77y\circ$. From table 2, we can see that there are exactly three such patterns: $772\circ$, $77\overline{5}\circ$ and $776\circ$. We note that none of them occurs in an **8**-flower.

Similar considerations hold with the petal at edge $\overline{2}$ which is $1\overline{22}\circ$. Such a petal abuts to an **8**-centre and to a G_r-one by its two edges $\overline{2}$. And so, the second edge $\overline{2}$ of this petal is in contact with a G_r-centre. As v is adjacent to this second edge $\overline{2}$, it is also in contact with the G_r-centre, see Figure 34. By the successor constraint and the orientation induced by a G_r-centre, we conclude that $v = 1$. Accordingly, the pattern of the parental petal at edge 1 is $1\circ u1$. Table 2 shows us that there are exactly three such patterns: $1\circ 61$, $1\circ 21$ and $1\circ\overline{3}1$. We note that here also, none of these patterns occurs in an **8**-flower. This confirms that there cannot be more than one **8**-flower around

a red-vertex.

We shall consider each case with the petal at edge 7 and, at the same time, we shall determine the third petal and the third centre to which it abuts.

Consider 772∘. Table 2 shows that this petal occurs only with an F-centre. With the successor constraint and the orientation induced by the F-centre, this entails $\alpha = 1$. There are a lot of patterns $1\beta\gamma\circ$. Table 2 gives us all of them: $1\overline{3}1\circ$, $1\overline{4}7\circ$, $141\circ$, $1\overline{22}\circ$, $151\circ$, $137\circ$ and $157\circ$.

This gives us $\gamma \in \{1, \overline{2}, 7\}$. Next, the successor constraint on γ and u indicates that for $\gamma = 1$ $u \in \{2, \overline{2}, 7\}$. And so, the single possibility is $1\circ 21$ which corresponds to a G_ℓ-centre. For the third petal, we have then three possibilities, the patterns with $\gamma = 1$: $1\overline{3}1\circ$, $141\circ$ and $151\circ$. Table 2 indicates that the corresponding flower is, respectively, an F-flower, a G_ℓ-flower and a G_r-flower. This corresponds to the fact that in a G-flower, the flower which is on the right-hand side of the F-son is a G_ℓ-flower. This is also the case in an F-flower for its right-hand side F-son. Figure 34 shows us that indeed, petal $1\overline{3}1\circ$ stands between the right-hand side F-son of an F-flower and the G_ℓ-son which is on its right-hand side.

Now, consider the case when $\gamma = \overline{2}$. This induces tile $1\overline{22}\circ$ which is in contact with both an **8**-flower and a G_r-flower by its edges $\overline{2}$. Now, as the **8**-flower cannot abut with u as no petal at edge 1 of the main centre can belong to an **8**-flower at its edge u, we have that u is in contact with a G_r-centre. Accordingly, by the successor constraint and the orientation, $u = \overline{3}$ and this gives us $1\circ\overline{3}1$ as the petal at 1. Note that the fact that the third flower is an **8**-centre is in correspondence with the fact that the G_r-centre is on the right-hand side of the F-centre.

At last, consider $\gamma = 7$. The patterns $1u7\circ$ are: $1\overline{4}7\circ$, $137\circ$ and $157\circ$. They fit either with an F-centre or an **8**-one. Accordingly, taking into account the orientation, the successor constraint gives $u = 6$ which provides us with $1\circ 61$ for the parental petal at edge 1. All the patterns we have just seen are possible for the third petal. We can see that $137\circ$ and $157\circ$ give rise to an **8**-flower only, corresponding to the petal which is between the second and the third F-son of an **8**-flower and the third and fourth, respectively. For what is $1\overline{4}7\circ$, it is possible with an **8**-flower: it is then between the first and the second F-son. It is also possible with an F-flower: it is then between the two F-sons of the flower.

Now, consider the case when the petal at edge 7 is $77\overline{5}\circ$. This tile occurs

only with G_ℓ-centres. Accordingly $x = 5$ and, from the successor constraint and the orientation, $\alpha = \overline{6}$. And so, the third petal is $\overline{66}7\circ$. This gives us $\gamma = 7$ and so, from the successor constraint, $u \in \{6, \overline{6}, 1\}$. As $u = 1$ corresponds to a pattern which does not exist in table 2, we conclude that only $1\circ 61$ matches with the constraints for the parental petal at edge 1. This corresponds to an F-flower.

As we know, a petal $\overline{66}7\circ$ is in contact with both a G_ℓ-centre and an **8**-one by its edges $\overline{6}$. We know that the parental petal at edge 7 is also in contact with a G_ℓ-flower by its edge $\overline{5}$. Accordingly edge α of the third petal is also in contact with this G_ℓ-flower. And so, the second edge $\overline{6}$ of the third petal is in contact with an **8**-flower. This corresponds to the fact that we have a G_ℓ-flower on the left-hand side of an F-son of a flower. This may occur only in **8**-flowers as already noted. In the other flowers, the flower which is on the left-hand side of an F-son or the left-most F-son is a G_r-flower.

At last, consider the case when the parental petal at edge 7 is $776\circ$. From table 2, we can see that such a tile only occurs in G_r-centres. Accordingly, the orientation and the successor constraint give $\alpha = 7$. From table 2 again, the patterns of the form $7\beta\gamma\circ$ are: $772\circ$, $7\overline{5}7\circ$, $737\circ$, $77\overline{5}\circ$, $747\circ$ and $776\circ$.

From the possible patterns of the parental petal at edge 1, we know that $u \in \{2, \overline{3}, 6\}$ and from what we have above we can see that $\gamma \in \{2, \overline{5}, 6, 7\}$. If $u = 2$, we have $1\circ 21$ at edge 1 of the main centre. But as a non-parental petal, $1\circ 21$ only belongs to G_ℓ-flowers. Accordingly, due to the orientation and from the successor constraint, we should have $\gamma = 1$ which is impossible. If $u = \overline{3}$, we have petal $1\circ\overline{3}1$ which requires a G_r-flower from table 2. But in this case, we need $\gamma = \overline{2}$, which is not the case.

We remain with $u = 6$ which yields $1\circ 61$, a petal which occurs with F-flowers only according to table 2. From the orientation and the successor constraint, this gives us $\gamma = 7$, which is possible. Then, we obtain the following patterns for the third petal: $7\overline{5}7\circ$, $737\circ$ and $747\circ$. From table 2, we get that the third centre is of type F, G_ℓ and G_r, respectively. All these cases are possible as the situation of a G_r-flower at the left-hand side of an F-son occurs in these cases exactly.

We can sum up this results in tables 5. The first one gives the parental tiles. For each couple of parental tiles, the second gives the third petal and the third centre.

	F-F	F-G_ℓ	F-G_r	G_ℓ-F	G_r-F
1	11∘6	11∘2	11∘$\overline{3}$	11∘6	11∘6
7	2∘77	2∘77	2∘77	$\overline{5}$∘77	6∘77

	F-F				F-G_r	G_ℓ-F
3rd	1$\overline{4}$7∘	1$\overline{4}$7∘	137∘	157∘	1$\overline{22}$∘	$\overline{66}$7∘
	F	**8**	**8**	**8**	**8**	**8**

	F-G_ℓ			G_r-F		
3rd	1$\overline{3}$1∘	141∘	151∘	7$\overline{5}$7∘	737∘	747∘
	F	G_ℓ	G_r	F	G_ℓ	G_r

Table 5 *Above: the possible values of the parental tiles of an* **8***-flower. Below, in two tables, the third petal and the third centre.*

Note that table 5 shows that the two centres defined by the petals at edge 7 and at edge 1 cannot be both G-centres, a situation which was already ruled out by the definition of the splitting.

Accordingly, the proof of Lemma 5 is completed. ■

5.2.2 The algorithm

In Lemma 2, we already indicated that the mantilla can algorithmically be constructed.

In this section, we precisely describe the construction algorithm. This algorithm is an important piece for the proof of the main theorem of this report. The algorithm which we shall use later is an adaptation of this one to the changes which will introduce in the set of tiles itself. Basically it will be the present algorithm.

The algorithm works on two copies of the grid $\{7, 3\}$. We may imagine that one of them is transparent and that it is laid on the other. This boils down to assume that we have a bijection between the two copies of the grid. This bijection can be materialized by the coordinates which were introduced in [3]. We then fix a central tile in each copy which, by definition, receives coordinate 0.

One copy is the **background**. It is used by the algorithm to compute a sequence of balls B_n: B_n is the set of tiles which are at a distance at most n from the central tile.

The other copy is the **main plane** where the algorithm constructs the mantilla.

To that purpose, we make use of **truncated sectors** built from the sectors which we defined in section 3.2. For this, we define **levels**.

Definition 2 *Two neighbouring tiles are at the* **same level** *if and only if they share a green side. A centre is at the level of the majority of its non-parental tiles.*

This definition can be extended by transitivity. Accordingly, by definition, two tiles τ_b and τ_e are at the same level if and only if there is a sequence τ_i of tiles with $i \in \{0..k\}$ for some natural number k such that $\tau_i = \tau_b$, $\tau_k = \tau_e$ and τ_i and τ_{i+1} share a green side for $i \in \{0..k-1\}$. Now, the relation **to be at the same level** is an equivalence relation and, by definition, a **level of the mantilla** is an equivalence class for this relation. Next, we can order the levels. To this purpose, we fix a tile T_0 which, by definition, will be at level 0. The class of all tiles at the same level as T_0 define **level 0** of the mantilla.

Now, consider the levels inside a sector. The connections are as follows:

Lemma 6 *In the sector headed by an F-flower or a G-flower, the centres of the F- and G-sons are at the same level as well as the* **8***-sons which are in contacts with its petals at edges* 6 *and* 2 *in the case of an F-flower, at edges* 2 *and* $\overline{5}$ *in the case of a G_ℓ-flower, at edges* $\overline{3}$ *and* 6 *in the case of a G_r-flower. In the sector headed by an* **8***-flower, the centres of its F-sons are also at the same level as well as the centres of the two G-flowers which are in contact with the parental petals of the* **8***-flower.*

Proof. Obvious.

At this point, we remind the reader of the fact that the splitting of a sector, whichever it is, generates a tree which we call the **spanning tree** of the splitting, see [12, 18].

Now, as indicated by Figures 38, 39 and 40 below, we have that a level of the mantilla inside a sector follows a level of the spanning tree for this sector.

Now, following the levels on neighbouring sectors, we can see that the majority of the non-parental tiles of the F- and G-flowers whose parental tiles

are at level 0, are at the same level and we define this level as **level 1**. It is plain that this definition can be repeated by giving to level 1 the rôle of level 0. By induction, we construct such a numbering, downwards and upwards. The number attached to a level is called its **depth**. As a consequence, we define an **order** of the levels which is induced by their depth. Again following levels in a sector, we can see that a level which does not contain the leading centre of the sector but another tile inside the sector defines a level which splits its complement in the sector into two regions: one contains the levels which are higher than this one, the other the levels which are lower.

Now, we can define a sequence of sectors $\{\Sigma_n\}_{n\in I\!N}$ such that $\Sigma_n \subset \Sigma_{n+1}$ and $\bigcup_{n\in I\!N} \Sigma_n = I\!H^2$. We call such a sequence a **covering** sequence of sectors. This construction reminds a construction which we performed in [18]. The proof is based on the property that a sequence of angular sectors may cover the hyperbolic plane, whatever we choose the angle for the members of the sequence.

We already saw in the proof of Lemma 2 that it is possible to construct a covering sequence of sectors by the completion process of sectors. Taking a sequence of covering sectors Σ_n of the hyperbolic plane we get:

Lemma 7 *Let $\mathcal{P}_n$ be a level of the mantilla where n is its depth. Then the complement of $\mathcal{P}$ in the hyperbolic plane consists of two regions. One is the union of levels $\mathcal{P}_m$ with $m < n$, it is said to be* **upper** *than $\mathcal{P}_n$. The other region is the union of levels $\mathcal{P}_m$ with $m > n$ and is said to be* **lower** *than $\mathcal{P}_n$.*

Evidently, we have the following:

Lemma 8 *In an F-flower, the parental tiles and the centre are at level n and the non-parental tiles are at level $n+1$. In an* **8***-flower, the centre and all the petals are at the same level. In a G_ℓ-flower, the parental petals, the centre and the petal at edge $\overline{2}$ are at level n while the remaining petals are at level $n+1$. In a G_r-flower, the parental petals, the centre and the petal at edge $\overline{6}$ are at level n while the remaining petals are at level $n+1$.*

Accordingly, we consider a truncated sector as the intersection of a sector with the levels which are lower than a fixed one. To avoid trivialities, we assume that the fixed level intersects the sector.

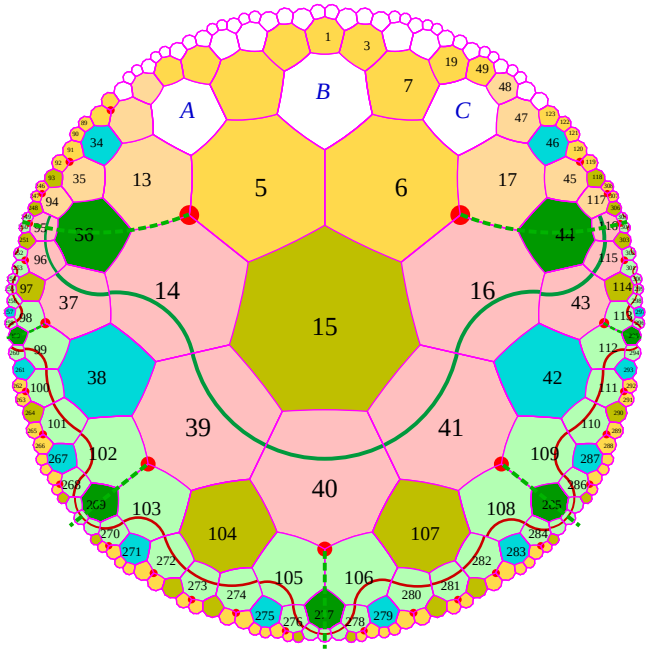

Figure 38 *Level* 0 *and level* 1 *in an* F*-sector.*

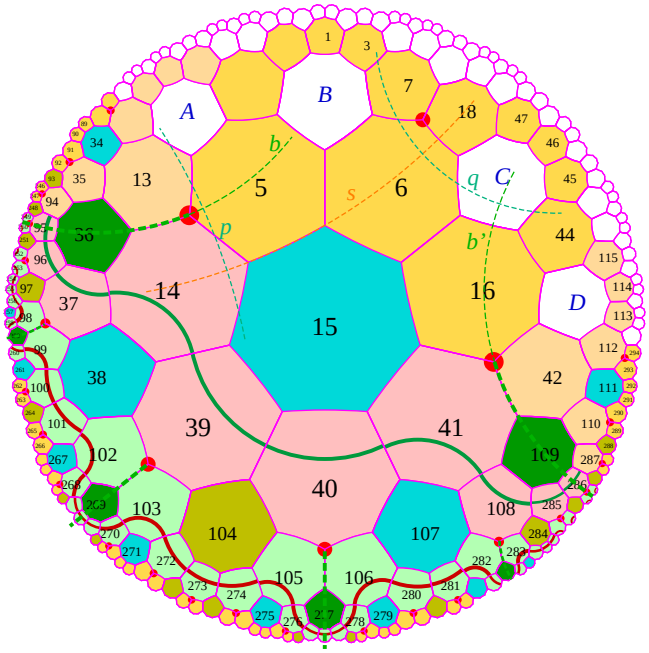

Figure 39 *Level* 0 *and level* 1 *in a* G*-sector.*

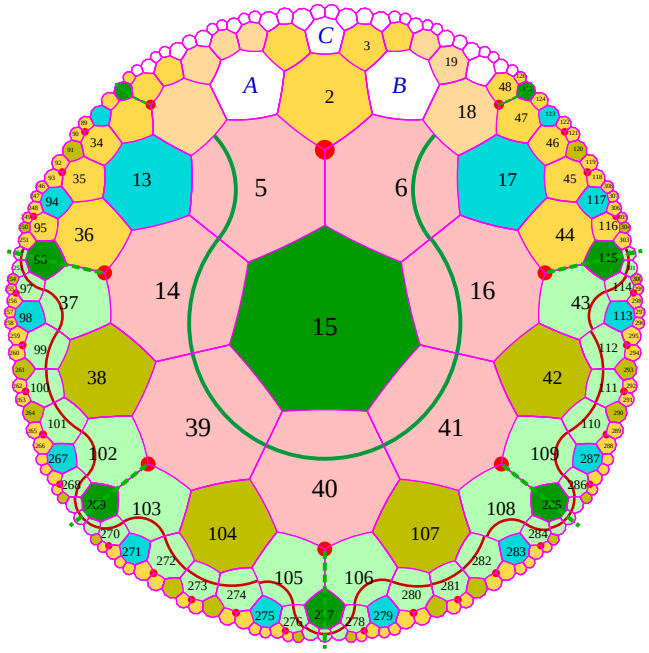

Figure 40 *Level* 0 *and level* 1 *in an* **8***-sector.*

Now, we consider the algorithm of Figure 41.

Accordingly we proved:

Lemma 9 *The mantilla can be constructed by the set of* 21 *prototiles given by tables* 2 *and* 1 *as well as Figure* 42 *applying the algorithm of Figure* 41.

Now, we can indicate another property of the algorithm. As it clearly appears on its description itself, the algorithm is fully deterministic for the construction of a sector once its leading centre is fixed. But it is non-deterministic in the construction of the next leading centre. It is not difficult to see that there are infinitely many different constructions for the mantilla. Indeed we have continuously many such solutions as it is clear from step 3 of the algorithm.

1. Pick at random a tile T_0 from the set of tiles of Figures 26 and 27. This is time t_0.
2. If T_0 determines a centre C_1, take and complete the non-parental tiles of C_1. If T_0 does not determine a centre, take at random a tile (petal or centre) which matches with T_0. Then, C_1 is determined and complete its non-parental tiles. This is level 0 of the sector. Next, choose an F-son of C_1 to be the centre B_0 of the balls. Now, go on in the sector, until its level 1 is complete. When this is done, it is time t_1. Then B_1, the ball of radius 1 around B_0 is contained in the union of the tiles which are placed up to now. Say that C_1 is the leading centre of the sector. Recall that once a tile is placed it cannot be removed.
3. At time t_n, choose at random two tiles among the possible parental tiles of C_n, using tables 3, 4 and 5. If C_n is an F- or G-centre, the parental tiles determine a centre C_{n+1} which defines a new sector which contains B_{n+1}. If C_n is an **8**-flower, the parental tiles determine two centres A and B which share a third tiles which has a red-vertex in common with the parental tiles. Also choose the third tile at random among the possible ones using the appropriate tables 5. It determines a centre C_{n+1} which leads a sector which contains B_{n+1}. Once C_{n+1} is obtained, complete the new sector led by C_{n+1} downto level ℓ_{n+1} such that B_{n+1} is covered. When the sector up to level ℓ_{n+1} is complete, it is time t_{n+1}.
4. Increment n. Go to step 3.

Figure 41 *The algorithm to construct the mantilla.*

We already indicated a point which we shall prove later: there are indeed many periodic solutions among the ones which can be produced by the algorithm. Now, we turn to the main property of the algorithm:

Theorem 3 *The algorithm of Figure* 41 *can produce all the possible realizations of the mantilla.*

Proof. Assume that we have a solution for the mantilla. We shall apply the algorithm. But we run it in **checking mode**. This means that each random choice indicated in Figure 41 is replaced by what is given by the solution at this point of the construction. As any possible solution must conform to tables 3, 4 and 5, our claim is proved. ■

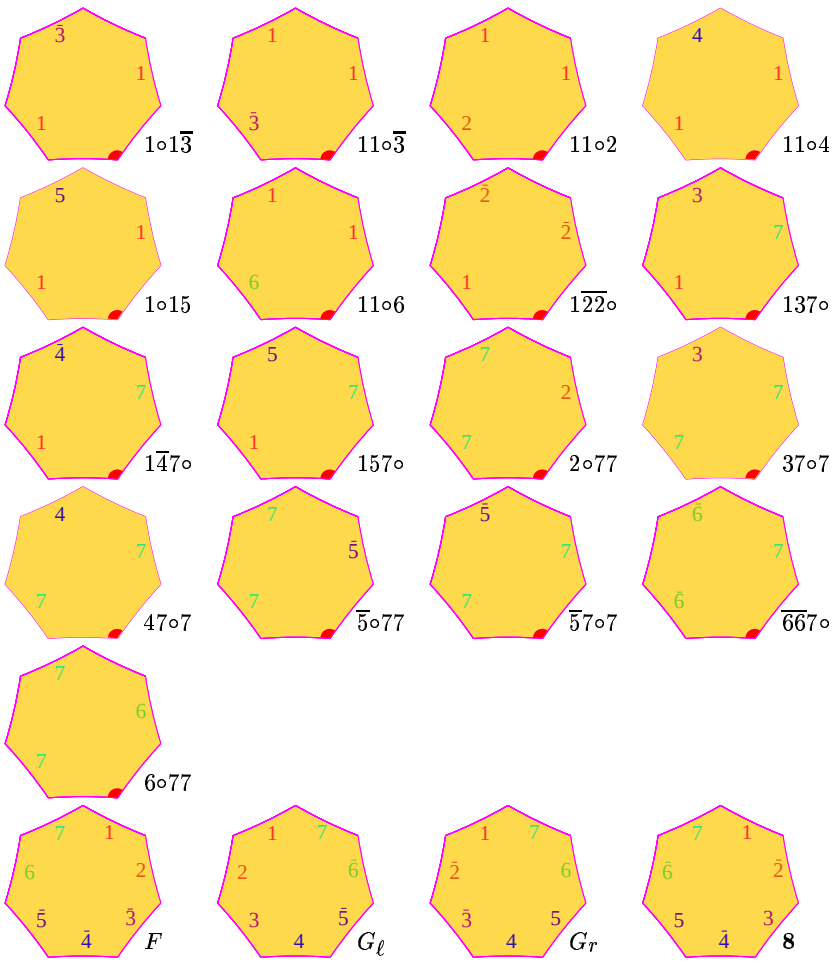

Figure 42 *The* 21 *prototiles for the mantilla. The lowest row indicates the tiles for the centres. The petals of the flowers are to be taken among the first* 17 *prototiles of the other rows.*

Figure 42 does not yet display the set of prototiles for the skeleton. This will be done later by the change of four tiles which are the nonparental tiles of a G-flower which are parental tiles of their F-sons.

5.3 The computing regions

Here, computing regions are defined with the help of Fibonacci trees which will be generated by a simple rule. We shall study the properties of the trees

in order to select some of them which will constitute the computing regions. The selection will keep infinitely many such regions.

Then, we shall explain how we proceed to the computation. In both cases, we also consider the needed set of tiles.

5.3.1 The trees

First, we define what we shall from now on call a tree.

Definition 3 *Say that a set of tiles of tiling* $\{7, 3\}$ *is within a* **tree** *if the centres of the tiles belong to the angular sector defined by two mid-point lines* β_1 *and* β_2 *issued from the mid-point* A *of an edge* η *of the tiling whose angle is* α*, the angle which defines the angular sectors of tiling* $\{7, 3\}$*. We also assume that the line supporting* η *is the bisector of the angle made by* β_1 *and* β_2 *at* A*. The set of tiles is called the* **area** *delimited by the tree or, simply, the* **area of the tree**.

Next, we define where the trees are placed. To this aim, we use a very simple criterion:

Definition 4 *In the mantilla, we call* **candidate to a computing region**, *simply* **candidate**, *the area of a tree whose root is the centre of an* F*-flower which is the* F*-son of a* G*-flower.*

We shall prove two basic properties of the candidates to computing regions: they are completely contained in the sector defined by the F-flower whose centre is their root. We also prove that two candidates have either distinct areas or the area of one contains the other area.

Lemma 10 *In the mantilla, a candidate is completely contained in the sector defined by the* F*-flower which defines the root of its tree.*

Proof. Consider Figure 43. Using the numbering of the tiles, note that a tree is rooted in tile 104 and that the mid-point lines which define it start on the mid-point of the edge shared by tiles 39 and 40. Denote by β_ℓ and β_r the respective left- and right-hand mid-point lines which we just considered. Tile 104 is the centre of an F-flower whose sector is delimited by the lines which support the common edge of tiles 102 and 103 on the left-hand side

and the common edge of tiles 105 and 106 on the right-hand side. Denote these lines by δ_ℓ and δ_r respectively.

Now, it is not difficult to see that the line γ_ℓ which is shared by the tiles 39 and 15 in Figure 43 is perpendicular to both β_ℓ and δ_ℓ. And so, as these lines are non-secant, two of the half-planes which they define are disjoint. They are precisely the half plane containing the tree, delimited by β_ℓ, and the half-plain delimited by δ_ℓ which does not contain the sector.

A similar result holds for γ_r, the line which supports the common edge between tile 40 and tile 15: $\gamma_r \perp \beta_r$ and $\gamma_r \perp \delta_r$. With a similar remark about the half-planes defined by β_ℓ, β_r, δ_ℓ and δ_r, we conclude that the tree is strictly contained in the sector. ■

Indeed, we can say more: between the leftmost branch of the tree and the left-hand border of the sector, new trees appear. This can be seen in Figure 43. The configuration of tile 104 is exactly that of tile 2. Note that tile 17 plays for tile 2 the rôle which is played by tile 277 for tile 104. There is a shift transforming the configuration of tile 2 into that of tile 104. The same shift applied to tile 104 provides us with a new tree between the rightmost branch of the tree rooted at tile 104 and the right-hand border of the region defined by the F-flower whose centre is tile 104.

Now, let us start from the parental petals of an F-flower which is the F-son of a G-flower. There are two possible couples of such petals: 37∘7 and 1∘14 in the case of a G_ℓ-flower, 47∘7 and 1∘15 in the case of a G_r-flower.

Consider the right-hand border.

We successively meet the following tiles, starting from the first one, say $1\circ 1\alpha$ with $\alpha \in \{4, 5\}$:

rank	1	2	3	4	5	6	7	8	9	10	11
tile	7	2	6	5	15	14	39	38	102	101	267
pattern	$1\circ 1\alpha$	F	$2\circ 77$	$1\circ 1\overline{3}$	G_ℓ	$11\circ 2$	$37\circ 7$	G_r	$6\circ 77$	$1\circ 15$	G_ℓ
sides	$\diamond$–1	1–2	2–$\diamond$	$\diamond$–1	1–2	2–$\diamond$	$\diamond$–7	7–6	6–$\diamond$	$\diamond$–1	1–2

Table 6 *The ultimately periodic path followed by the mid-point line of the rightmost branch of a computing tree. The table indicates the patterns of the tiles crossed by the mid-point lines. For each tile, it also indicates the sides of the tile which are crossed. The $\diamond$ sign indicates a green side.*

We note that the sequence of tiles crossed by the mid-point lines is ultimately periodic. The period involves six tiles and the aperiodic part at the

beginning of the sequence involves four tiles. Note that the table also indicates the sides which are crossed by the mid-point line for each tile involved by the border. In the table, a green side is represented by $\diamond$.

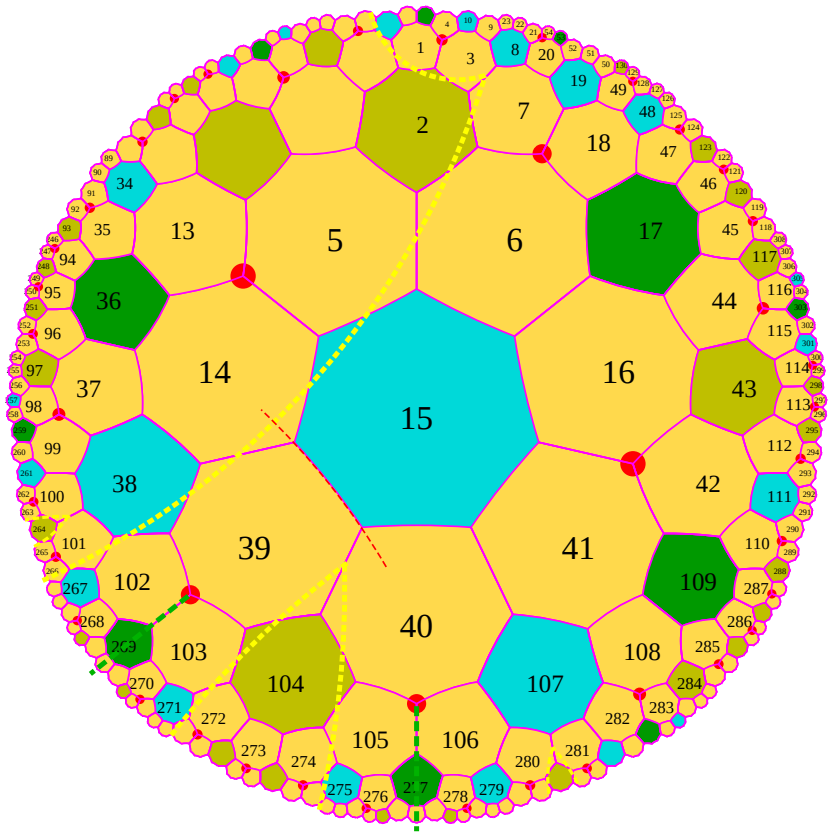

Figure 43 *The tree generated by an F-flower which is the son of a G-flower.*

A similar table can be established for the left-hand border where the first tile is $\beta 7 \circ 7$ with $\beta \in \{3, 4\}$:

rank	1	2	3	4	5	6	7	8	9	10	11
pattern	$\beta 7 \circ 7$	F	$11 \circ 6$	$\overline{57} \circ 7$	G_r	$6 \circ 77$	$1 \circ 15$	G_ℓ	$11 \circ 2$	$37 \circ 7$	G_r
sides	$\diamond$–7	7–6	6–$\diamond$	$\diamond$–7	7–6	6–$\diamond$	$\diamond$–1	1–2	2–$\diamond$	$\diamond$–7	7–6

Table 7 *The ultimately periodic path followed by the mid-point line of the rightmost branch of a computing tree. Same conventions as in table* 6.

Taking into account that the construction of the tiling is deterministic when we go from a centre to its non-parental petals, the sequences defined by tables 6 and 7 for the ranks, the patterns and the sides are the same for all trees. Accordingly, we proved the following result:

Lemma 11 *The sequence of the tiles crossed by the border of the tree is ultimately periodic. The period is the same for the right-hand- and for the left-hand borders.*

Let us look again at the tiles involved in the border.

The initial tiles $1\circ 1\alpha$ and $\beta 7\circ 7$ may occur in the period. This is the case for $\alpha = 5$ and $\beta = 3$ only. Consider a tile $1\circ 15$. When it is the first tile of a tree, the border is the right-hand one and it crosses sides $\diamond - 1$. We note that the concerned sides are on the left-hand side of edge 5 when the red-vertex is below this edge. When it appears in the periodic part of the border, the same tile is also crossed at sides $\diamond - 1$. As we can see on Figure 43, the crossed side are on the other side of edge 5, with the red-vertex again in a below position, see tile 101 in Figure 43. This means that another border may use this tile as indicated. A similar remark holds for tile $37\circ 7$. It is crossed along sides $\diamond - 7$. But the crossed sides are on the right-hand side of edge 3 when the red-vertex of the tile is below this edge. When tile $37\circ 7$ again appears in the period of a border, it is crossed also at edges $\diamond - 7$, but on the right-hand side of the tile when the red-vertex is below edge 3, as can be noted in Figure 43 with tile 39. This means that this tile may also be crossed by another border at the same time. In Figure 43, this is the case for tile 39.

Another tile can be crossed by two borders at the same time. It is, of course, the F-tile which is at the root of the tree. The involved edges are $1-2$ on one side and $7-6$ on the other.

Let us look at the other tiles. Using tables 6 and 7 and Figure 43, we have the following properties:

- tiles crossed by a right-hand border only: $1\circ 14$, at edges $\diamond - 1$ only; $2\circ 77$, at edges $2 - \diamond$ only; $1\circ 1\overline{3}$, at edges $\diamond - 1$ only;
- tiles crossed by a left-hand border only: $47\circ 7$, at edges $\diamond - 7$ only; $11\circ 6$, at edges $6 - \diamond$ only; $\overline{5}7\circ 7$, at edges $\diamond - 7$ only;
- tiles crossed by one border only, when the left-hand border, when the right-hand one: G_ℓ, at edges $1-2$ only; $11\circ 2$, at edges $2 - \diamond$ only; G_r, at edges $7-6$ only, $6\circ 77$ at edges $6 - \diamond$ only;

• tiles possibly crossed by two borders: F, always at both edges $1-2$ and $7-6$; $1\circ 15$ at edges $\diamond-1$, when both, when one of them; $37\circ 7$ at edges $\diamond-7$, when both, when one of them.

Next, we have the following property of the mid-point lines which we consider:

Lemma 12 *Consider two mid-point lines ℓ_1 and ℓ_2 of tiling $\{7,3\}$. Recall that we consider lines joining the mid-points of two consecutive edges of tiles of the tiling. Then if ℓ_1 and ℓ_2 do intersect, they meet at the mid-point of an edge of a tile.*

Proof. Indeed, assume that ℓ_1 and ℓ_2 meet at a point A. On a mid-point line of the tiling, any point is between two mid-points of two consecutive edges of a tile, as can easily be seen in Figure 43. Let A_1 and B_1 be the such points for ℓ_1 with respect to A and A_2 and B_2 for ℓ_2 with respect to A too. By construction of a mid-point line of the tiling, if A is inside a tile τ, A_1 and B_1 must be vertices of τ. It is clear that A_2 and B_2 must be the same vertices as this happens also on the same tile. And so, this is impossible if $\ell_1 \neq \ell_2$. Accordingly, A belongs to the border of a tile and, by construction of a mid-point line, it is the mid-point of an edge of a tile. ■

Now, if we look at what we observed on the tiles involved in borders, the single possible meeting of two borders is the mid-point of the common edge shared by tiles $37\circ 7$ and $1\circ 4$, or tiles $47\circ 7$ and $1\circ 15$.

Consequently:

Lemma 13 *The border of a tree does not meet the border of another tree.*

Proof. There is no tile which would allow to realize the meeting as the only ones which can contain the intersection of two mid-point lines are the parental petals of the root of the tree. ■

What we proved on the border of a tree and of a sector also proves Lemma 13. Figure 43 indicates that along a border, new trees appear, both outside and inside the area of the tree. They are generated by the G_ℓ's and G_r's tiles which periodically occur among the tiles crossed by the border. Tiles 39 and 101 are crossed by two borders and they illustrate both situations. At the same level, other F-sons of a G-centre are further and, indeed, they belong to different sectors. They belong either to a sector which is outside the sector defined by the root of the initially considered tree, or

they belong to a sector which is inside the area of the tree. In the first case, as sectors define a partition starting from a given level, the property of the lemma follows. In the second case, it is not difficult to see that the border of a sector involves **8**-centres which occur periodically along the border as we go down along it. As **8**-centres have only F-sons, these F-centres do not generate trees. This is why, trees are rather 'far' from such a border. And so, using the levels we introduced in the mantilla, we can see that the trees which are generated at the same level always occur in sectors which have no border in common. Look at Figures 38 and 39 and at Figures 18 and 19. Also, Figure 43 contains two examples of the situation when borders of different trees are closest at possible. Tile 39 and 101 are crossed by two borders. Tile 39 is crossed by the right-hand border of the tree rooted at 2 and it is also crossed by the created left-hand border of the tree rooted at tile 104. For tile 101, it is crossed by the right-hand border of the tree rooted at 2 and also by the just now created right-hand border of the tree rooted at tile 264 as the latter tree is inside the former. Note that this is the single possibility for a tree to be so closed to another one. 'Old' trees are indeed very far from each other.

Now we get an important corollary of Lemma 13:

Lemma 14 *In the mantilla, two trees have either disjoint areas or one area contains the other.*

Proof. Assume that we have two trees A_1 and A_2 such that their areas intersect and that none of them contains the other. Let τ_i be the root of A_i, $i \in \{1, 2\}$. Let τ be a tile of the intersection. In the tree A_1, there is a path from τ to τ_1 which consists of tiles of A_1. As $\tau_1 \notin A_2$, there is a last tile of A_1 on the path, say σ_1, which meets the border of A_2. As σ_1 is on the border of A_2, there is a last tile of A_2, among those which are on the border from σ_1 to τ_2, say σ_2 which meets the border of A_1. And so, σ_2 contains both the border of A_2 and the border of A_1. Considering the triangle defined by τ_1, τ_2 and σ_1, the border of A_2 must meet the border of A_1, a contradiction with Lemma 13. ■

Now, we define the following notion:

Definition 5 *A* **thread** *is a set $\mathcal{F}$ of trees of the mantilla such that:*

(i) if $A_1, A_2 \in \mathcal{F}$, then either $A_1 \subset A_2$ or $A_2 \subset A_1$;

(ii) if $A \in \mathcal{F}$, then there is $B \in \mathcal{F}$ with $B \subset A$, the inclusion being proper;

(iii) if $A_1, A_2 \in \mathcal{F}$ with $A_1 \subset A_2$ and if A is a tree of the mantilla with $A_1 \subset A$ and $A \subset A_2$, then $A \in \mathcal{F}$.

Definition 6 *A thread $\mathcal{F}$ of the mantilla is called an* **ultra-thread** *if it possesses the following additional property:*

(iv) there is no $A \in \mathcal{F}$ such that for all $B \in \mathcal{F}$, $B \subset A$.

Lemma 15 *A set $\mathcal{F}$ of trees of the mantilla is an ultra-tread if and only if it possesses properties (i) and (ii) of definition 5 together with the following:*

(v) for all $A \in \mathcal{F}$ and for all tree B of the mantilla, if $A \subset B$, then $B \in \mathcal{F}$.

Proof. Indeed, an ultra-thread satisfies (v). Otherwise, let $A \in \mathcal{F}$ and B be a tree of the mantilla such that $A \subset B$ and $B \notin \mathcal{F}$. From (iii) we get that for any tree C of the mantilla such that $B \subset C$, then $C \notin \mathcal{F}$. From Lemma 14, if $A \subset B$, A is a sub-tree of B and so, considering the path leading from the root of A to the root of B, there are at most finitely many trees D of the mantilla such that $A \subset D \subset B$. Note that if two trees D_1 and D_2 of the mantilla contain A, we have $D_1 \subset D_2$ or $D_2 \subset D_1$ by Lemma 14. And so, considering the biggest tree D between A and B with $D \in \mathcal{F}$, we obtain an element D in $\mathcal{F}$ such that for all $A \in \mathcal{F}$, $A \subset D$. This contradicts (iv). And so, if B is a tree of the mantilla which contains A, it belongs to $\mathcal{F}$.

Conversely, if a set $\mathcal{F}$ of trees of the mantilla satisfy (i), (ii) and (v), it obviously satisfies (iii) and (iv). ■

Accordingly, an ultra-thread is a maximal thread with respect to the inclusion.

Note that the mantilla may possess ultra-threads and it may possess none of them. Indeed, consider the algorithm of Figure 41 and apply the following strategy:

- at time t_{2n}, in step 3, for the choice of C_{n+1}, we take an F-centre;
- at time t_{2n+1}, in step 3, for the choice of C_{n+1}, we take a G-centre, choosing at random between a G_ℓ- and a G_r-centre.

Then it is clear that the sequence constructed by C_n defines an ultra-thread.

Consider now another execution of the algorithm of Figure 41 where the strategy is now:

- at time t_n, in step 3, take for C_{n+1} an **8**-centre.

Then as the sectors defined by C_n are increasing sectors, all the threads existing at time t_n have a maximal tree at some level with respect to C_n. As the sequence of flowers above C_n do not contain the root of a tree, we have that the maximal trees we define at time t_n are not included in a tree, by induction on the construction of sequence $\{C_n\}$. The tree which appear at higher levels generate trees which are all outside the sector defined at time t_n.

Here are additional properties of the ultra-threads.

Lemma 16 *Let $\mathcal{U}$ be an ultra-thread. Then, $\mathcal{U} = \{A_n\}_{n\in\mathbb{Z}}$, where $A_n \in \mathcal{U}$ for all $n \in \mathbb{Z}$ and $A_n \subset A_{n+1}$, the inclusion being proper. We also have that $\bigcup_{n\in\mathbb{Z}} A_n = \mathbb{H}^2$.*

Proof. By properties (ii) and (v) of the ultra-threads, there is a sequence $\{C_n\}_{n\in\mathbb{Z}}$ such that $C_n \subset C_{n+1}$ for all n in $\mathbb{Z}$, the inclusion being proper. As C_n is a sub-tree of C_{n+1}, there is a path which goes from the root of C_n to that of C_{n+1}. Along these paths, there are finitely many trees of the mantilla. By (v), these trees also belong to $\mathcal{F}$. Accordingly, we obtain $\{A_n\}$ by appending these trees to $\{C_n\}$.

From our study of trees issued from a G-centre crossed by the border of a given tree of the mantilla, we know that we have the following property. If A and B are two trees of the mantilla with $A \subset B$, the inclusion being proper, consider the set of tiles A' which is obtained by appending a layer of one tile along the borders of A and outside A. Then, we have that $A' \subseteq B$.

Now, fix a tile τ_0 in A_0. From what we just noted, we obtain that $B_1 \subset A_1$ and, by induction, that $B_n \subset A_n$ where B_h is the ball of radius h around τ_0. Accordingly, $\bigcup_{n\in\mathbb{Z}} A_n = \mathbb{H}^2$. ■

Lemma 17 *Let $\mathcal{U} = \{A_n\}_{n\in\mathbb{Z}}$ and $\mathcal{V} = \{C_m\}_{m\in\mathbb{Z}}$ be two ultra-threads. Then, there are two integers n_0 and m_0 such that $A_n = C_m$ for all n and m such that $n - n_0 = m - m_0$.*

Proof. Indeed, consider A_0. Then, as $\bigcup_{n\in\mathbb{Z}} C_n = \mathbb{H}^2$, there is m_0 such that C_{m_0} contains the root of A_0. Now, by Lemma 14, necessarily, $A_0 \subset C_{m_0}$ and so, $C_{m_0} \in \mathcal{U}$ by property (v) of the ultra-threads. This means that there is n_0 such that $A_{n_0} = C_{m_0}$. Now, by construction of $\{A_n\}$ and $\{C_m\}$, there is no tree of the mantilla between A_n and A_{n+1} and, similarly, between C_m and C_{m+1}. Accordingly, $A_{n_0+1} = C_{m_0+1}$. By induction, we get $A_{n_0+k} = C_{m_0+k}$ for all $k \in \mathbb{N}$. ■

5.3.2 The refined mantilla and its set of tiles

In order to define the computation areas, we need to define infinitely many of them and, if possible, in a such a way that they do not intersect. We shall start from the trees and, due to Lemma 14, it will be enough to prevent any tree to embed another one.

The previous lemmas, especially Lemma 17, indicates that if a mantilla does possess ultra-threads, morally it has a single one at infinity. Consequently, we may view mantillas with ultra-threads as particular cases and so, we shall restrict our attention to mantillas **without** ultra-threads.

Now, we define the following **sieving** procedure: as each thread has a maximal element, we select this element which will be called the **selected tree** and we erase all the other trees inside the selected tree. What we obtain by applying this procedure is called the **refined mantilla**.

Now, we turn to the description of the tiles which are needed to construct the refined mantilla. As previously, we deal with **prototiles** which are the tiles which can be copied as many times as needed.

We define the new set of tiles as follows:

First we duplicate the set of tiles of the mantilla and we call one set the **orange tiles** and we call the other the **green tiles**. We may imagine that the tiles have a coloured background: orange in the first set of tiles, green in the second. We shall consider that the orange tiles are involved in the construction of the original version of the mantilla and that the green tiles are involved to mark the areas of the selected trees of the refined mantilla. The representation of these tiles are given, below, by Figures 45 and 48.

Next, we make a change in the orange tiles: we **replace** tiles with patterns $1 \circ 14$, $1 \circ 15$, $37 \circ 7$ and $47 \circ 7$ by similar tiles which bear a green mark on the sides crossed by the border, see their representation in Figure 44, below and also in Figure 45.
In the set of green tiles, we do not put marks, see Figure 48 again. As a consequence, a tree cannot be built inside an area of green tiles.

Now, we define a new set of tiles for the border of the selected trees. These tiles are illustrated by Figures 46 and 47, below. They have two parts: an orange one and a green one. Both parts are separated by a piece of line which materializes the border. In our sequel, we shall use the following convention: we say that a border tile is orange or green depending on which colour the central part of the tile is.

We can subdivide the new set into three parts.

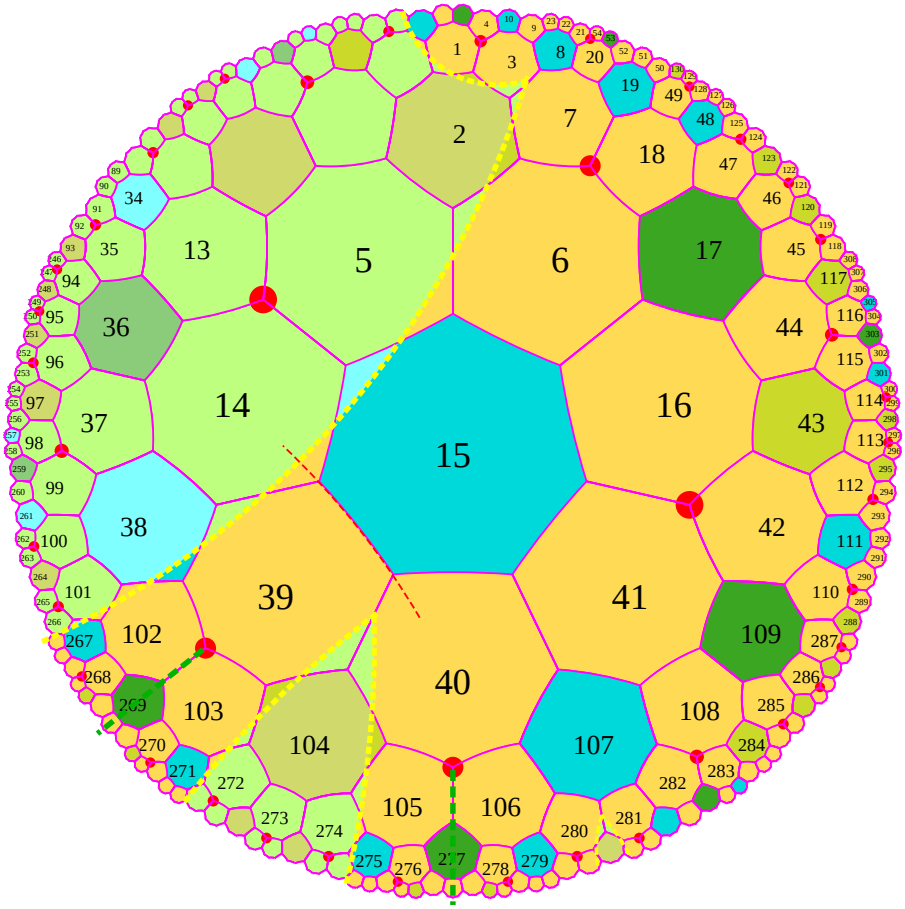

Figure 44 *Two selected trees in the refined mantilla. Note the green background of the selected trees. Also note that tile* 294 *is an F-son of a G-centre but, as it is inside a selected tree, it does not generate a tree.*

The first part consists of three tiles. Their characteristic property is that they are crossed at the same time by two borders which defines three parts for the colouring of the background of the tile. First, we have the F-tile which is the root of a tree of the refined mantilla. It is a green tile according to the above convention, but it has two orange parts corresponding to the beginning of the two borders. Then we have two orange tiles with patterns 1∘15 and 37∘7 which have two small green parts. They correspond to the case when two selected trees are very close to each other, because one of them has its root very close to the border of the other. Tile 37∘7 corresponds to

the case when the new tree is on the right-hand side of the older one. Tile 47∘7 corresponds to the case when the new tree is on the left-hand side.

pattern	$1\circ 1\alpha$	F	$2\circ 77$	$1\circ 1\overline{3}$	G_ℓ	$11\circ 2$	$37\circ 7$	G_r	$6\circ 77$	$1\circ 15$	G_ℓ
colour	or.	gr.	or.	gr.	or.	gr.	or.	gr.	or.	gr.	or.
sides	$\diamond$–1	1–2	2–$\diamond$	$\diamond$–1	1–2	2–$\diamond$	$\diamond$–7	7–6	6–$\diamond$	$\diamond$–1	1–2

pattern	$\beta 7\circ 7$	F	$11\circ 6$	$\overline{5}7\circ 7$	G_r	$6\circ 77$	$1\circ 15$	G_ℓ	$11\circ 2$	$37\circ 7$	G_r
colour	or.	gr.	or.	gr.	or.	gr.	or.	gr.	or.	gr.	or.
sides	$\diamond$–7	7–6	6–$\diamond$	$\diamond$–7	7–6	6–$\diamond$	$\diamond$–1	1–2	2–$\diamond$	$\diamond$–7	7–6

Table 8 *The colours are* **orange** *for* or. *and* **green** *for* gr.. *They are the colours of the central part of the considered tile. All tiles have two colours: a smaller part is in the other colour. Above: for the right-hand border; below: for the left-hand one.*

The second part corresponds to the tiles which are involved by a right-hand border. In the aperiodic part, besides the parental tiles of the root and the F-centre which is the root itself, we have tiles $2\circ 77$ and $1\circ 1\overline{3}$. The first one is orange while the second is green, see Figure 47, below. Then we have the tiles for the periodic part. Here, we have six new tiles: G_ℓ, $11\circ 2$, $37\circ 7$, G_r, $6\circ 77$ and $1\circ 15$. All these tiles are crossed by a single border defining two coloured back-grounds. Above, table 8 indicates which is the main colour of each tile, according to the border where it is used, see also Figures 47 and 46.

The third part corresponds to the left-hand border. We have tiles $11\circ 6$ and $\overline{5}7\circ 7$ for the aperiodic part. They are orange for the former and green for the latter. We have also six tiles for the periodic part. The patterns are the same as previously, but the colouring is different: green and orange parts are exchanged with respect to the tiles for the right-hand border.

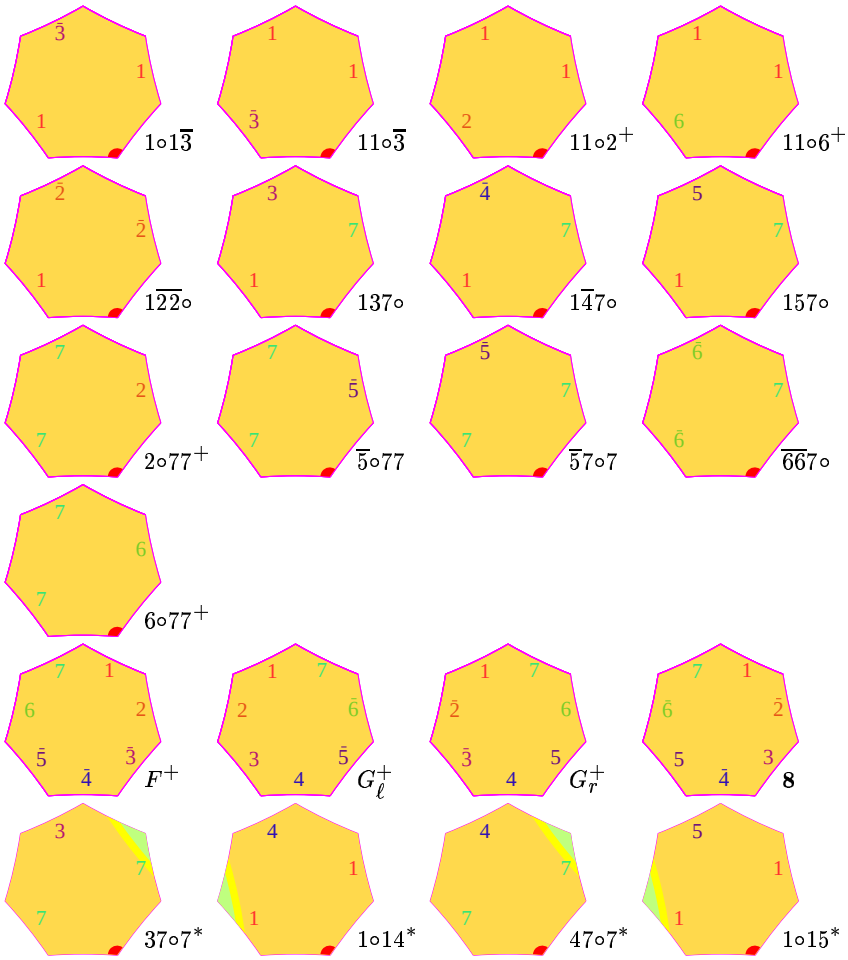

Figure 45 *The* 21 *tiles of the shrunken mantilla.*
Note the tiles which start the construction of a selected tree.

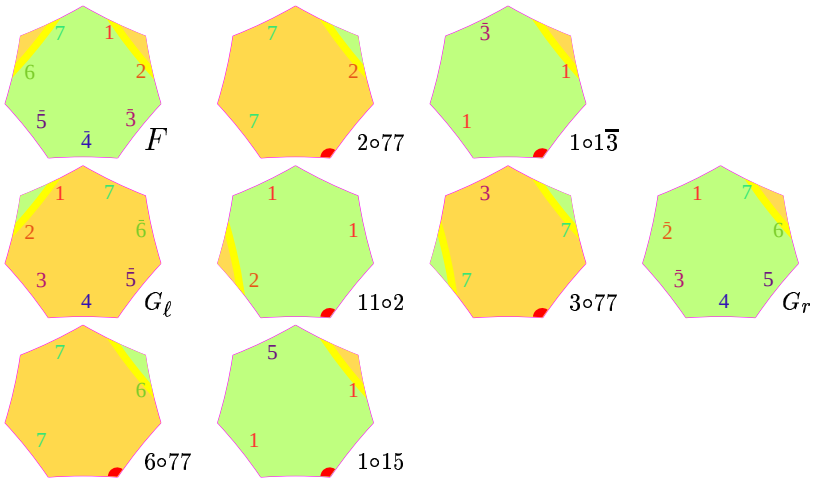

Figure 46 *The* 9 *tiles of the right-hand border of a selected tree.*
First, the 3 *tiles of the aperiodic part of the border: an F-centre and then two of its petals:* 2∘77 *and* 1∘$\overline{3}$1.
Second, the periodic part: three tiles belonging to the shrunken mantilla: tiles G_ℓ, 37∘7 *and* 6∘77*; three tiles belonging to the area of the selected tree:* 11∘2, 6∘77 *and* 1∘15.
Note that tile 37∘7 *also starts another selected tree.*

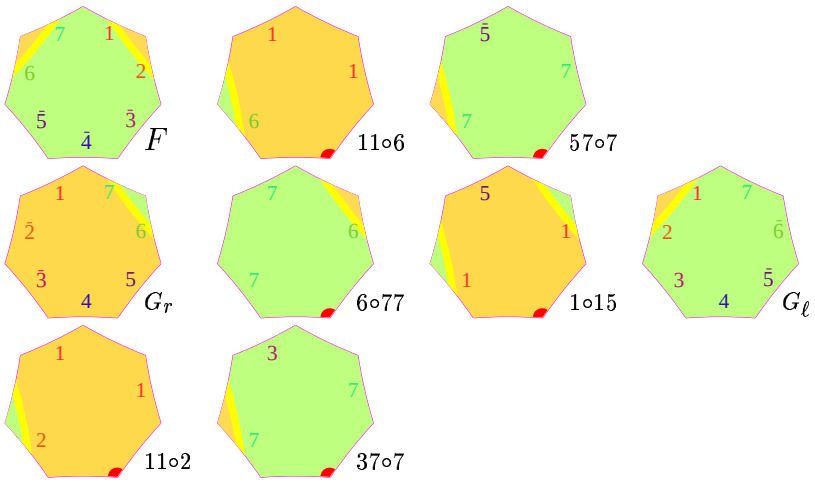

Figure 47 *The* 9 *tiles of the left-hand border of a selected tree.*
First, the 3 *tiles of the aperiodic part of the border: the F-centre, again, and then two of its petals, this time:* 11∘6 *and* $\overline{5}$7∘7.

Second, the periodic part: three tiles belonging to the shrunken mantilla: tiles G_r, 1∘15 *and* 11∘2*; three tiles belonging to the area of the selected tree:* 6∘77, G_ℓ *and* 37∘7.

Note that tile 1∘15 *also starts another selected tree.*

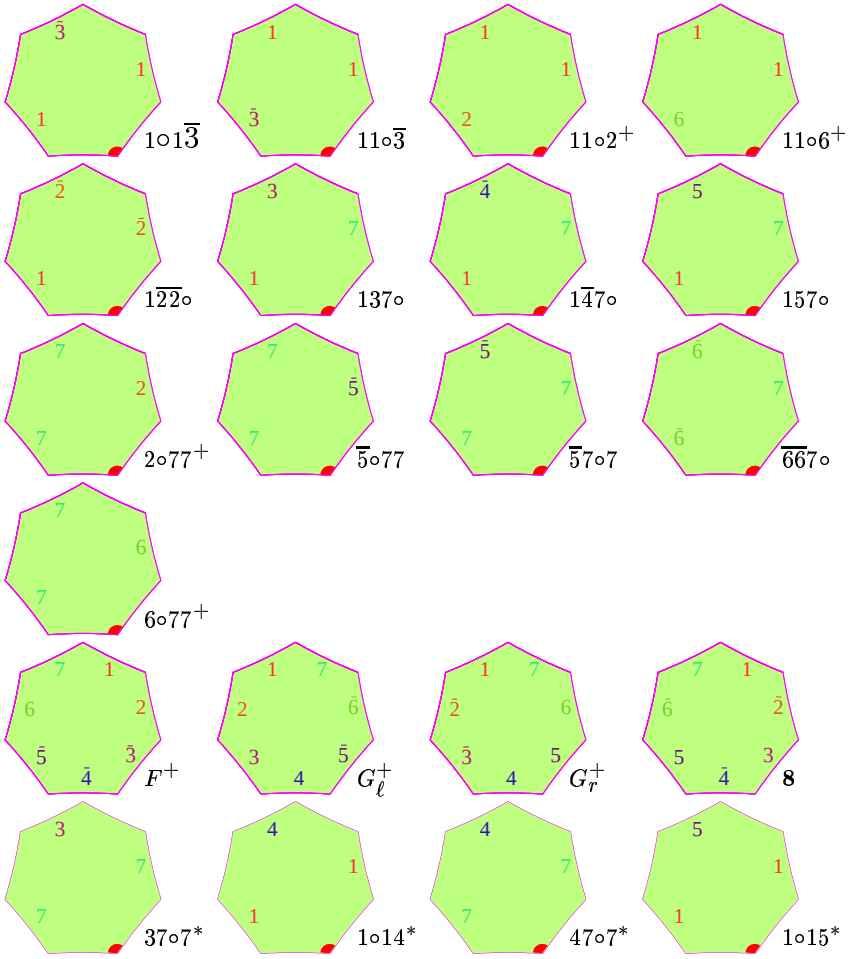

Figure 48 *The* 21 *tiles of the inside of the selected tree.*

Note that the tiles are obtained from the set of 21 *tiles for the shrunken mantilla by simply changing the background of the tile, four tiles being excepted: tiles* 37∘7, 1∘14, 47∘7 *and* 1∘15. *The new tiles have the new background but they no-more bear the marks of another part of the tiling. As a consequence, no tree can be created in this area.*

Next, we modify the algorithm of Figure 41 as follows. In step 1, we do not pick at random a tile from the set of all tiles but only in the set of the 21

modified orange tiles. Later on, we call the modified algorithm **algorithm for the refined mantilla**.

Lemma 18 *The algorithm for the refined mantilla always produces a realization of the refined mantilla. It exactly yields all the possible solutions of the refined mantilla.*

Proof. It is straightforward and it runs as the proof of theorem 3. In particular, there is no need to change the *wording* of Step 3 in Figure 41. However, it is worth noticing that the difference with theorem 3 lies in the application of the algorithm. In the case of theorem 3, consider the first action in Step 3. It consists in chosing at random the parental tiles of C_n among what is possible. When C_n is an F-centre, it may happen that this choice yields a G-centre, which means that a new tree is created. In the case of the refined mantilla, this must be ruled out. Otherwise, the trees being present in Σ_n would be contained in the tree created at time t_{n+1}, which violates the definition of a refined mantilla: it contains no ultra-thread. However, this never happens in the case of the algorithm of the refined mantilla. Indeed, the centre induced by the choice of the parental tiles at time t_{n+1} is always an **orange** tile. Assuming that this is the case for C_n, it is clearly the case for C_{n+1} when C_n is a G- or **8**-centre. When C_n is an F-centre, we first remark that there is a single orange F-centre in the set of prototiles. Next, we note that the petals which give rise to an F-son in a G-flower are $37\circ7$, or $1\circ14$, or $47\circ7$ or $1\circ15$. There are six of them in the set of prototiles and all have a small green part in contact with the edges 1 and 7 of the F-centre. As an orange F-centre has no green part, the above petals cannot match with it. And so, when C_n is an orange F-centre, the possible parental tiles are those for an F-centre or for an **8**-centre. This means that the number of possibilities for a random choice is six instead of eight for the ordinary mantilla. This is not really a big change from the point of view of the number of solutions.

The above argument shows that with respect to Σ_n, new trees created in Σ_{n+1} are either in the continuation of Σ_n but at a deeper level, or rooted in $\Sigma_{n+1}\backslash\Sigma_n$ but not containing any tree of Σ_n. And so, the algorithm produces a refined mantilla, *i.e.* without ultra-thread.

The proof that all the realizations of the refined mantilla are produced is as in the proof of theorem 3: the algorithm works in checking mode. ■

Before turning to the simulation of the computation of a Turing machine, we want to stress on a very important property.

It was foreseen by Robinson in his solution of the partial problem, see [29]: *it may happen that the universality problem and the aperiodic one are there not related* while they are closely related in the Euclidean case. Indeed, we have the following result.

Lemma 19 *There are infinitely many realizations of the refined mantilla which are periodic.*

Proof. Consider a G-centre A. We may assume A to be the first sector constructed by the algorithm for the refined mantilla. Accordingly, the F-son of A is the root of a selected tree. We note that the sons of a flower define a partition of the sector. Consequently, when we remove a selected tree, this does not affect the other sectors at the same level of the spanning tree for the mantilla. Now, in terms of petals, only two non-parental petals are concerned by the creation of the selected tree. The other non-parental petals are connected to the parental ones and they are the parental petals of the other sub-sectors: again two G-sectors and also two **8**-sectors. Consequently, by an easy induction on the levels of the spanning tree of the mantilla splitting, we can see that what remains from the sector when we remove the tiles belonging to the areas of all selected trees sons of the sector is a connected set of tiles.

In particular, the G-centre which is over the root of a selected tree is connected to A by a path which does not meet any selected tree. Also the path goes always from a tile which belongs to one level to a tile belonging to another level or which is the centre to which the previous tile is attached.

Consider such a path from A to B, another G-centre. We may assume that we have taken for B the same kind of G-centre as the kind of A. In this case, as the construction of the tree downwards is deterministic, this path will be repeated if we go downwards beyond B. Now, we can take the reverse path when we choose a new C_n in order to tile the plane in steps 3 of the algorithm. This will leads us to a tile C and the relations between C and A are in all respects those between A and B. Consequently, starting from C, we may again apply the same reverse path. By the end we obtain a periodic tiling: it is invariant under the shift along the mid-point line defines by the mid-point of edge 1 of A and the mid-point of edge 1 of B.

This construction is valid for any choice of B and there are infinitely many of them. ■

The property is perhaps more striking by the following fact: the converse of Lemma 19 is true, as proved by the following lemma.

Lemma 20 *There are countably many periodic realizations of the refined mantilla.*

Proof. First, we note that the construction which we indicated in the Lemma 19 is not the single one. We can repeat it *mutatis mutandis* with an F- or an **8**-center. Each time, we shall get another tree and indeed, different periodic realizations of the refined mantilla.

From what we already established, assuming that we have a period, *i.e.* a shift under which the considered realisation of the refined mantilla is periodic, it is enough to show that the line of the shift goes inside the sector defined by a a certain flower. Denote by Σ_M the sector headed by a centre M.

Assume that the considered realisation is invariant under a shift σ along a line ℓ. Let G be a G-flower giving rise to a selected tree as close as possible to ℓ. From the splitting property of the mantilla, Σ_G and $\Sigma_{\sigma(G)}$ are either disjoint of one of them contains the other.

If one contains the other, we are done and this realisation belongs to one of those which are depicted by Lemma 19.

Assume that the sectors are disjoint.

From the construction of the mantilla, there is another sector Σ_Φ, headed by a flower Φ, such that Σ_Φ contains both Σ_G and $\Sigma_{\sigma(G)}$. Now, by the properties of a hyperbolic shift and as the tiling is invariant under σ, it is not difficult to see that Φ and $\sigma(\Phi)$ are the same kind of centre. As Σ_Φ contains both G and $\sigma(G)$, we get that $\sigma(\Sigma_\Phi)$ contains both $\sigma(G)$ and $\sigma^2(G)$ and so, $\sigma(G) \in \Sigma_\Phi \cap \sigma(\Sigma_\Phi)$.

As distinct sectors are either disjoint or embedded, we obtain the inclusion $\Sigma_\Phi \subset \sigma(\Sigma_\Phi)$ or the opposite: $\sigma(\Sigma_\Phi) \subset \Sigma_\Phi$.

And so, the lemma is proved. ■

Note that the tilings constructed in Lemma 19 share the following property: for any pair of disjoint G-sectors Σ_{G_1} and Σ_{G_2}, there is a third one Σ_{G_3} which contains both of them. If we consider an F-centre F_0 and we take the shift which transforms this centre in its left-hand son F_1, it is not difficult to see that Σ_{G_0} is disjoint from Σ_{G_1} where G_0, respectively G_1, is the left-hand G-son of F_0, respectively F_1. Then it is not difficult to see that in the periodic tiling generated by the shift which transforms F_1 into F_0, Σ_{G_0} and Σ_{G_1} are not contained in any sector Σ_M when M is a G-centre.

Still about this property of periodic realizations of the refined mantilla, we can indicate some remarkable constructions which are illustrated by Figure 49, below.

A line of G_ℓ-centres:

Start from a G_ℓ centre A. Take its left-hand G_ℓ-son B. Let ℓ be the line which passes through the mid-points of the edges 7 and $\overline{5}$ of A. This line is also a line of mid-points but it is different from those which we consider in this report. We shall see another one in the second example of a periodic solution only. Indeed, this line joins the mid-points of two sides of an heptagon such that two end points of these sides are the vertices of a third edge of the heptagon. It is not difficult to see that in the tiling $\{7, 3\}$, this property is observed for all heptagons crossed by such a line. In particular, as can easily be seen in Figure 19, ℓ also crosses the edges 7 and $\overline{5}$ of B. This defines a period along ℓ and B is the image of A under the corresponding shift along ℓ. We may remark that the bisector of edges $\overline{6}$ of A and B are both perpendicular to ℓ.

A line of F-centres:

Start from an F-centre A. Take its left-hand F-son B. Let m be the mid-point line which cuts the edges 7 and $\overline{5}$ of A. This line is again a line of mid-points of the same kind as ℓ. From Figures 18 and 34, we can see that after A, m cuts the petal $\overline{5}7\circ 7$ at the mid-point of the first edge 7 after edge $\overline{5}$ of the petal and then it crosses B at the mid-points of its edges 7 and $\overline{5}$. This defines the period along m and the shift along m defined in this way transforms A into B. We may remark that the bisector of the edges 6 of A and B are both perpendicular to m.

A line of 8-centres:

Start from an **8**-centre A. Take the bisector p of its edge $\overline{4}$ which also passes through the red vertex of A. Consider the F-son C of A whose parental tiles are the tiles $157\circ$ and $1\overline{4}7\circ$ of A. Let B be the **8**-centre defined by C whose red vertex is shared by the petal $1\overline{4}7\circ$ of A. Then p is also the bisector of the edge $\overline{4}$ of B. This defines the period along p and it also defines a shift along p which transforms A into B. By construction, the edges $\overline{4}$ of A and B are both perpendicular to p.

A half-plane solution:

Consider again a G_ℓ-centre A and assume that it is an orange tile at the border of a selected tree. As A is an orange G_ℓ-centre, we know that

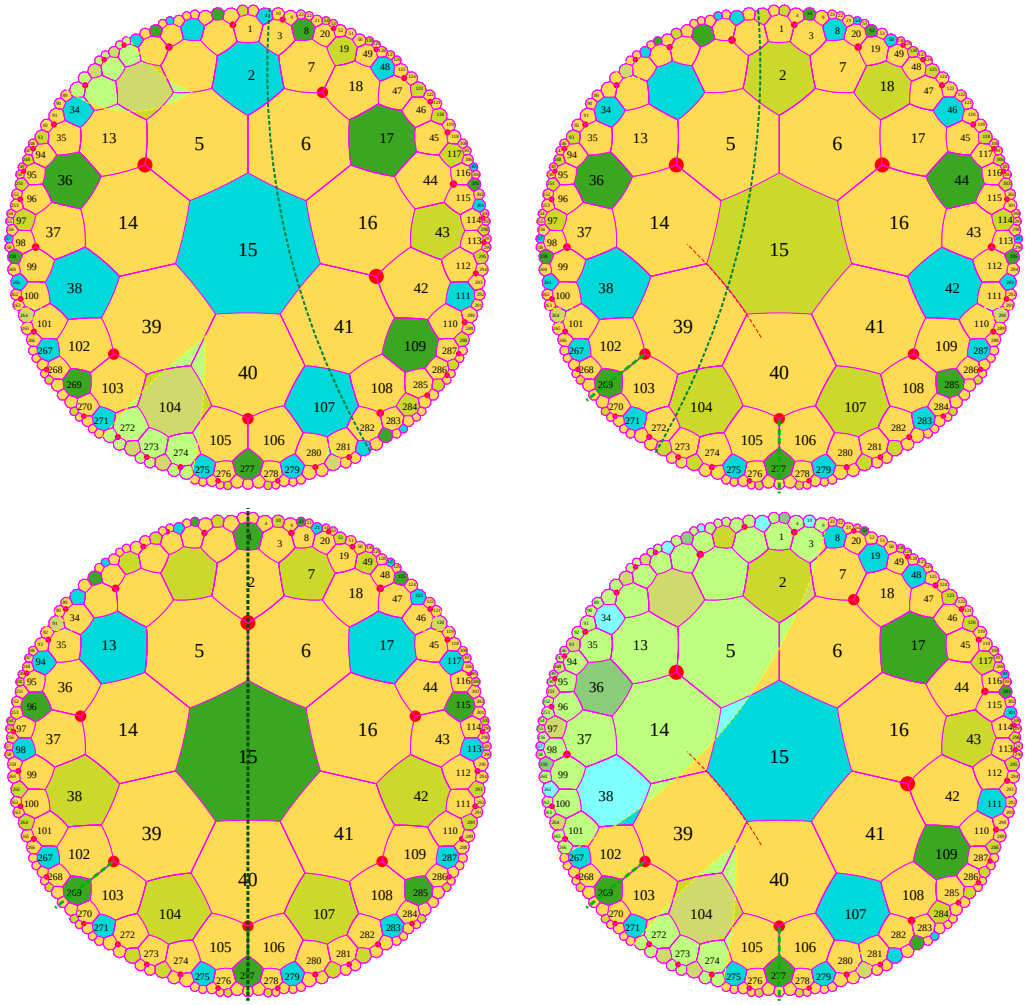

Figure 49 *Periodic realizations of the refined mantilla.*

Above: on the left-hand side, the period is generated by a mid-point line of G_ℓ-centres. On the right-hand side, it is generated by a mid-point line of F-centres.

In both cases, the mid-point lines are of the kind joining mid-points of non contiguous sides.

Below: on the left-hand side, the period is generated by a line of **8***-centres. On the right-hand side, a half-plane solution, here defined by G_ℓ flowers at the border, but outside the selected half-plane. There is another such solution with G_r flowers.*

it is on the right-hand border. We also know that the border is materialized by the 'ordinary' mid-point line ℓ which cuts its edges 1 and 2. Looking at the ultimate periodicity of the border, we know that G_ℓ belongs to the periodic part of the border and we know that the periodic

part goes downwards. When completing the refined mantilla starting from A, if the right-hand border goes on, it goes along ℓ again. We may decide to put a G_r-centre C at the parental petals of A or to put an F-centre. In the latter case, the F-centre defines the root of the selected tree whose right-hand border is materialized by ℓ. In the former case, we may also decide to put again a G_ℓ-centre at the parental petals of C. If we go on this alternation of G_ℓ- and G_r-centres, we get that the selected tree becomes a half-plane: it is the limit case of a tree whose root is removed to infinity. It is not difficult to see that the period between two consecutive G_ℓ-centres along ℓ defines a shift which leaves the tiling invariant. The half plane is also invariant under the shift.

Call **shrunken mantilla** the set of tiles which we get when we remove all tiles belonging to a selected tree. From the argument of the proof of Lemma 19, we derive another property of the refined mantilla:

Lemma 21 *The shrunken mantilla is a connected set of tiles.*

Proof. Consider Σ_n the sequence of modified sectors constructed by the algorithm for the refined mantilla. Define Σ'_n as the complement in Σ_n of all tiles belonging to a selected tree rooted in Σ_n. Then, by repeating the induction argument of the proof of Lemma 19 which is based on the levels of the mantilla we have that each Σ'_n is connected. Now, as $\bigcup_{n\in I\!N} \Sigma_n = \boldsymbol{H}^2$, we have that $\bigcup_{n\in I\!N} \Sigma'_n$ is the shrunken mantilla. Accordingly, as $\Sigma'_n \subset \Sigma'_{n+1}$, the shrunken mantilla is also connected. Note that from the proof of Lemma 19 and from the present argument, connectivity can be understood as the possibility to join any pair of tiles by a path of tiles which all lie in the shrunken mantilla. ■

Now, we state another important property of the shrunken mantilla.

Lemma 22 *For any tile τ of the shrunken mantilla, there is a G-flower at a distance at most* 6 *from τ.*

Proof. Obvious from the figures of the splitting of the sectors, see Figures 18, 19 and 20. ■

5.3.3 The delimitation of the computing regions

Now, we turn to the description of the tiles which delimit the trees in which the computation will proceed.

Before turning to the description of the prototiles used for the computation, we have to indicate how the computation is handled in connection with the algorithm of construction of the tiling.

Previously, we indicated that the computation of the partial problem will be put in the selected trees of the refined mantilla. This is true, but this does not necessarily mean that the border of the selected tree is also the border of the computation area.

Let us see why this cannot be the case. Assume for a while that the border of the selected tree is also the border of the harp. From the working of the algorithm for the refined mantilla, a border tile β may be chosen at random and, in particular, it may turn out to be a computational tile, far away from the beginning of the computation while the computation did not yet started because β is the first tile of the tree in our process of construction. Of course, as a placed tile cannot be removed, we may refrain to place β until we may actually start the computation. Then, at some point, we find the exact place of β and we put it. There are two objections. First, a mild one is that it may happen that we shall never find a place for β as β may turn out to be never used in the computation which we are simulating. As the reachability problem is undecidable for Turing machine, we cannot do otherwise than put aside β until we find its place. We shall have to return to the processing of such a case in the final algorithm. Second, and this is a serious objection, it may turn out that in the construction of the tiling, we shall find a border of a half-plane and not of a selected tree. In this case, as we are waiting for the root of the selected tree, the algorithm will simply not tile the plane. And the fact that this happens with a very low probability if not probability 0 changes nothing.

This is why the computation area does not coincide with the selected tree in our setting. In fact, it will be a subtree inside of the selected tree. The complement of the computation area inside the selected tree is called the **shield**. It is not difficult to see that as we put the computation area inside the selected tree, the shield has two parts connected by the root of the selected tree: one part lies between the left-hand border and the computation area and the other lies between the computation area and the right-hand border. And this is enough to answer the above question. If we find a border tile β, it will be a tile of the shield. We may place it as it does not bare any computation. Later, the final algorithm will contribute to fill up the shield in such a way that if the root of the selected tree is never found out, the resulting half-plane will nonetheless be constructed by the algorithm.

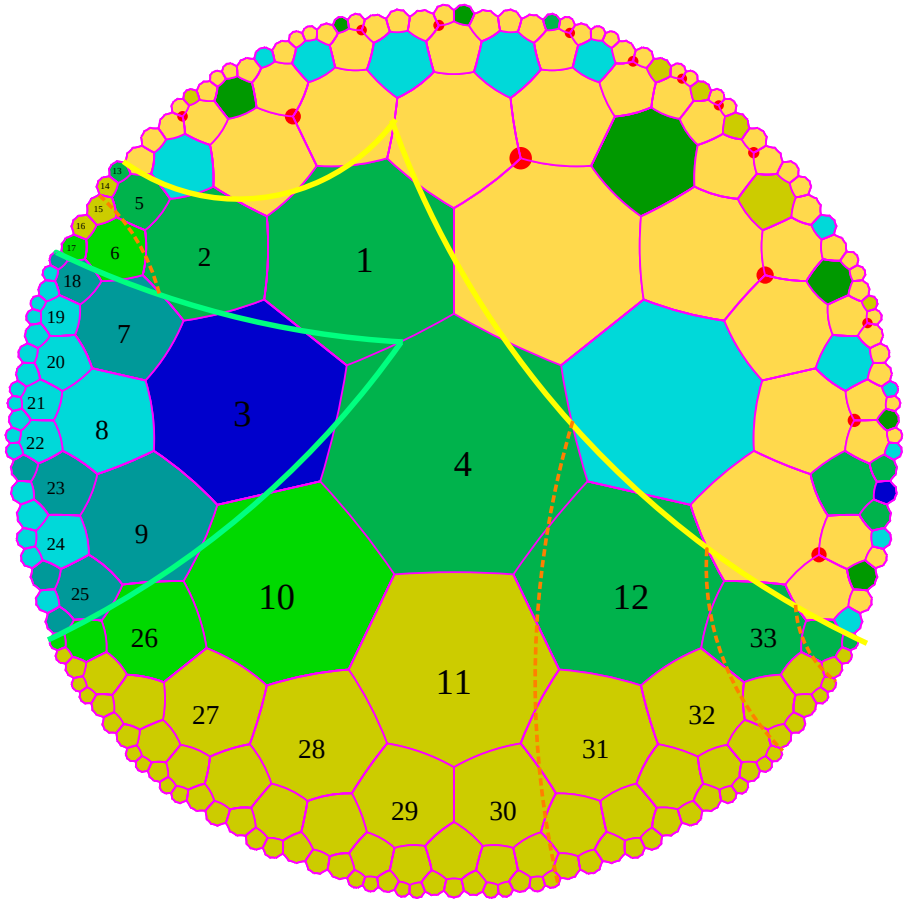

Figure 50 *The insertion of the harp, in blue, inside the selected tree, in green. On the right-hand side of the selected tree with numbered tiles, note another selected tree at three tiles on the right-hand side of tile* 33*. This new selected tree is generated by the* G_ℓ*-centre which is adjacent to tiles* 4 *and* 12*.*

Accordingly we shall get a complete tiling.

This also answers the mild objection. As we shall soon see, the construction of the computation area always start from the root and so we are never faced to the situation which is considered in the mild objection.

The situation of the computation area, now call it the **harp**, is depicted by Figure 50, above. As seen in the figure, the root of the harp is a son of the root ρ of the selected tree, it is its middle son in the sense of the Fibonacci structure. It is delimited by two mid-point lines. The left-hand border of the harp is defined by the mid-point ray γ which starts from the mid-point

of edge $\overline{3}$ of ρ and which passes through the mid-point of edge $\overline{4}$ of ρ. The right-hand border is the mid-point ray δ which is the reflection of γ in the support of edge $\overline{3}$ of ρ.

As the new name suggests it, we implement the description of section 4.1 in the harp placed in any selected tree of the refined mantilla.

5.3.4 The final set of tiles

Now, we turn to the description of the final set of prototiles for our problem.

As previously, the set of prototiles splits into several subset. The first subset is the **skeleton** which allows to construct the shrunken mantilla. And we know from Lemma 21 that the shrunken mantilla is a connected set of tiles.

The skeleton contains the previous set of 21 orange tiles in which four tiles have a small green part in their background, see Figure 51, above. It is the tiles with pattern 47∘7, 1∘15, 37∘7 and 1∘14, respectively. By definition, the skeleton is the set of tiles which can be used in step 1 for the choice of the first tile. As we wish that the first tile could be any tile of the shrunken mantilla, we have to append the **orange** tiles of the border of the shrunken mantilla with the selected tree. We know that these orange tiles have also a small green part, due to their border position. It is the tiles: 11∘6, G_r, 1∘15, 11∘2 of Figure 53 and the tiles: 2∘77, G_ℓ, 37∘7, 6∘77 of Figure 54. Also, any tile of the skeleton will be used infinitely many times, as proved further.

The second subset of tiles consists of the tiles for the inside part of the shield. They are copies of tiles (5) and (6) of Figure 23. We just change the colour of the background which is green as we are inside a selected tree.

This set matches with the third subset of prototiles which has more prototiles and which is the set of tiles for the border of the shield with the shrunken mantilla.

First, we have the root ρ of the selected tree which bears all the marked sign of an F-flower, see Figure 52. Its background is green and so, it belongs to the shield. Also, it has three smaller parts in other colours: two are in orange to match with the orange tiles of the shrunken mantilla. One is in blue to match the starting part of the root of the harp. Then we have the left-and right-hand sons of ρ. These sons of ρ have also three colours for the background. Their main part is green as they belong to the shield, but they have a blue part to match with the root κ of the harp and an orange part to match with the shrunken mantilla. They also have numbered marks:

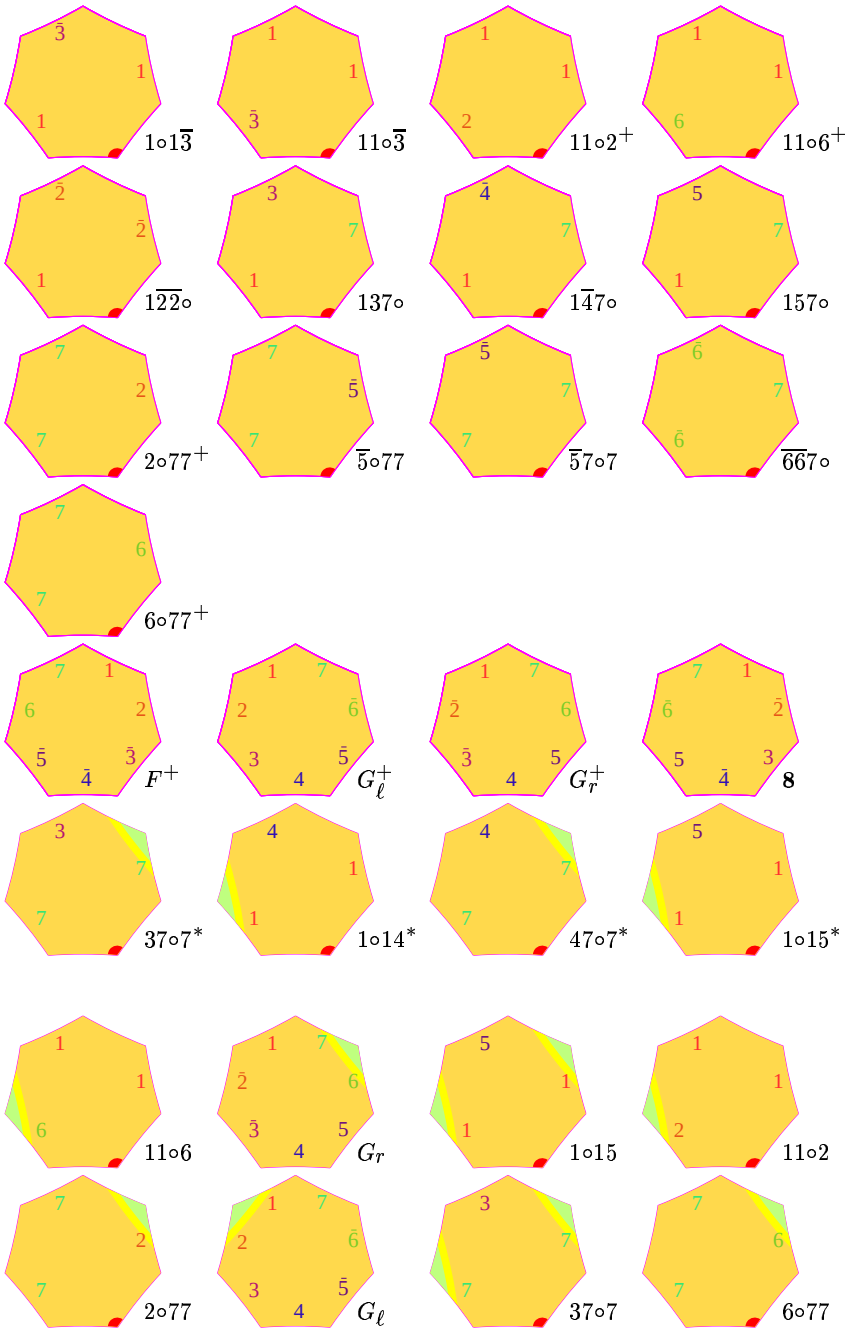

Figure 51 *The 29 tiles of the shrunken mantilla.*
Note the tiles which start the construction of a selected tree.

Also note the orange tiles of the borders with the shield of a computing area.

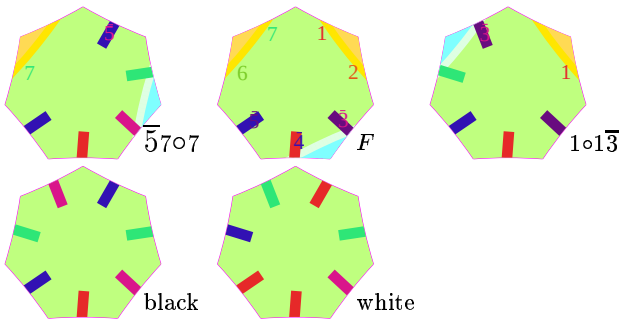

Figure 52 *The* 5 *tiles of the shield.*
Above, in the middle, the root of the shield. The tile is called by tiles 1∘14, 1∘15, 37∘7 *and* 47∘7 *of the shrunken mantilla. Note that tiles* $\overline{5}$7∘7 *and* 1∘1$\overline{3}$ *are changed.*
Below, the two tiles inside the shield. The border with the shrunken mantilla and with the harp is displayed below.

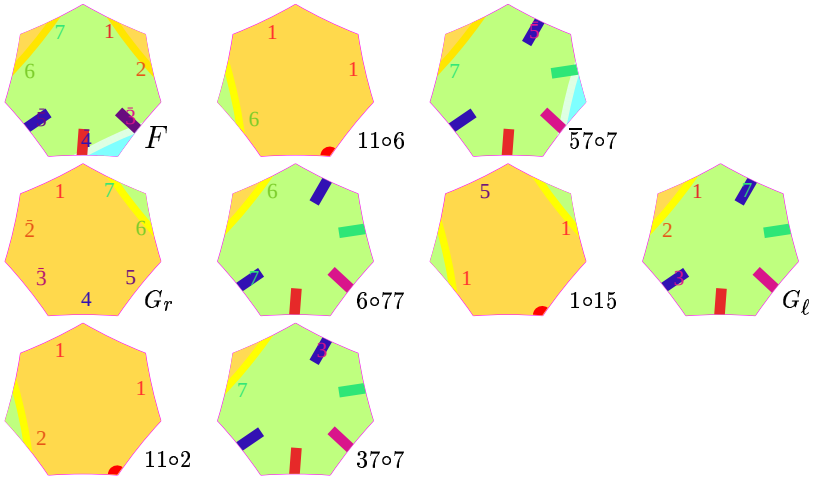

Figure 53 *The* 9 *tiles of the border between the shrunken mantilla and the left-hand part of the shield.*
Above, we have the aperiodic part; below, the periodic part.
Note that only 3 *tiles are new: the new* 6∘77, G_ℓ *and* 37∘7. *Note that these tiles do not bear all the numbered marks of standard tiles as they belong to the shield. They also lost their red-vertex for the same reason.*

one mark replicates the mark of the edge of ρ at which they abut; the other mark reminds the petal numbering and is used to easily place the tiles of the border which are in the shield.

The other tiles of the border have this latter characteristics: they still bear two marks from the mantilla tiles in order to match with the tiles of the shrunken mantilla. Indeed the border tiles of the shrunken mantilla still bear all their numbered marks when they are orange tiles. The border tiles of the shield exactly reproduce the periodicity observed when defining the tiles of the refined mantilla. This requires to partially use the numbered marks. It is needed for the edges close to the border only: the third number which is deeper inside the tree is no more useful. It is also removed, to match more easily with the Fibonacci tiles. This subset of tiles is illustrated below in Figures 53 and 54.

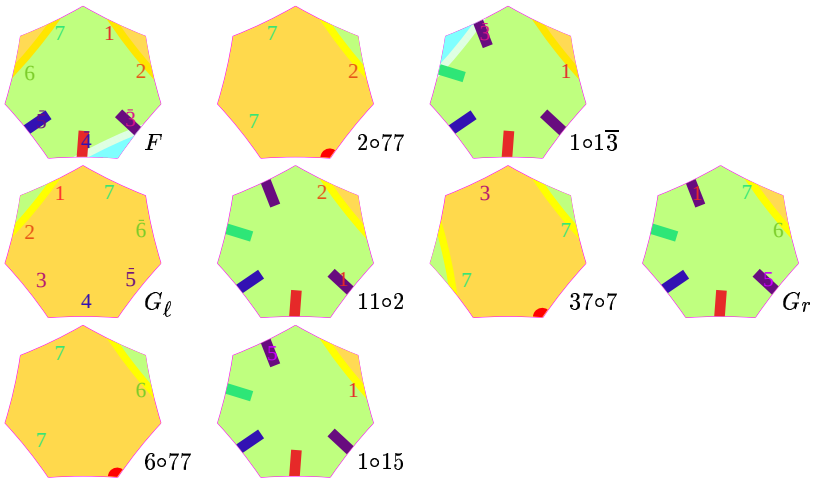

Figure 54 *The 9 tiles of the border between the shrunken mantilla and the right-hand part of the shield.*
Above, we have the aperiodic part; below, the periodic part.
Note that only 3 tiles are new: the new 11∘2, G_r *and* 1∘15. *Note that these tiles do not bear all the numbered marks of standard tiles as they belong to the shield. They also lost their red-vertex for the same reason.*

The fourth set of tiles is the borders between the shield and the harp. We take tiles (c), (i), (e), (m) and (n) and we modify them as now described. First, they have mainly a blue background but they have a small green part to match with the tiles of the shield. We shall say that they are blue tiles and we consider them as belonging to the harp. Next, tiles which are alike

tiles (e), (m) and (n) have Fibonacci marks on the border sides: they have to match with the Fibonacci marks of the shield as they globally belong to the same selected tree. Accordingly these tiles have a green Fibonacci mark on the right-hand side topmost edge and the next edge, clockwise going, bears a light purple mark to a tile of the shield on the next level.

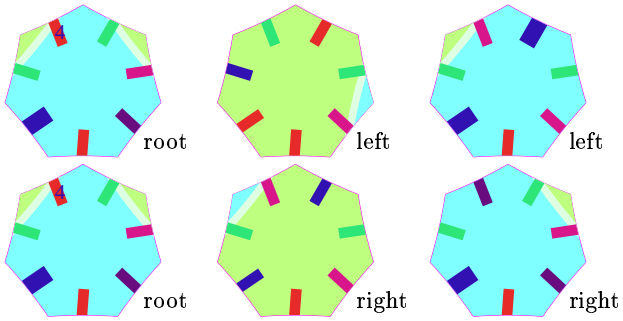

Figure 55 *The tiles of the borders between the shield and the harp. Above, we have the aperiodic part; below, the periodic part.*

It is important that the border maintains the lateral connections represented by the green marks: they indicate the levels of the Fibonacci trees. They allow us to harmonize the levels between the harp and the shield in order to define unique levels in the selected tree itself.

The fifth set of tiles is the set of tiles of the harp, border excluded. Here, we just changed the background of the tiles: now, it is blue. As in the case of the harp, these tiles as well as the border tiles which are mainly inside the harp are prototiles of prototiles. They bear the supports for the Turing signal but they have not the exact indication of states or tape symbols. The prototiles are obtained from these tiles by putting all possible marks of state and tape symbol corresponding to the instruction table of the simulated Turing machine. However, for the counting of the number of tiles, we only count the prototiles of prototiles for the Turing signals. We just note that tiles which are alike tiles (c) and (i) have a similar one in the subset of tiles for the borders of the harp with the shield. In the border situation, there is only one possible kind of Turing signal for a state in a tile of type (i): the signal must go back to the right. But it is enough to have this kind of tile for the border, as illustrated by the third tile of the first row of Figure 56, and not the tiles alike to (f) for instance.

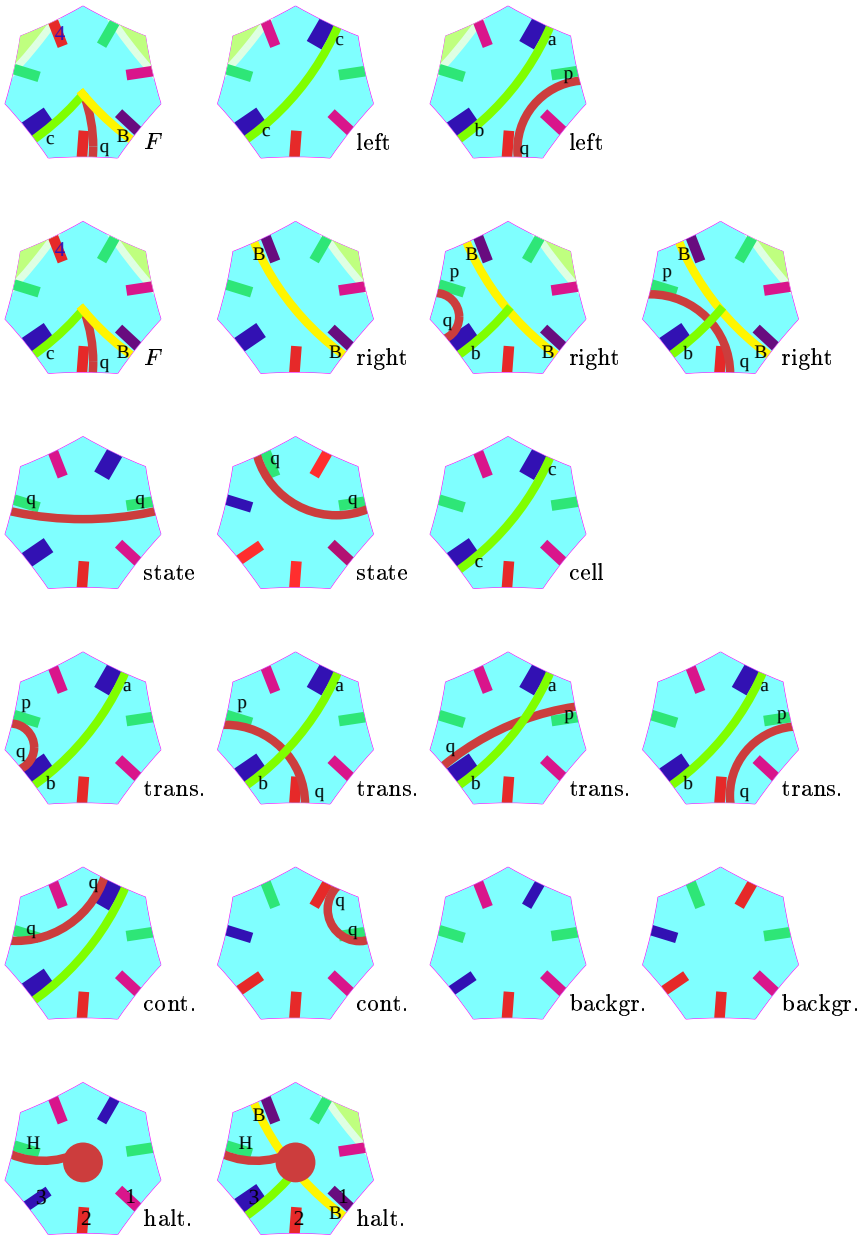

Figure 56 *The tiles for the harp and its computation.*
The first row indicates the left-hand border of the harp.
The second row indicates the right-hand border.
The third row indicates the tile for a passive propagation of the signals: for the state, for the content of the squares of the tape.

The fourth row implements the transition. The continuation of the new signal is indicated by the first two tiles of the fifth row.
The last two tiles of the fifth row indicates the tiles for the back ground of the harp.
The tiles of the sixth row indicates the tiles for the halting.
Note that we already met some of the present tiles but without the Turing signals.

Taking into account all what we up to now listed we obtain that the set of prototiles contains 64 tiles.

5.4 The algorithm, revisited

We revisit the algorithm for the refined mantilla and that of Figure 41.

Now, in step 1, we require that the first tile should be taken from the skeleton, exactly as in the algorithm for the refined mantilla.

Steps 2. and 3. are modified in order to take into account the new properties of the border between the shrunken mantilla and the shield of the selected tree.

In both cases, in the process of completing a sector, we have to take into account that the sector constructed by the algorithm may meet several selected trees. There are two situations: either the root of the selected tree is already placed or it is not.

In the case when the root of the selected tree is already placed, there is indeed little to do. As the computation goes on downwards, it is deterministic and the single point is the growth of the tiled area inside selected trees. The easiest way is to follow the levels of the Fibonacci tree inside selected trees in place of following levels of the mantilla.

Of course, there is a discrepancy. As can be noted in Figures 38, 39 and 40, mantilla levels are larger than Fibonacci ones. Locally, a mantilla level can spread over three Fibonacci levels. From this, we easily deduce that level n of the mantilla reaches at most level $3n$ of the Fibonacci tree, the extremal value being reached, if we assume that levels 0 are the same for the mantilla and for the tree at the root of the tree. Accordingly, as a Fibonacci tree of height h has a level h of length K^h, where $K > 1$, indeed K is the square of the golden mean, we conclude that if L is the length of the Fibonacci level λ, the level reached by the mantilla level which coincide with λ on the borders of the tree reaches a Fibonacci level which is $M \log L$ deeper than the level of λ, where M is a positive constant. In this argument we assume that the mantilla level which coincides with λ on a border of the tree also coincides with λ on the other border. This is true because a

selected tree is symmetric under the reflection in the axis of the F-sector which generates the tree. Remind that this axis is also the bisector of edge $\overline{4}$ in an F-centre. It is also obvious from Figure 18 that an F-sector is invariant under this reflection.

If the root of the selected tree is not already placed, it may happen that we deal with a half-plane and not with a selected tree. Accordingly, we have to grow up the tiled area of the shield in a way which does not lead to a contradiction. Taking into account that the process is deterministic as we go downwards, each time a new tile ν of the border is placed, the algorithm fills up the tree rooted at ν down to the current level inside a selected tree. In this way, we obtain what would be developped if the root were already placed but no more.

Accordingly, consider the case when a new sector is determined at step 3 of the algorithm and that we have a shield border without root. Let α be the upmost tile of this border at this stage of the construction, just before time t_{n+1}. The algorithm places the tiles defined deterministically by the choice of C_{n+1} until they meet the continuation of the border above α. Then we go along this border tile by tile starting from α. Each new tile is determined by the new sector. If it is still the continuation of the border, the algorithm fills up the corresponding tree after up-dating what corresponds to the change of level induced by the new sector Σ_{n+1} lead by C_{n+1}. If it is a root ρ of the selected tree, then the harp can be constructed up to the level defined by Σ_{n+1}. If the new sector still brings a tile above ρ, then we can construct the continuation of the shrunken mantilla on the other side of the selected tree rooted at ρ and we can again go down to the required level of the mantilla thanks to the remark on the symmetry of the selected trees. If, when placing the root, it happens that the new sector does not bring in a tile of the mantilla above the root, we just construct the harp with its right-hand side border and we wait for the next sector, Σ_{n+2} in order to construct the right-hand part of the shield and the continuation of the shrunken mantilla over the right-hand border of the selected tree. If during this process we have only continuations of the border, when the time for C_{n+2} is reached we have constructed a far larger part of the shield. Also, this appending of trees at each step guarantees that the new Σ_{n+1} also contains B_{n+1} if B_n was contained at the previous step: it is plain that a new layer of at least one tile is put uniformly on the previous border of Σ_n. Consequently, if the root is never found, the unrooted shield will converge to a half-plane which will be covered by the algorithm.

We may consider the case of a half-plane as a limit case of selected tree:

the root of the tree is moved to infinity and, as a consequence, the harp is thrown away, beyond the points at infinity of the hyperbolic plane.

And so, the modified algorithm always construct a solution, provided that the simulated Turing machine does not halt. We also obtain that all the tiles of the skeleton are used infinitely often.

Now, it is not difficult to see that if we have a solution, picking at random a tile in the shrunken mantilla and taking it as the tile chosen at step 1, we again obtain this solution by running the algorithm in checking mode.

Accordingly, we proved the following result:

Lemma 23 *The algorithm of Figure* 41 *modified by the indications of section* 5.4 *yields all the solutions of the generalzed origin-constrained problem for the refined mantilla in the case when the simulated machine does not halt.*

Taking into account the remarks of the beginning of section 4.2.1, in particular the fact that the tiles of the skeleton are used infinitely many often and the density property indicated by Lemma 22, we proved the main result of this report:

Theorem 4 *The generalized origin-constrained problem of tiling the hyperbolic plane defined by the conditions* (*i*) *and* (*ii*) *of the introduction is undecidable. The set of prototiles of the proof contains* 64 *tiles,* 29 *constituting the skeleton of the construction. This set of prototiles has the property that when the simulated Turing machine does not halt, among the continuously many possible realizations of the tiling, countably many of them are periodic.*

Before turning to another application of our construction, we may note the following property of the skeleton:

Lemma 24 *There is a slight modification of the algorithm defined in lemma* 23 *such that starting from the skeleton alone, the algorithm constructs a realization of the shrunken mantilla. The modified algorithm also yields all the possible realizations of the shrunken mantilla.*

The modification consists in the fact that the algorithm knows that the tiles 37∘7 and 1∘15 are necessary connected with the border tiles 6∘77, 11∘ of Figure 53 and the tiles 2∘77, 11∘2 of Figure 54 respectively. This is forced by the whole set of prototiles with the algorithm of lemma 23. If the other tiles of the border are not present, then the matching can be done with the

ordinary tiles. An alternative solution consists in appending specific marks to the considered tiles. It will be a redundent information for the algorithm of lemma 23 but the same algorithm applied to the skeleton only will provide the shrunken mantilla. A third solution, which allows us to apply the algorithm of lemma 23 is to append new tiles to the skeleton: all the tiles which have an orange part. In this case, the other tiles of the border allow us to obtain the correct matching of the orange tiles of the border without additional mark or without putting the corresponding information in the memory of the algorithm.

6 Nonrecursive tilings

In this section, we apply the method of [9] to prove the result of [9, 24] for the hyperbolic plane, namely:

Theorem 5 *There is a finite set of prototiles $\mathcal{S}$ such that there is a nonrecursive way to tile the hyperbolic plane using copies of the tiles of $\mathcal{S}$ and that any recursive method to tile the hyperbolic plane starting from $\mathcal{S}$ will fail.*

Before turning to the easy proof of theorem 5, we make a detour through the notion of **carpet** which we already mentioned.

6.1 Coordinates

Up to now, we used coordinates for tiles just in a few pictures, see Figures 18, 19, 20, 21, 22, 24, 38, 39, 40, 43, 44 and 50. In these figures, we use the simple coordinates introduced in [12] and which we remembered in section 2.3.

As mentioned in the introduction, in [18], I introduced a new system of coordinates which can work both for the pentagrid and for the heptagrid. It is attached to the notion of **carpet** to which we referred when we constructed the mantilla.

Consider the heptagrid. As we know and as shown in [18], we define a sequence of increasing angular sectors defined by lines of mid-points, see Figures 4 and 6, whose union is the whole hyperbolic plane. We may fix the choice of the sectors in such a way that the head of each sector is the middle son of the head of the next sector, looking downwards. Now, we can number these sectors using integers in $\mathbb{Z}$ and then, using the coordinates of section 2.3 and [12] in each part of the tree which is not covered by the next

sector. In this way defined in [18], a couple of integers is attached to each tile as its coordinate. In this section, we assume that this system is defined for the tiles of the refined mantilla, considered as tiles of the heptagrid.

6.2 Recursive and nonrecursive tilings

Accordingly, a finite set of prototiles $\mathcal{T} = \{T_1, \ldots, T_k\}$ being defined, we say that a tiling is **recursive** if there is a total recursive function f on $\mathbb{N} \times \mathbb{N}$ such that $f(i,j) = h$ with $h \in \{1..k\}$ and tile $T_{f(i,j)}$ is placed on the tile of the heptagrid with coordinate $((-1)^{i \bmod 2} \lfloor \frac{i}{2} \rfloor, j)$, using the well known encoding of $\mathbb{Z}$ by $\mathbb{N}$ in which negative numbers are encoded by odd numbers.

It is not difficult to see that among the solutions of the refined mantilla given by the algorithm defined in section 5.4. there are nonrecursive solutions as there cannot be more than countably many recursive tilings: although they cannot be enumerated, as total recursive functions cannot be, they constitute a subset of partial recursive functions which, as well known, can be enumerated.

Transporting the construction of [9, 24] to the refined mantilla, we can explicitly construct a finite set of prototiles which can tile the hyperbolic plane, only in a nonrecursive way.

The idea is to transport the construction into the harp. There is just a little adaptation. In order the reader could clearly understand the construction, first we remind Hanf's construction.

The idea is the following: a Turing machine contains in its program the computation of two total recursive functions f and g which enumerate two recursively enumerable sets, A and B respectively which are supposed to be infinite, disjoint and recursively unseparable, see [25]. The machine has a semi-infinite input tape which is read-only and whose cells have coordinates in $\mathbb{N}$ denoted by $c(n)$. The machine performs the loop of Figure 57.

It is not difficult to implement this machine in the harp. Remember that all the levels of the Fibonacci tree intersect the rightmost branch of the harp exactly once: the level 0 at the root, the level 1 at the rightmost son of the root and so on. We again consider that the machine works on a semi-infinite tape materialized by the rightmost branch of the harp. We shall call **even chords** the chords of the harp which are issued from a cell of the rightmost branch with an even level. Similarly, we call **odd** the branches issued from the cells of the rightmost level with an odd level. We consider that the

even chords are devoted to the input tape of the above Turing machine. Accordingly, once the corresponding tiles are put on the rightmost branch, the information which they contain is never change along the corresponding chord, whatever the moves of the head of the machine are. Similarly, the odd chords are used by the head of the machine to perform the required computations and then the reading of the appropriate cell of the input tape.

$i := 0$;
`loop`
    compute $g(i)$;
    look at cell $c(g(i))$ of input tape;
    if $c(g(i))$ contains 0, `exit`;
    compute $h(i)$;
    look at cell $c(h(i))$ of input tape;
    if $c(h(i))$ contains 1, `exit`;
    $i := i+1$;
`end loop`;
`stop`;

Figure 57 *The loop performed by the program of the Turing machine.*

Once this has been precisely indicated, the needed details are easy to be provided. Accordingly, theorem 5 is proved. Note that it is proved both in a *partial* variant and in a *generalized* one thanks to the construction described in the report.

7 Conclusion

As a conclusion, we cannot say at the present moment how far this solution is from the solution of the general problem. If the general problem turns out to be decidable, the present solution will be an optimal one if not the best which could be done. If the general problem turns out to be undecidable, it is difficult to say whether we just need a slight improvement or completely different new ideas.

References

[1] Berger R., The undecidability of the domino problem, *Memoirs of the American Mathematical Society*, **66**, (1966), 1-72.

[2] C. Carathéodory. Theory of functions of a complex variable, vol.II, 177–184, Chelsea, New-York, 1954.

[3] Chelghoum K., Margenstern M., Martin B., Pecci I., Cellular automata in the hyperbolic plane: proposal for a new environment, *Lecture Notes in Computer Sciences*, **3305**, (2004), 678-687, proceedings of ACRI'2004, Amsterdam, October, 25-27, 2004.

[4] Chelghoum K., Margenstern M., Martin B., Pecci I., Skordev G., Tilings $\{p, q\}$ of the hyperbolic plane are combinatoric, *Proceedings of* **WTCA'2004**, Auckland, New-Zealand, December, 12, 2004.

[5] Sur les groupes hyperboliques d'après Michael Gromov, E. Ghys, P. de la Harpe (ed.), Progress in Mathematics, **83**, Birkhäuser, (1990).

[6] A. S. Fraenkel, Systems of numerations, Amer. Math. Monthly, **92** (1985), 105-114.

[7] Goodman-Strauss Ch., A strongly aperiodic set of tiles in the hyperbolic plane, *Inventiones Mathematicae*, **159**(1), (2005), 119-132.

[8] M. Gromov, Groups of polynomial growth and expanding maps, *Publications Mathématiques de l'IHES*, **53**, (1981), 53-73.

[9] Hanf W., Nonrecursive tilings of the plane. I. *Journal of Symbolic Logic*, **39**, (1974), 283-285.

[10] D. Hilbert, *Grundlagen der Geometrie*, B.G. Teubner, Stuttgart, 1968, (10^{th} ed.), 271p.

[11] M. Hollander, Greedy numeration systems and regularity, *Theory of Comput. Systems*, **31** (1998), 111-133.

[12] Margenstern M., New Tools for Cellular Automata of the Hyperbolic Plane, *Journal of Universal Computer Science*, **6**,, No12, (2000), 1226–1252.

[13] Margenstern M., A contribution of computer science to the combinatorial approach to hyperbolic geometry, **SCI'2002**, July, 14-19, 2002, Orlando, USA, (2002).

[14] Margenstern M., Revisiting Poincaré's theorem with the splitting method, talk at **Bolyai'200**, International Conference on Geometry and Topology, Cluj-Napoca, Romania, October, 1-3, 2002.

[15] Margenstern M., Cellular automata in the hyperbolic spaces. A survey, *Romanian Journal of Information Science and Technology* **5**, 1-2, (2002), 155-179.

[16] Margenstern M., Cellular Automata and Combinatoric Tilings in Hyperbolic Spaces, a survey, *Lecture Notes in Computer Sciences*, **2731**, (2003), 48-72.

[17] Margenstern M., The tiling of the hyperbolic $4D$ space by the 120-cell is combinatoric, *Journal of Universal Computer Science*, **10,** N°9 (2004), 1212-1238.

[18] Margenstern M., A New Way to Implement Cellular Automata in the Penta- and Heptagrids, *Journal of Cellular Automata*, **1**, (2006), 01-24.

[19] Margenstern M., Morita K., NP problems are tractable in the space of cellular automata in the hyperbolic plane, *Theoretical Computer Science*, **259**, (2001), 99-128.

[20] M. Margenstern, G. Skordev, Fibonacci Type Coding for the Regular Rectangular Tilings of the Hyperbolic Plane, *Journal of Universal Computer Science* **9**, N°5, (2003), 398-422.

[21] Margenstern M., Skordev G., Tools for devising cellular automata in the hyperbolic 3D space, *Fundamenta Informaticae*, **58,** N°2, (2003), 369-398.

[22] Margulis G.A., Mozes S., Aperiodic tilings of the hyperbolic plane by convex polygons, *Israel Journal of Mathematics*, **107**, (1998), 319-325.

[23] Meschkowski H., Non-euclidean geometry, translated by A. Shenitzer. Academic Press, New-York, 1964.

[24] Myers D., Nonrecursive tilings of the plane. II. *Journal of Symbolic Logic*, **39**, (1974), 286-294.

[25] Oddifredi P., Classical Recursion Theory, North-Holland, 1989.

[26] Poincaré H., Théorie des groupes fuchsiens. Acta Mathematica, **1**, 1–62, (1882).

[27] A. Ramsay, R.D. Richtmyer, Introduction to hyperbolic geometry. Springer-Verlag, 1995.

[28] Robinson R.M. Undecidability and nonperiodicity for tilings of the plane, *Inventiones Mathematicae*, **12**, (1971), 177-209.

[29] Robinson R.M. Undecidable tiling problems in the hyperbolic plane. *Inventiones Mathematicae*, **44**, (1978), 259-264.

[30] Wang H. Proving theorems by pattern recognition, Bell System Tech. J. vol. **40** (1961), 1–41.